

Final Report

Test bench measurements of a 250 kW hydrostatic drivetrain WP1: System design for 250 kW

Client: Bosch Rexroth AG

Contractor: Institute for Fluid Power Drives and Controls (IFAS)

Head of Department: Prof. Dr.-Ing. H. Murrenhoff

Official in Charge: G. Matthiesen, M.Sc., M.Sc.

Project Number: 79 Hy 1056b

Aachen, September 2014

Table of contents

I	Table of formulae	ii
II	Table of abbreviations	iv
1	Introduction	5
2	Generation of a drivetrain	7
2.1	The underwater turbine	7
2.2	Design of the hydrostatic drivetrain	10
3	Control Strategy	18
3.1	TSR-controller with knowledge of current speed	18
3.2	TSR-controller without knowledge of current speed	18
3.3	Limitations of input power without knowledge of current speed	21
3.4	Start up procedures for the turbine.....	22
3.4.1	Start up of the turbine using the grid	23
3.4.2	Start up of the turbine without using the grid (respectively the generator).....	26
3.5	Stop procedures for the turbine	32
3.5.1	Stop of the turbine using pressure control	32
3.5.2	Stop of the turbine using the main pressure relief valve (emergency stop)	34
3.5.3	Overview of the different control algorithms	37
3.5.4	Overview of further required components for a hydrostatic drivetrain	38
4	Build-up of the Simulation Model	39
5	Simulation of the HDT	43
5.1	Start up of the rotor	44
5.1.1	Start up with the grid	44
	Start up with the grid in an overload scenario	49
5.1.2	Start up without the grid	50
5.2	Simulation of an overload scenario	51
5.3	Simulation of an “over speed configuration”	52
5.4	Stop procedures for the system	55
5.4.1	Stop procedure with braking torque applied by the motors.....	55
5.4.2	Stop procedure with braking torque applied by the PRV	56
5.5	Load-cycle: Start – Overload – Stop	58
6	Proposed layout for a test bench	59
7	Summary and Outlook	61
III	Bibliography	62
IV	Table of figures	63
V	List of tables	66
VI	Appendix	67

I Table of formulae

A_0	Cross sectional area	[m ²]
c_m	Torque coefficient	[-]
c_p	Power coefficient	[-]
J_m	Motor inertia	[kg m ²]
J_p	Pump inertia	[kg m ²]
$M_{L,m}$	Motor torque losses	[Nm]
$M_{L,p}$	Pump torque losses	[Nm]
M_{Rotor}	Rotor torque	[Nm]
n_m	Motor rotation speed	[rpm]
n_{Rotor}	Rotor rotation speed	[rpm]
P_H	Kinetic power	[W]
P_{mec}	Mechanical power	[W]
P_{Rot}	Rotor power	[W]
$Q_{L,m}$	Motor leakage volume flow	[l min ⁻¹]
$Q_{L,p}$	Pump leakage volume flow	[l min ⁻¹]
$Q_{m,eff}$	Motor effective volume flow	[l min ⁻¹]
$Q_{p,eff}$	Pump effective volume flow	[l min ⁻¹]
R	Rotor radius	[m]
v_c	Current velocity	[m s ⁻¹]
V_m	Motor displacement	[cm ³]
V_p	Pump displacement	[cm ³]
α	Swash plate angle of motors	[-]
Δp	Pressure difference	[bar]
$\eta_{m,c}$	Constant displacement motor efficiency	[-]
η_{motors}	Efficiency of all motors	[-]
$\eta_{m,var}$	Variable displacement motor efficiency	[-]
η_p	Pump efficiency	[-]
η_{Rotor}	Rotor efficiency	[-]

η_{total}	Overall efficiency	[-]
λ	Tip speed ratio	[-]
ρ	Fluid density	[kg m ⁻³]
Ω	Rotor rotation speed	[rad s ⁻¹]

II Table of abbreviations

IFAS	Institute for Fluid Power Drives and Controls
HDT	Hydrostatic drivetrain
HP	High pressure
LP	Low pressure
CP	Control pressure
PRV	Pressure relief valve
PTO	Power take off unit
TSR	Tip speed ratio

1 Introduction

The aim of this project is the development and analysis of a hydrostatic drivetrain (HDT) for a marine current power system. A concept from the company AQUANTIS for such a system is shown in Figure 1-1. Two turbines capture power from the streaming water similar to a wind turbine. The slow rotation of the rotor has to be transferred to electric power.

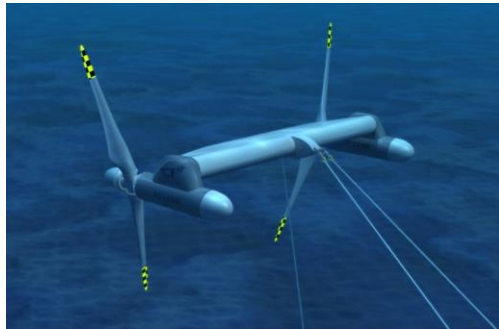


Figure 1-1: Concept of a marine current turbine

A HDT makes up the connection between the slow turning rotor shaft and the high speed shaft driving a generator. In order to do so the turbine directly drives a hydraulic pump transferring the entire power to a high pressure oil flow. Hydraulic motors convert the hydraulic power back into a mechanical rotation of a defined speed. In this case no mechanical gearbox is needed. To fulfill these tasks the required components have to be selected and the system layout has to be determined. Therefore static and dynamic simulations are used. The design methodology used in the scope of the project is illustrated in figure 1-1.

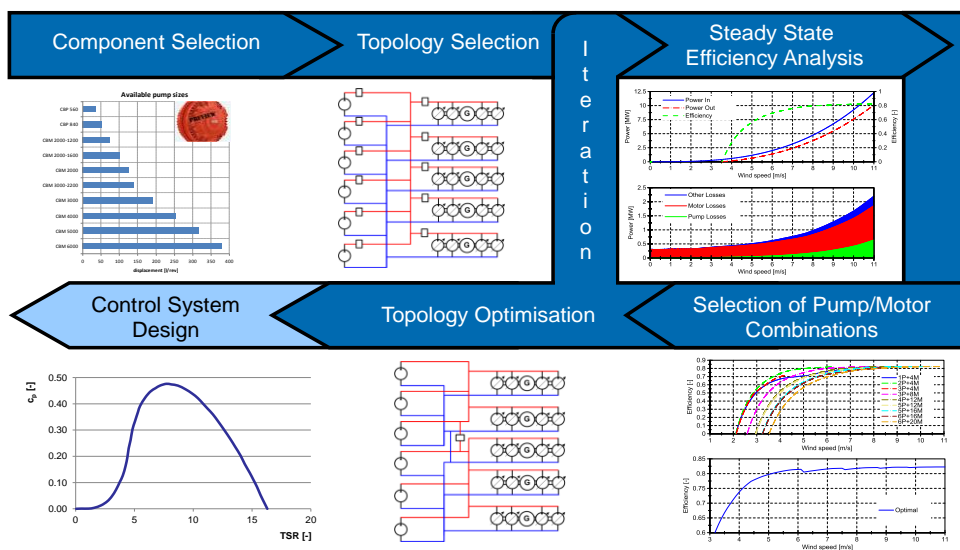


Figure 1-1: Design Methodology

To aid and evaluate each step in this process, static and dynamic system simulations were used. This final report gives an overview of the development and explains the results of the analysis. To begin with the basic theory used for the design of a hydrostatic drivetrain is explained. In a next step the generation of three different layouts is conducted. The layouts are then discussed and based on the overall efficiencies and operating parameters (e.g. high pressure during operation or potential for over speed) only one layout is selected for further investigation in a simulation environment.

The control strategy as well as strategies for start up, stop and reactions to overload scenarios for the system are presented. These strategies are tested in a simulation environment subsequently. Finally the results of the simulations are presented and discussed.

2 Generation of a drivetrain

2.1 The underwater turbine

The underwater turbine used in this project has been developed by AQUANTIS. Necessary data for the generation of different hydrostatic drivetrain layouts is shown in Table 2-1.

Rated rotor speed	12 [rpm]
Rated current velocity	1.6 [m/s]
Rated rotor mechanical power	275.1 [kW]
Optimal tip speed ratio	8
Blade radius	9.8 [m]
Fluid density	1025 [kg/m ³]
Number of blades	2
Estimated inertia of rotor	229820 [kg m ²]

Table 2-1: Parameters of the turbine model

The kinetic power of a current can be described as a product of the fluid density ρ , the cross sectional area of the flow A_0 and the current velocity v_c .

$$P_H = \frac{1}{2} \rho A_0 v_c^3 \quad \text{eq. 2-1}$$

The rotor is able to transfer only part of that energy to mechanical power, which is expressed in a power coefficient c_p .

$$c_p = \frac{P_{\text{Rot}}}{P_H} \quad \text{eq. 2-2}$$

The power coefficient c_p depends on the blades' hydrofoils and the tip speed ratio (TSR) λ which is the ratio of speed at the blade tip divided by the current speed and is given by eq. 2-3.

$$\lambda = \frac{\omega R}{v_c} \quad \text{eq. 2-3}$$

The power absorbed by the rotor is expressed by eq. 2-4.

$$P_{rot} = \frac{1}{2} c_p(\lambda) \rho A_0 v_c^3 \quad \text{eq. 2-4}$$

The power coefficient of the rotor designed by AQUANTIS is shown in Figure 2-1.

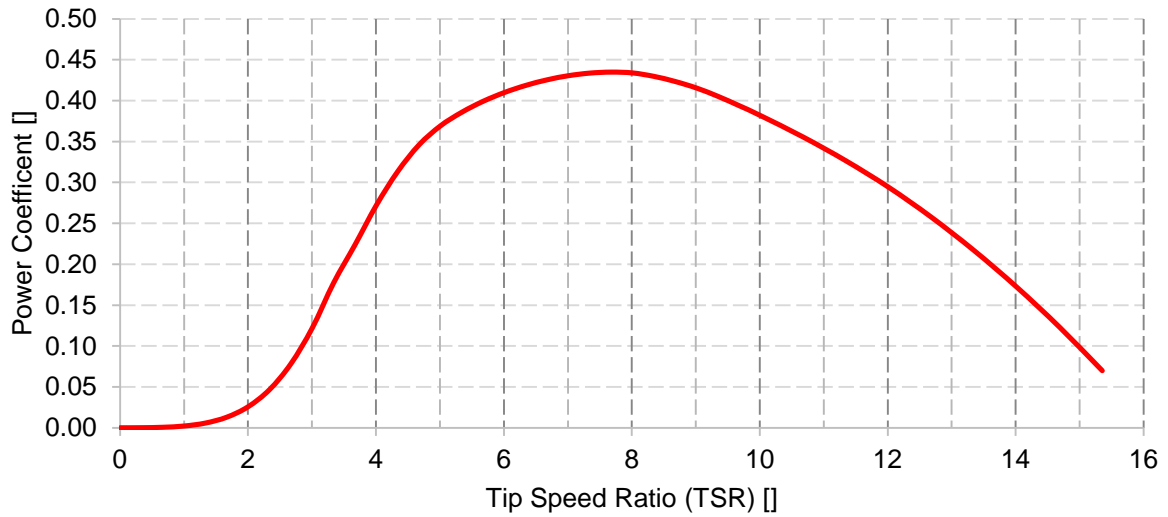


Figure 2-1: Power-coefficient c_p curves versus tip speed ratio

Similar to the power coefficient c_p a torque coefficient c_m is used to express the torque M_{Rot} that the rotor is able to generate [HAU08].

$$M_{Rot} = \frac{1}{2} c_m(\lambda) \rho A_0 R v_c^2 \quad \text{eq. 2-5}$$

The rotor torque can also be calculated by dividing the rotor power by the rotation speed. As a result the relation between the coefficients can be expressed as following.

$$c_p(\lambda) = \lambda c_m(\lambda) \quad \text{eq. 2-6}$$

The resulting torque coefficient c_m is shown in Figure 2-2.

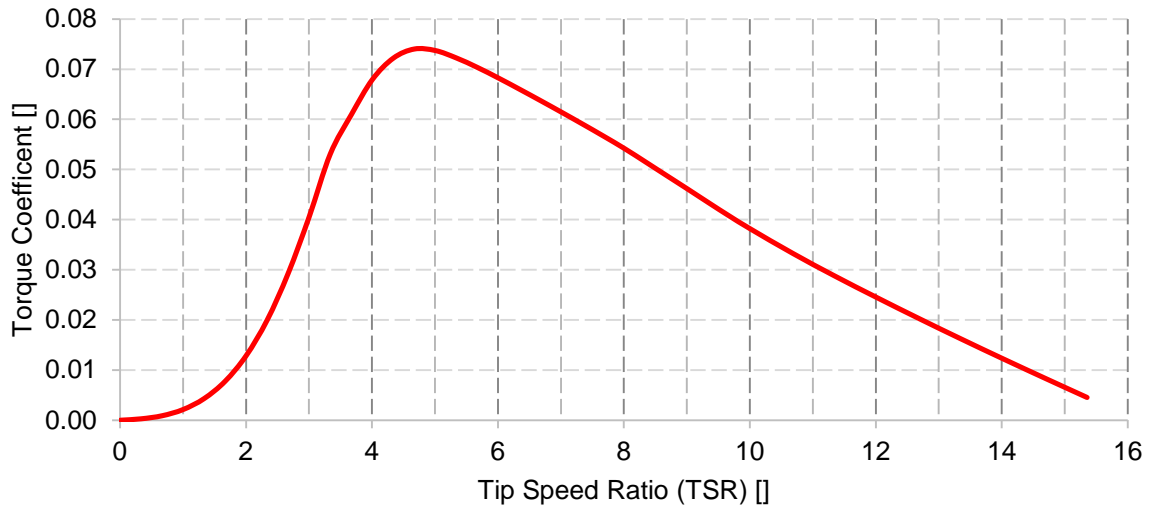


Figure 2-2: Torque-coefficient c_m curves versus tip speed ratio

As shown in Figure 2-1 each rotor is designed to absorb a maximum amount of power for a certain TSR (here $\lambda_{opt} = 8$). Assuming the rotor operates at this optimal TSR the current speed can be expressed by the rotor speed via eq. 2-3. Inserting this relation into eq. 2-5 the rotor torque $M_{Rot,opt}$ at the optimal operating points can be expressed as a function of the rotor speed:

$$M_{Rot,opt} = c_M(\lambda_{opt}) \frac{1}{2} \rho A_0 R^3 \left(\frac{2\pi}{\lambda_{opt}} n_{rot} \right)^2 \quad \text{eq. 2-7}$$

The absorbed input power at the optimal operating points $P_{rot,opt}$ can be calculated by eq. 2-8 and is depicted in Figure 2-3.

$$P_{Rot,opt} = c_p(\lambda_{opt}) \frac{1}{2} \rho A_0 R^3 \left(\frac{\lambda_{opt} 2\pi}{\lambda_{opt}} n_{rot} \right)^3 \quad \text{eq. 2-8}$$

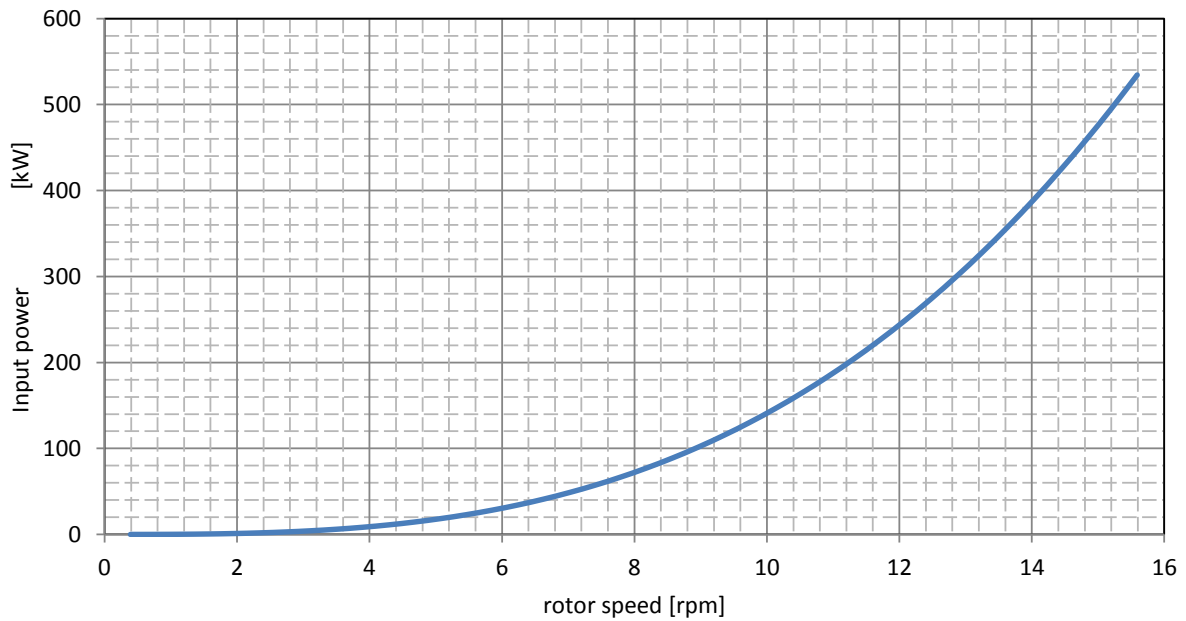


Figure 2-3: Optimal power curve of the rotor

2.2 Design of the hydrostatic drivetrain

In Figure 2-4 a sketch of the transmission system is shown. A hydrostatic transmission basically consists of a hydraulic pump connected to a hydraulic motor via a transmission line (pipe). The rotational kinetic energy of the rotor is converted to hydraulic energy by the pump and transported by the hydraulic fluid to the motor. Here, the hydraulic energy is converted back into rotational kinetic energy and then into electrical energy by the generator. In the presented layout the pump is directly mounted onto the rotor shaft.

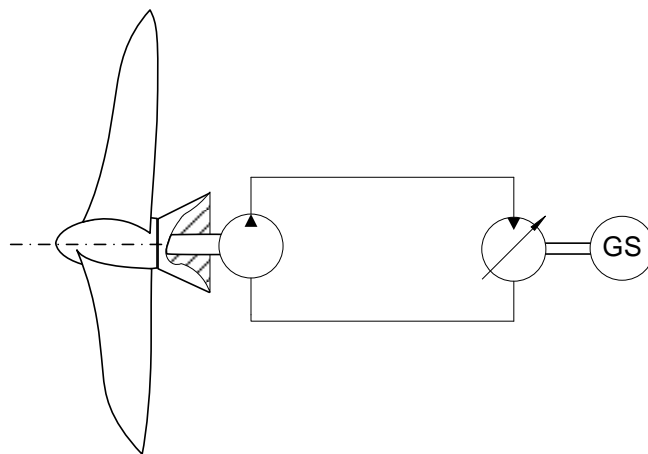


Figure 2-4: Sketch of the drivetrain under development

Using the data shown in Table 2-1 the input power provided by the turbine can be calculated for all operating points. Based on this data different hydrostatic drivetrain layouts are

developed. The overall efficiency of the system is assumed to be dependent on the variables shown in eq. 2-9 and the calculation of the efficiency is done considering only these.

$$\eta_{\text{total}} = \eta_{\text{Rotor}} \cdot \eta_p \cdot \eta_{\text{motors}} = f(V_p, V_m, v_c, n_{\text{rotor}}, n_m, \alpha, \Delta p)$$

$$\eta_{\text{motors}} = \frac{Q_{m,\text{var}}\eta_{m,\text{var}} + Q_{m,c}\eta_{m,c}}{Q_{m,\text{var}} + Q_{m,c}} \quad \text{eq. 2-9}$$

The variables are the pump displacement V_p and motor displacement V_m , current velocity v_c , rotational speed of rotor n_{rotor} and motors n_m , swash plate angles α and pressure difference Δp . Necessary periphery such as feeding pumps and control systems are not included. The power for hydraulic actuation systems i.e. valves or variable displacement motors are neglected as well. The losses at the piping between pumps, the valve block and the motors are included in the look-up table data used for modelling the mechanical and volumetric losses of the hydraulic components. Furthermore, the explicit influence of losses from additional tubing and fittings are neglected. Thus, the overall efficiency of a real drivetrain will be one to two percent lower, which is known from the hydrostatic drivetrain test bench at IFAS. The look-up tables are only available for several units of predefined sizes. In case of using other pumps and motors of a similar design it is possible to scale these look-up tables according to the ratio of the displacements [WAT09].

Limiting the possible solution space by explicitly setting variables simplifies the calculation of the overall efficiency of the HDT. Pump and motor displacements are predefined for each configuration. By calculating the torque equilibrium on the rotor shaft (eq. 2-10) the pressure can be calculated.

$$M_{\text{Rotor}}(v_c, n_{\text{Rotor}}) - \sum_i M_{L,p,i}(\Delta p, n_{\text{Rotor}}) = \frac{\Delta p \sum_i V_{p,i}}{2\pi} \quad \text{eq. 2-10}$$

By equating the flow leaving the pumps with the flow required by the motors at a constant motor speed (eq. 2-11) the calculation of the overall efficiency of the HDT here depends on the current velocity and the rotational rotor speed as shown in eq. 2-12.

$$\begin{aligned}
 n_{\text{Rotor}} \sum_i V_{p,i} - \sum_i Q_{L,p,i}(\Delta p, n_{\text{Rotor}}) \\
 = n_m \sum_j V_{m,j}(\alpha) + \sum_j Q_{L,m,j}(\Delta p, \alpha)
 \end{aligned}
 \tag{eq. 2-11}$$

$$\eta_{\text{total}} = f(v_c, n_{\text{Rotor}})
 \tag{eq. 2-12}$$

The three different drivetrain layouts shown in Figure 2-5 are derived and discussed in the following. All three configurations use the same pump configuration. On the motor side various combinations of fixed and variable displacement units are analysed. Configuration 1 and 2 use the same total displacement, whereas the ability to vary the displacement is changed. In Configuration 3 the displacement of the smaller motor is increased. This leads to a higher maximally transferable power of this drivetrain. However, the system should be designed for a certain maximum input power and the drivetrains should be compared, in regard to how each of them transfers the same amounts of energy. So for configuration 3 the swivel angle is limited to make the installed displacement on the motor side equal for all three configurations.

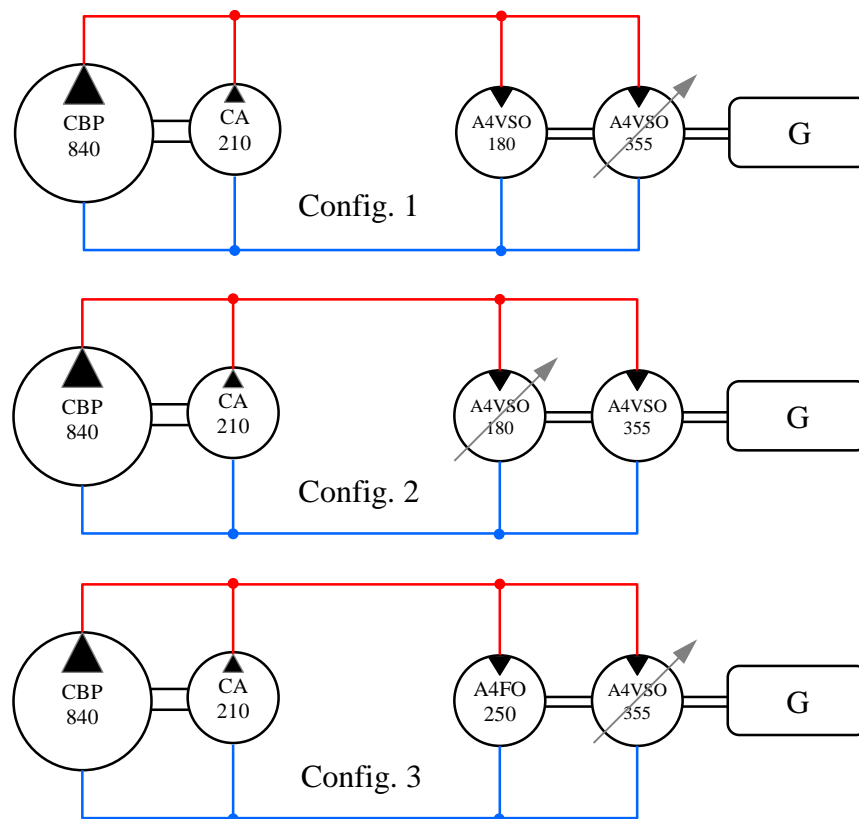


Figure 2-5: Main configurations of the HDT

The calculated overall efficiencies are presented in Figure 2-6. As operating point for each current the optimal rotor speed defined by the optimal TSR (TSR = 8) is chosen.

Losses in the variable motors are higher compared to constant units. So Configuration 2 achieves the highest overall efficiency due to the smallest variable displacement. Accordingly Configuration 3 shows the lowest estimates of the overall efficiency due to the higher variable displacement.

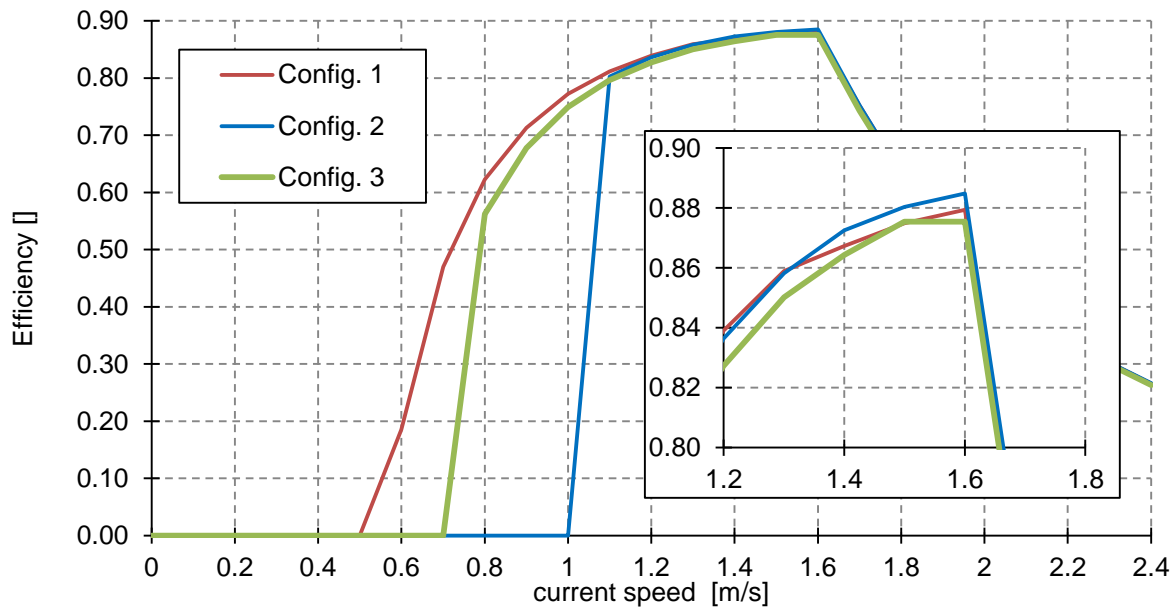


Figure 2-6: Efficiency curves of the drivetrains at optimal points of operation

The system pressure is defined by the installed displacement on the pump side and shown in Figure 2-7 for all configurations.

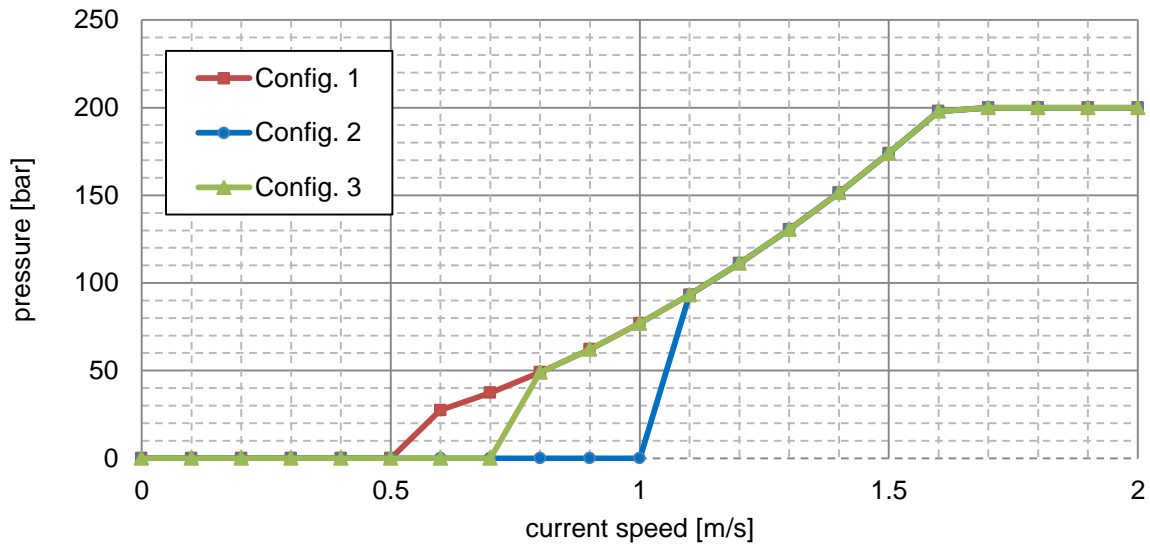


Figure 2-7: Pressure curves of the drivetrains at optimal points of operation

The optimal operating points for all three configurations are depicted in Figure 2-8. Due to the smallest constant displacement Configuration 1 shows the lowest cut-in-speed about $v_c = 0.5 \text{ m/s}$ whereas configuration 3 utilises the highest constant displacement that leads to a cut-in-speed of $v_c = 1 \text{ m/s}$.

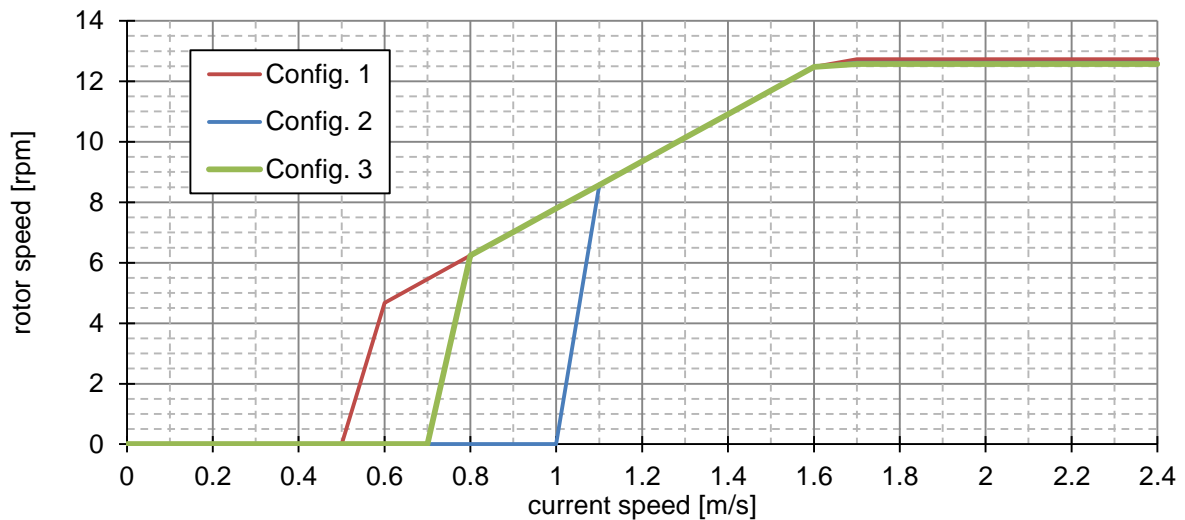


Figure 2-8: Points of operation for three configurations

The resulting power curves are depicted in Figure 2-9. Due to the smallest variable motor and the resulting losses Configuration 2 shows the highest output power at the operating point with the maximum rotor speed and system pressure.

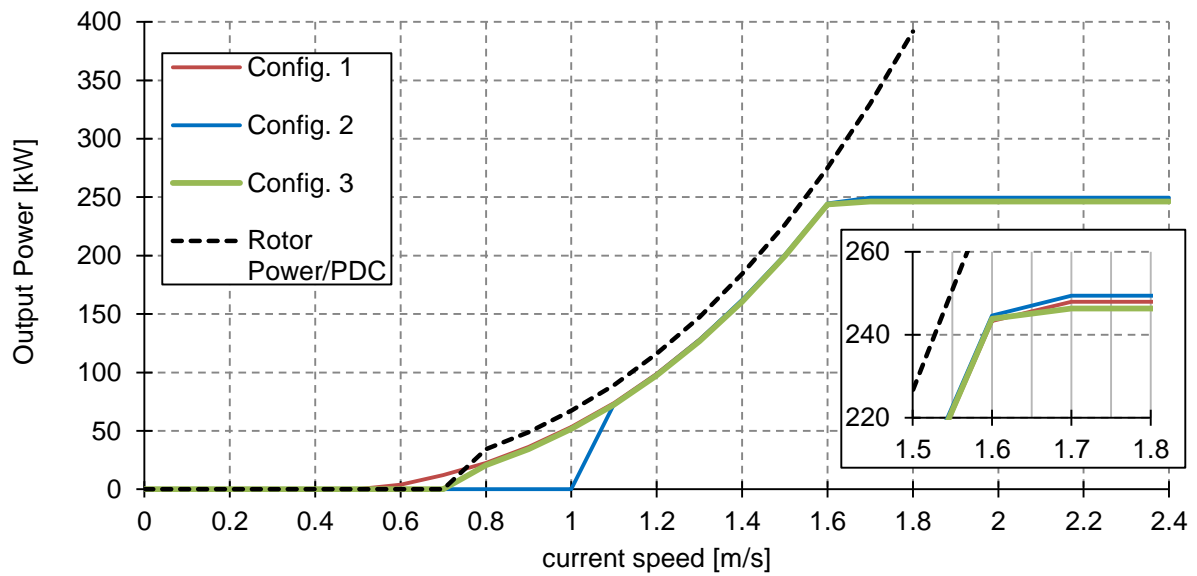


Figure 2-9: Power curves of the drivetrains at optimal points of operation

At this point it is not possible to compare the configurations because the drivetrains operate at different operating points. To estimate the expected output power per year, a frequency distribution of the current velocity at a specified location is used. This distribution is provided by AQUANTIS and shown in Figure 2-10.

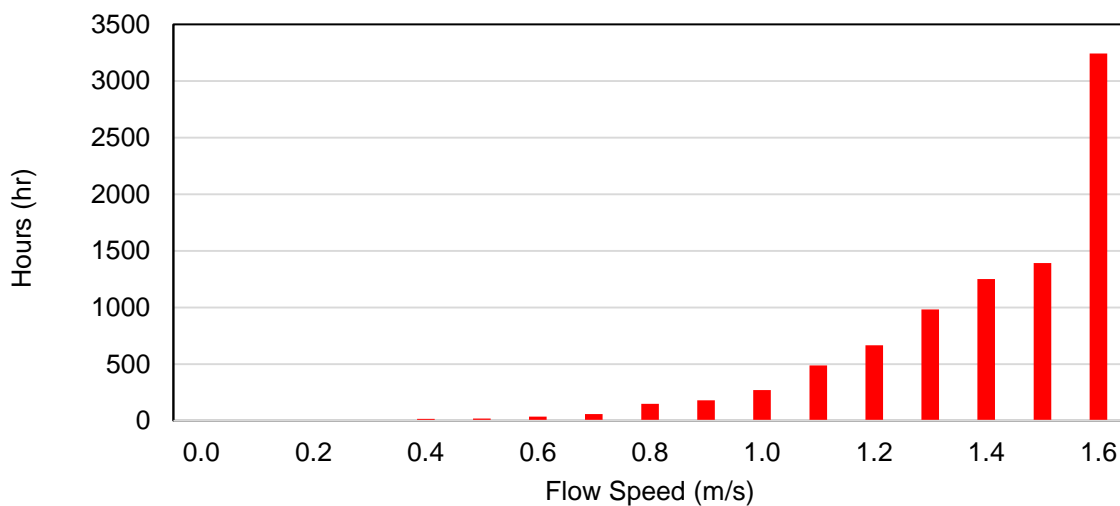


Figure 2-10: Relative frequency of current velocity provided by AQUANTIS

For each current speed the corresponding output power and frequency of the current speed are multiplied. In doing so the output power for these operation points is weighted. The different drivetrain layouts can now be compared. The weighted power outputs are depicted in Figure 2-11.

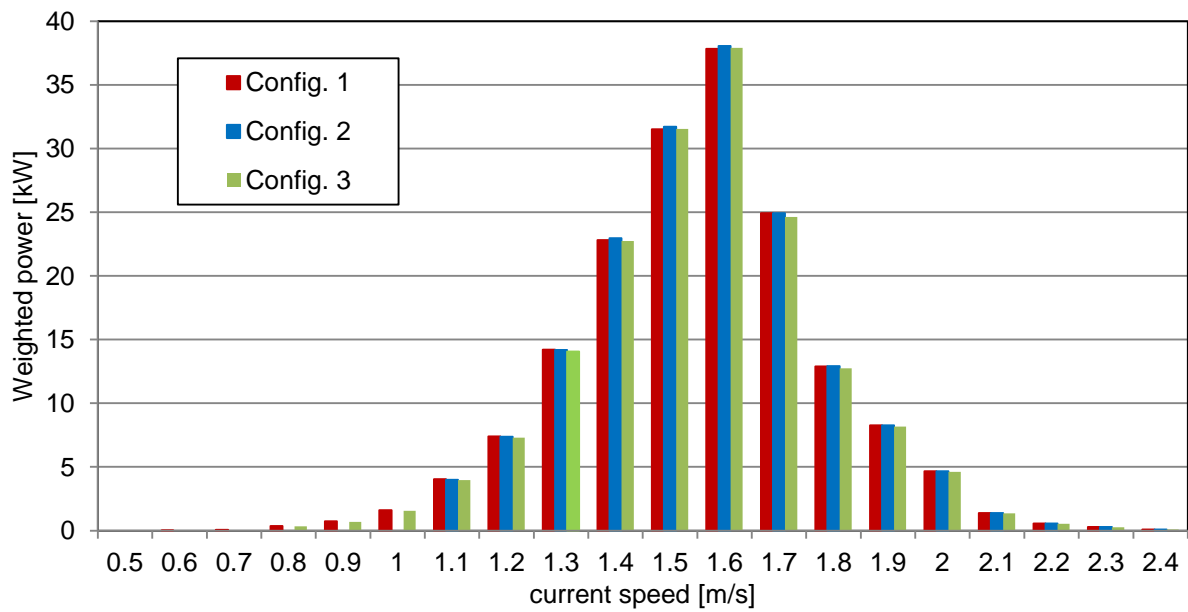


Figure 2-11: Comparison of weighted power for three drivetrain layouts

Finally for each configuration the weighted power values are summed up (shown in Figure 2-12) to get the expected power output per year. At the rated operating point the power output of all three configurations is only slightly different. For lower current speeds configuration 1 shows a considerably higher efficiency (see Figure 2-6), that leads to the highest estimated power output. Due to the highest variable displacement configuration 2 achieves the lowest estimate.

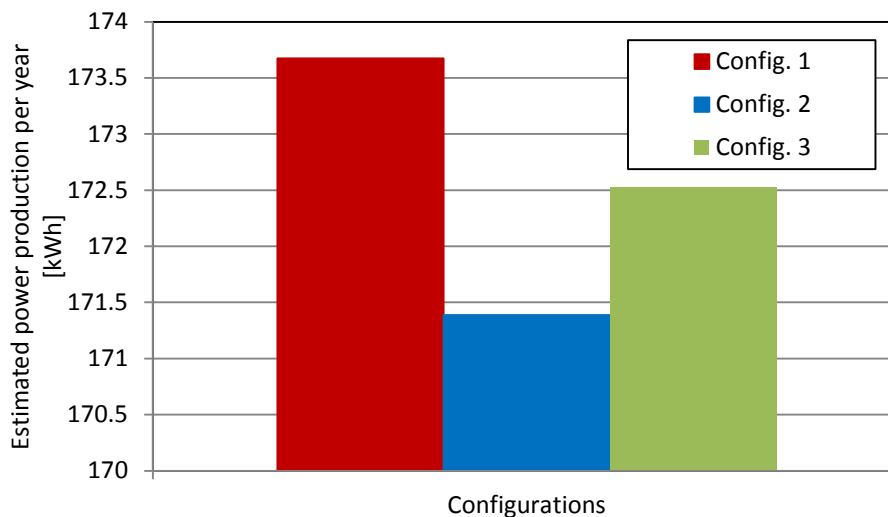


Figure 2-12: Comparison of estimated power for three drivetrain layouts

The differences in the estimates of the power outputs are comparatively low (maximum is 1 % between configuration 1 & 2), so more aspects are included to make a decision for a certain configuration. The drivetrain of configuration 1 reaches its maximum rotor speed at the rated operating point. Due the higher total displacement configuration 3 shows a wider range of possible operating points in the area around the rated operating point to handle overloads. Configuration 1 utilises a constant motor with a displacement of 180 ccm. Such a displacement is not available within the A4FO constant motor series of REXROTH. To implement such a displacement a variable displacement motor of the pricier A4VSO series must be used. A constant motor with a displacement of 250 ccm is available within the A4FO series. Considering costs and the ability to handle overloads configuration 3 is chosen to be further developed within this project.

3 Control Strategy

To absorb the maximum amount of energy available in the current it is necessary to control the rotor speed depending on the current flow speed. A speed controller would register the current flow speed, determine the optimal rotor speed and then regulate the rotor shaft using the hydraulic motors to ensure a constant TSR.

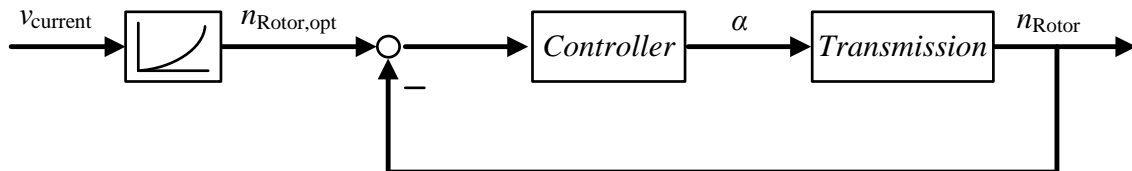


Figure 3-1: Speed Controller

3.1 TSR-controller with knowledge of current speed

Measuring the current speed and using this measured value as a control input to adjust the hydraulic motors poses two problems. First of all, measuring current speed is not a straightforward task. Due to the large area spanned by the blades, the current speed within this area varies in magnitude and direction. A single current speed sensor mounted on top of the nacelle can hardly detect all these effects and can at most deliver approximate values /Sch12/.

3.2 TSR-controller without knowledge of current speed

Another method to ensure operation at the required tip speed ratio, without knowledge of the current speed, is to indirectly control the turbine speed by using a torque/pressure controller, Figure 3-2. The rotor speed is measured and the optimal torque, determined using the relation in eq. 2-7, is sent to the controller.

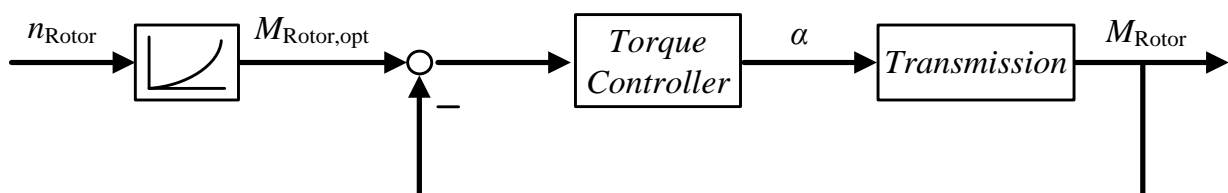


Figure 3-2: Torque Controller

At first look, the control scheme shown above does not indicate how such a strategy can ensure operation at the optimal TSR. To understand how this works, it is necessary to look at the forces acting on the rotor shaft, Figure 3-3. If the hydrodynamic torque is greater than the brake torque the rotor will accelerate, vice versa the rotor will decelerate. Only when both quantities are of the same magnitude can equilibrium be reached and a constant rotor speed is established.

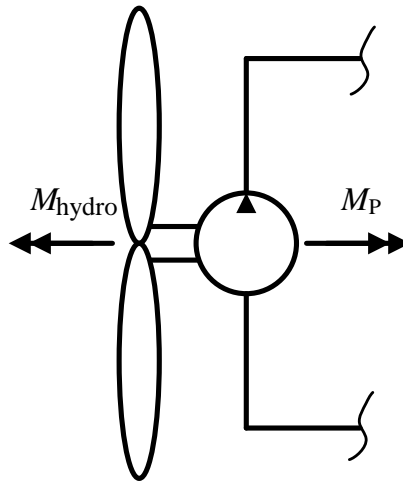


Figure 3-3: Forces acting on rotor shaft

Figure 3-4 shows the hydrodynamic torque acting on the rotor (black) and the optimal torque (blue) used by the controller above. If the controller is designed appropriately, the brake torque generated by the transmission will follow the optimal torque line. At a constant current speed, the curve describing the hydrodynamic torque is bell-shaped and intersects the optimal rotor torque curve at one point.

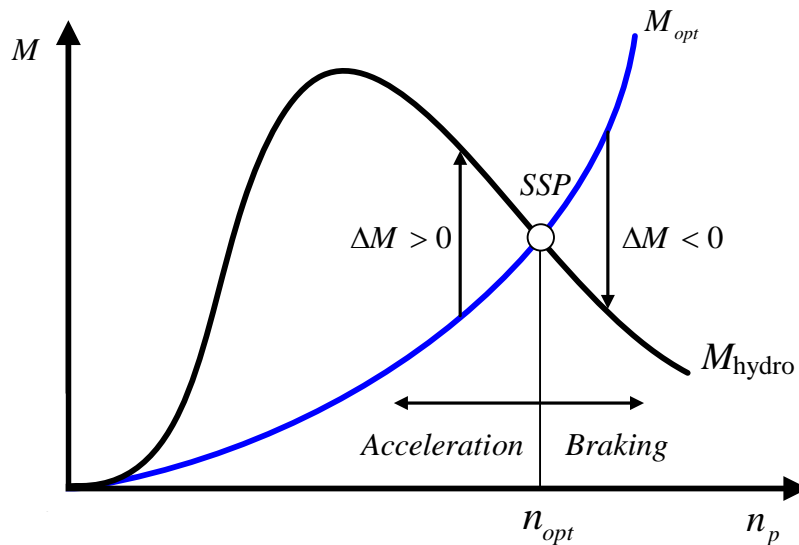


Figure 3-4: Torque control strategy

Left of the intersection point the rotor will tend to accelerate and right of the intersection point it will decelerate. The control system will drive the rotor to the intersection point, which also corresponds to the optimal rotor speed for the current flow speed. Figure 3-5 shows the situation when the current speed increases. The new current speed follows a slightly different bell shaped curve. The previous steady state point $SSP1$ is now in a region of acceleration because the aerodynamic torque is greater than the brake torque produced by the transmission. The rotor accelerates and moves to the new equilibrium condition $SSP2$. Therefore, it is clear that such a control strategy will ensure operation at the optimal TSR. The distinct advantage of this method is that it requires no knowledge of the current flow speed.

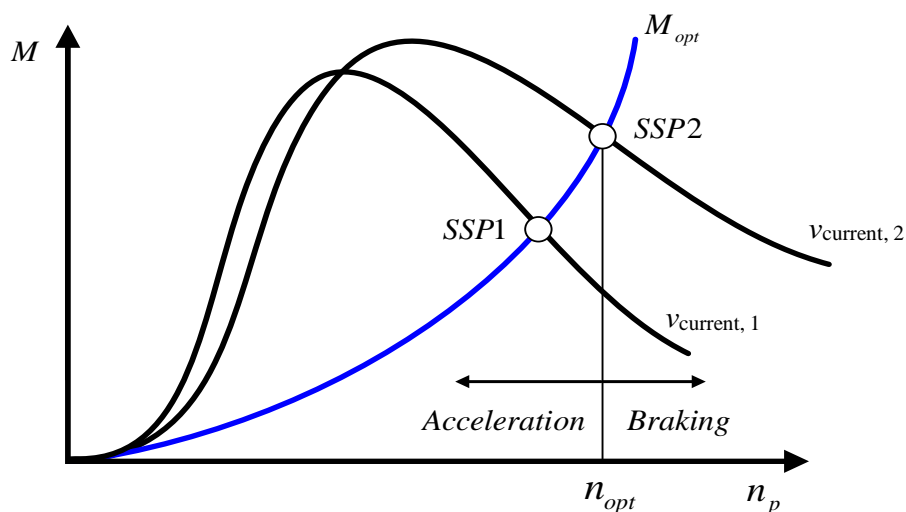


Figure 3-5: New equilibrium point with change in current speed

3.3 Limitations of input power without knowledge of current speed

The control strategy shown in section 3.2 stabilizes the turbine for each current speed at the optimal rotor speed, where the rotor absorbs the maximum amount of power. As the optimal tip speed ratio remains constant the optimal rotor speed increases proportional with the current and likewise the rotor input power increases. The resulting input power depending on the optimal rotor speeds is plotted in Figure 2-3.

The allowable input power of the drivetrain is limited to a certain level depending on the components e.g. the pumps, motors and generator. Therefore, a strategy to reduce the input power is needed to operate the turbine in overload scenarios. Most common systems use a pitch system to limit the input power, which is a method to react to overloads quickly by changing the blades' angle of attack. However, the proposed rotor design does not consider a pitch system. Instead a "passive depth control" is considered. If the current speed increases above the rated current speed and likewise the input power, the turbine dives deeper into the water due to the increasing hydrodynamic forces. The turbine stops diving, when it reaches a lower sea level, where the current speed equals the rated current speed. This method of limiting the input power might react slowly to overload scenarios and a second more dynamic power control strategy may be needed.

As the hydrostatic drivetrain is capable of operating at variable rotor speeds the input power can be limited by shifting the operating point into regions of lower input power. For a given current speed this means slowing down the rotor. But as the rotor speed for the maximum power is not the same as the rotor speed for the maximum rotor torque, slowing down the rotor at first leads to an increase in input torque. This leads to a higher system pressure compared to the desired level during normal operation. This issue can be seen in Figure 3-6, where the rotor torque is shown for different current speeds. The maximum input power is assumed to be 275 kW and limited by the capacity of the generator and the electric hardware. The red line marks this limit, below which the input power is less than 275 kW. The optimal points of operation, where the rotor maximizes the input power, are marked by the green line. Under normal conditions the turbine is operated along this line ('Desired Control Curve') by the proposed torque/pressure control, which means that for a given rotor speed the corresponding optimal braking torque is applied to the rotor shaft. Above the intersection of the green and red lines this control strategy would lead to operating points with an input power higher than the chosen limit of 275 kW. Therefore, the control strategy is changed and the turbine is operated along the red line controlling the input

power. At the same time the ‘passive depth control’ should start working and the turbine should start diving deeper into sea, which leads to a decrease in the current speed. While the system dives the turbine is operated along the red line moving the operating point back towards the intersection. When a sea depth, where the rated current speed is applied to the rotor, is reached the turbine stops diving, the input power is below the power limit and the control strategy switches back to the torque/pressure control along the green line.

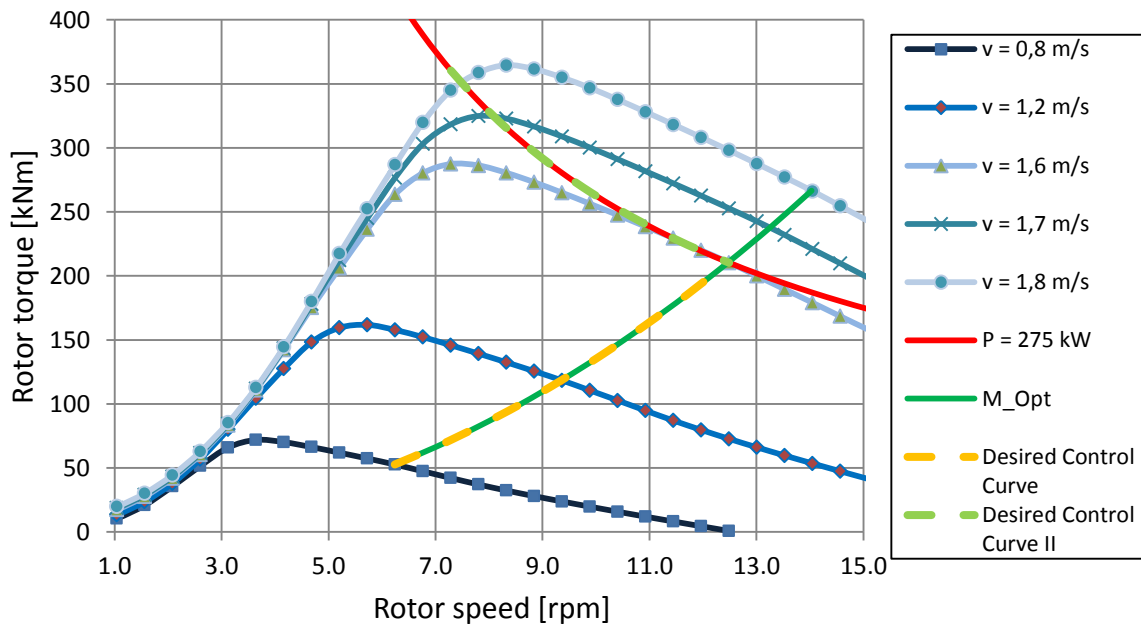


Figure 3-6: Limiting the input power by shifting operating points

3.4 Start up procedures for the turbine

For low rotational speeds the torque coefficient of the rotor (see Figure 2-2) becomes very small or near zero. Consequently for a whole spectrum of low rotational speeds (resulting in a small TSR) the input torque remains too small to overcome the mechanical losses in the drivetrain e.g. rotor seal friction or mechanical losses in the pumps and motors. To overcome this issue the rotor needs to be sped up into regions of higher rotational speed (likewise regions of higher TSR) leading to higher torque coefficients and resulting in higher rotor torques. Once this region of small rotor speeds is passed, the generated input torque is sufficient to speed up the rotor itself. Therefore a mechanism is needed that applies the necessary start up torque to overcome the losses during the initial start up phase until the rotor speeds up itself.

For the start up of the system two procedures are proposed, one using the grid and the generator side for speeding up the rotor and another procedure using an electrically driven boost pump for the initial acceleration of the rotor.

3.4.1 Start up of the turbine using the grid

At the beginning of the start up procedure the rotor is locked via a mechanical brake (see Figure 3-7). A boost pump sets the pressure on the low pressure side to the level needed for operation (nearly 10 bar).

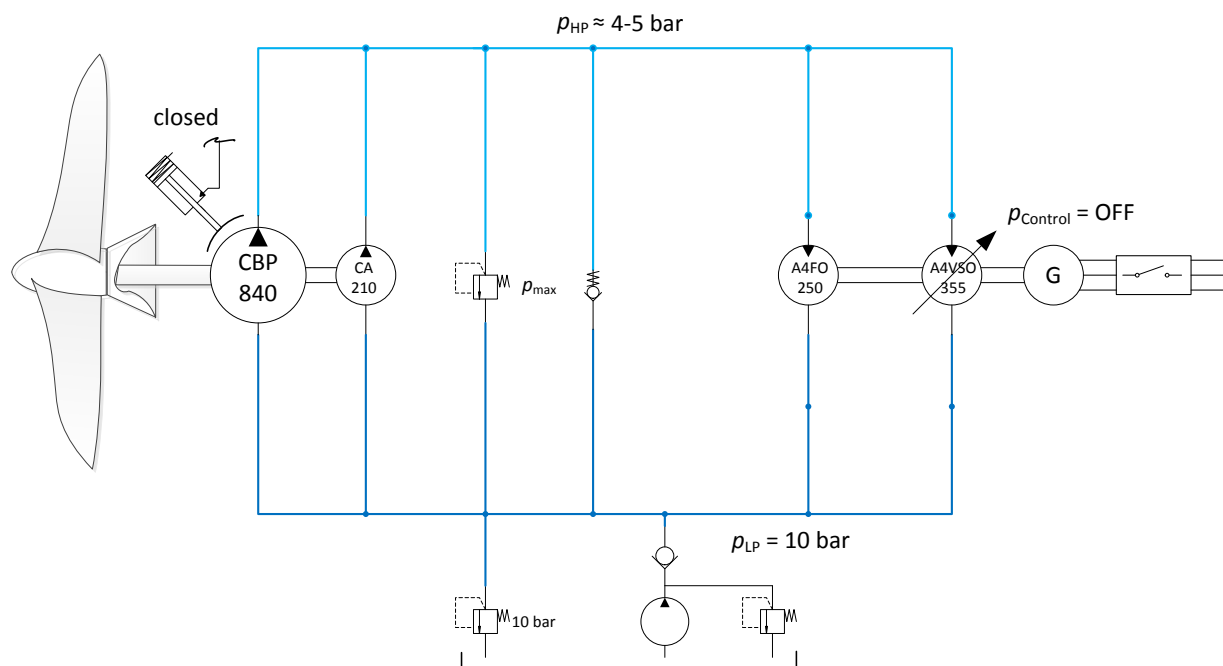


Figure 3-7: Start up of the turbine using the grid – Step one

Next the generator is sped up using the electrical grid (see Figure 3-8 for current operating condition of the drivetrain). At the same time the motors directly mounted on the generator shaft start to operate, whereby the swivel angle of the variable motor is set to zero resulting in a flow of this unit close to zero. Hence only the flow of the constant motor needs to be replaced at the high pressure side. After the mechanical brake has been unlocked the rotor speed is still very slow and the flow generated by the pumps also very small. As the constant displacement unit is operating at the rated speed and transferring flow from the high pressure side to the low pressure side, this flow needs to be replaced, which is done by the check valve (see left diagram in Figure 3-9).

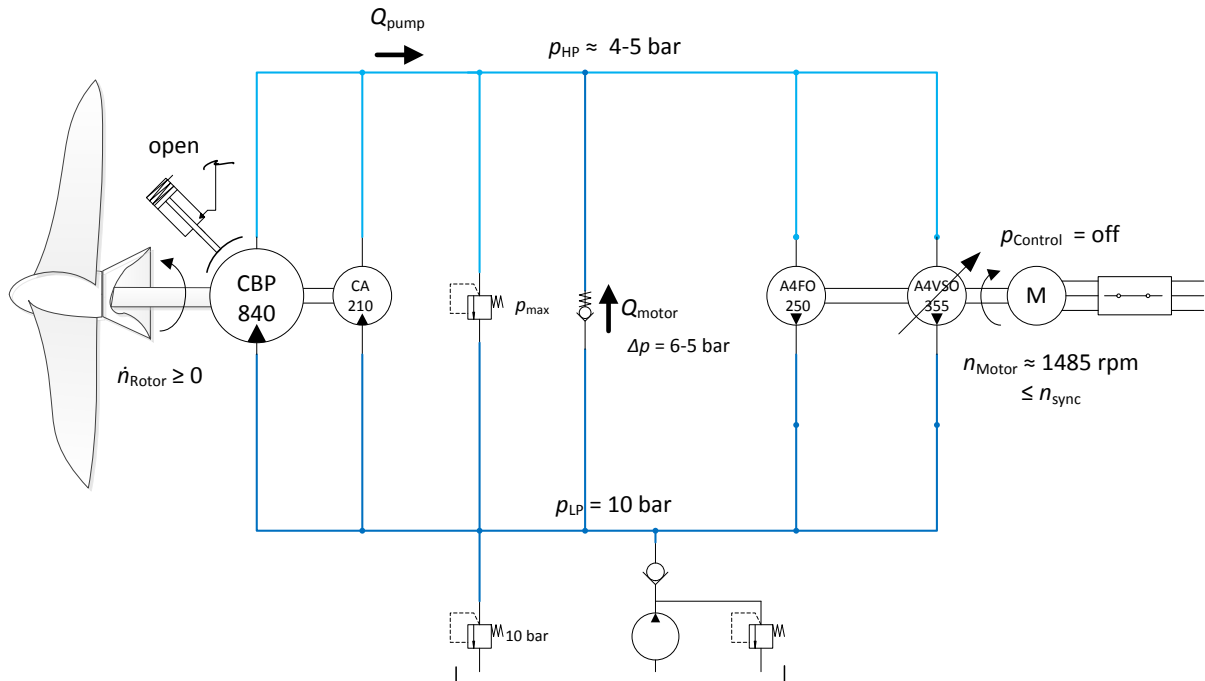


Figure 3-8: Start up of the turbine using the grid – Step two

To speed up the rotor an initial start up torque must be applied to the pumps. To generate this torque a pressure difference is required. Considering the rotational direction of the rotor and the resulting direction for the initial start up torque, the pressure at the high pressure side has to be lower compared to that at the low pressure side. Whereas both sides of the circuit are named after the conditions under normal operation, during the start up phase these conditions change. In fact, the high pressure side becomes the low pressure side and vice versa. The pumps connected to the rotor operate as motors and the constant displacement motor on the generator side operates as a pump.

The characteristic curve of the check valve is chosen to have a steep slope and an offset as shown in Figure 3-9 to the right. Only if the pressure difference is above 5 bar does a flow pass the check valve. While the check valve is active the pressure difference between both sides is not less than 5 bar. At the beginning of the start up phase the flow generated by the pumps is small and the flow taken from the motors has to be replaced primarily by a high flow rate passing the check valve leading to a pressure difference close to 6 bar (see Figure 3-9). As the rotor speeds up the flow passing the check valve becomes smaller.

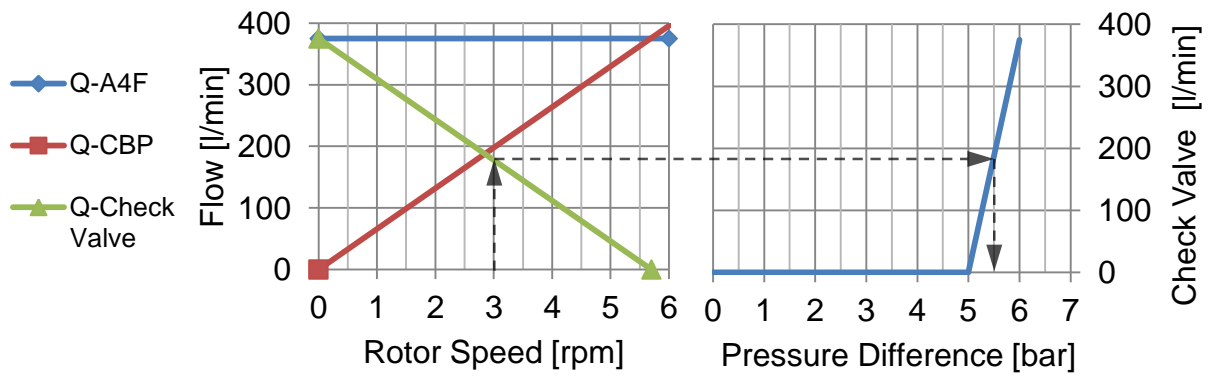


Figure 3-9: Flow rates during start up by strategy one

When the rotor speed is approximately to 5.7 rpm the flow from the pumps equals the flow of the constant displacement motor, no additional flow is needed and the check valve closes. At this point the pressure at the high pressure side rises above the pressure at the low pressure side (see Figure 3-10 for the current operating conditions of the drivetrain). The pressure controller is activated and turbine is operated with the control strategies proposed in 3.2 and 3.3. The magnitude of the initial torque applied to the rotor by the pumps and consequently the pressure on the low pressure side depends on the magnitude of the seal friction that has to be overcome during the start-up. Further results of the simulations for this start up procedure can be found in section 5.1.1.

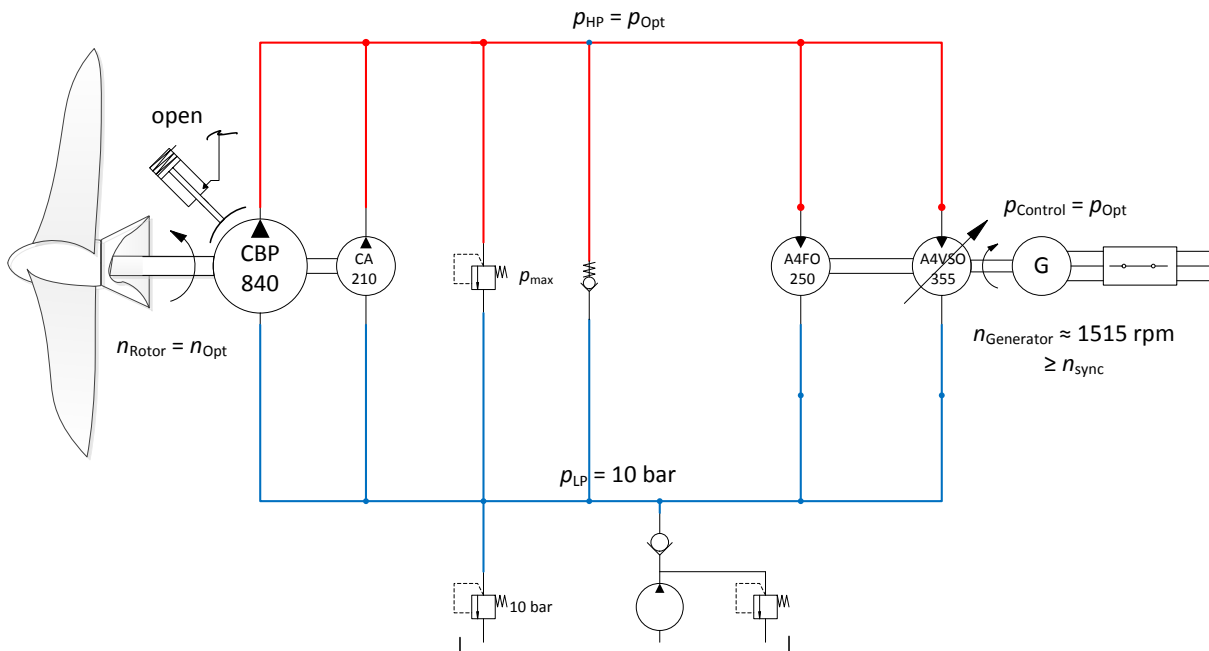


Figure 3-10: Start up of the turbine using the grid – Step three

3.4.2 Start up of the turbine without using the grid (respectively the generator)

At the beginning of the start up procedure the rotor is locked by a mechanical brake (see Figure 3-11). A boost pump sets the pressure at the low pressure side to the level needed during operation. Here the level is chosen to be 14 bar. The higher the chosen low pressure level is the faster the rotor will speed up. At the beginning of the start up procedure the pressure level on the high pressure side is close to zero. Due to the pressure difference between both sides, the motors mounted to the generator shaft would start rotating opposite to the desired rotational direction. As long as the generator is not connected to the grid no load can be applied on the generator side and the generator shaft acts as flywheel. To avoid this problem, the rotational speed of the generator shaft is kept at 0 rpm by applying a negative swivel angle to the variable displacement motor. In doing so the torques generated by the motors are opposite and compensate each other. As a result the generator shaft is unable to rotate and no flow is transferred by the motors except leakage.

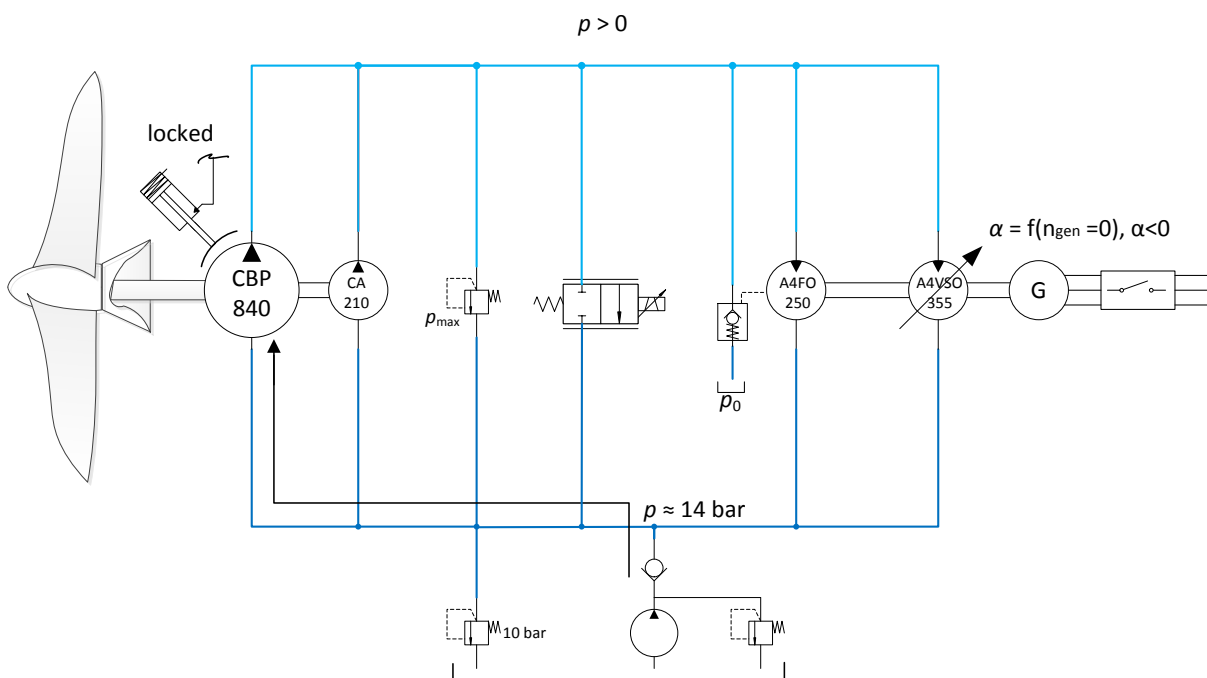


Figure 3-11: Start up of the turbine using the boost pump – Step one

In the next step the mechanical brake is unlocked. To speed up the rotor an initial torque and consequently a pressure difference between both sides is needed. Therefore the flow transferred into the high pressure line by the pumps needs to be removed. For this purpose a switchable check valve is used connecting the high pressure side directly to the reservoir. The operation curve of this check valve is chosen to generate a minimum pressure differ-

ence between the high pressure and the reservoir of 5 bar. The oil flow during the initial start up phase is shown in Figure 3-12.

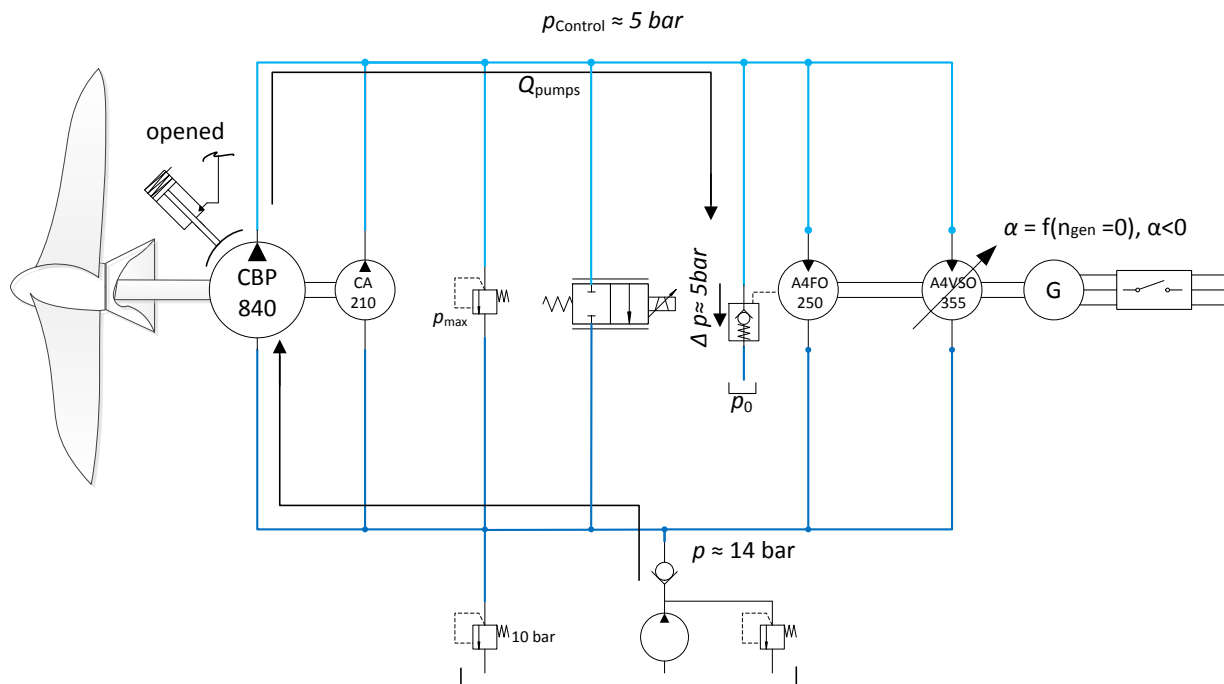


Figure 3-12: Start up of the turbine using the boost pump – Step two

After the rotor has reached a rotational speed of about 2 rpm it is able to speed up itself. At this speed the rotor torque increases at a very high rate compared to the increase of the rotor speed (see Figure 3.6). If no braking torque is applied here, nearly 2 sec are enough to reach the maximum rotational speed of the system, which is constrained by the operation curve of the check valve. The rotor speeds up until a state of equilibrium for flow and pressure is reached on the high pressure side. The equilibrium depends on the operation curve of the check valve and the current speed acting onto the rotor. As the flow characteristic of the check valve cannot be changed here, only one equilibrium state can be chosen in advance and only for one current speed will the equilibrium state be known. For all other conditions the equilibrium state and the behaviour of the rotor remains uncertain, which is not optimal for safe operation. To overcome this obstacle a servo valve is used connecting the high and low pressure side as shown in Figure 3-13. This way the high pressure can be controlled, a braking torque is applied to the rotor and finally the rotor can be controlled during start up. The position of the servo valve is set by the pressure control algorithm (see 3.2), which is used to control the turbine during normal operation. This way the rotor is sped up until the operating point for the present current speed is reached. Simultaneously the rotor is moved over the torque peak to the side, where it is easier to control.

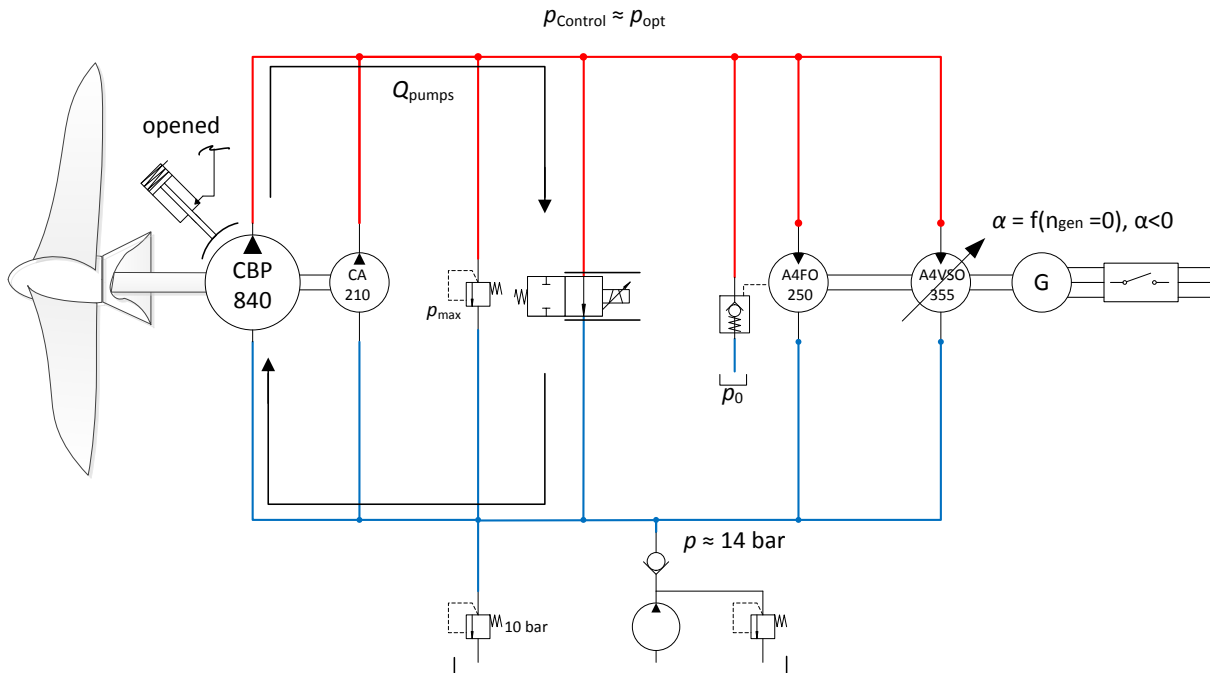


Figure 3-13: Start up of the turbine using the boost pump – Step three

The flow and pressure equilibrium on the high pressure side are shown in Figure 3-14 for a current speed of 1.6 m/s. When the pressure desired by the control equals the high pressure the equilibrium state is reached and the rotor speed is controlled with the pressure controller using the servo valve. At this point the torque loaded onto the motors is used to speed up the generator shaft. To avoid an overshoot of the generator shaft's rotational speed, the acceleration of the shaft is controlled. As shown in Figure 3-15 during this phase the flow generated by the pumps passes the servo valve and the motors as well.

The exemplary flow rates shown in Figure 3-14 shall give an overview, where oil flows occur in the system during the start up procedure (here at 1.6 m/s). Whereas the servo valve is activated always at a rotor speed of two rpm and the check valve closed due to the pressure set by the servo valve, the rotor speed, where the motors are activated, depends on the equilibrium between rotor torque and brake torque applied by the controller. So this rotational speed differs with the current speed (see blue area in Figure 3-14 for feasible rotor speeds). After the generator shaft has reached its rated rotational speed, the servo valve is closed slowly. During this procedure oil is transferred by both the motors and the servo valve.

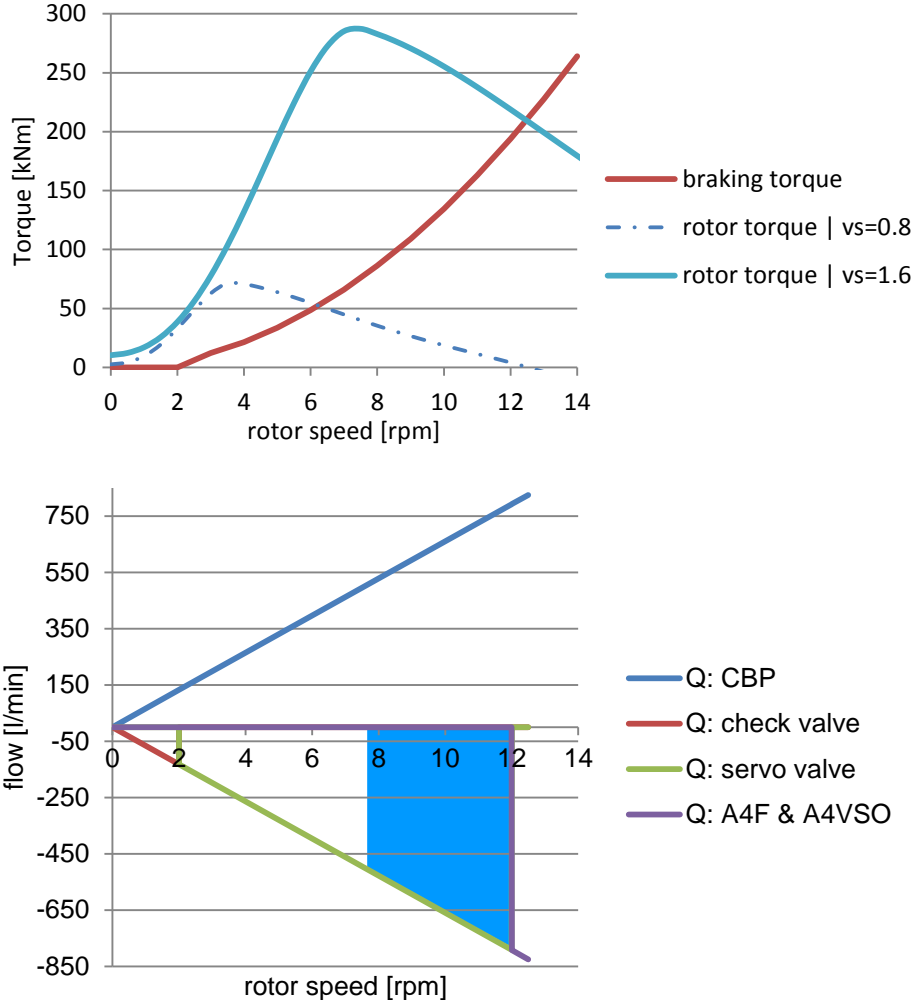


Figure 3-14: Torques and flow rates during start up strategy two

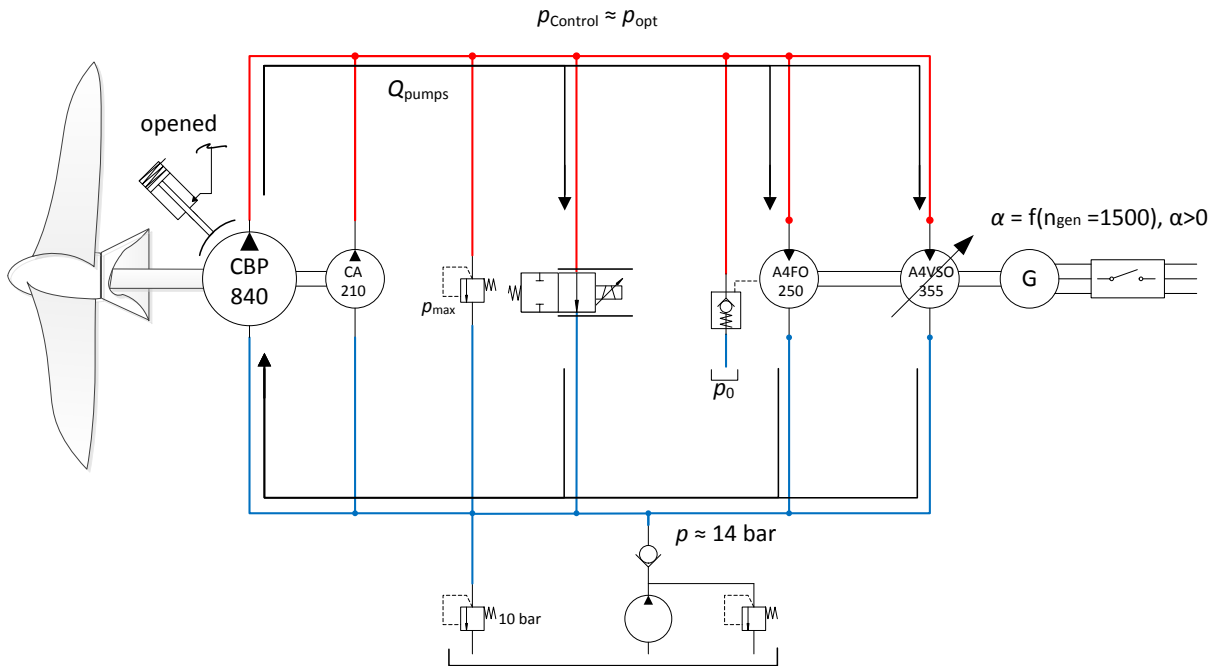


Figure 3-15: Start up of the turbine using the boost pump – Step four

When the rated generator speed is reached, the generator is connected to the grid and the servo valve is closed slowly to avoid pressure peaks. As the flow passing the servo valve decreases the flow through the motors increases and consequently the power transferred to the generator.

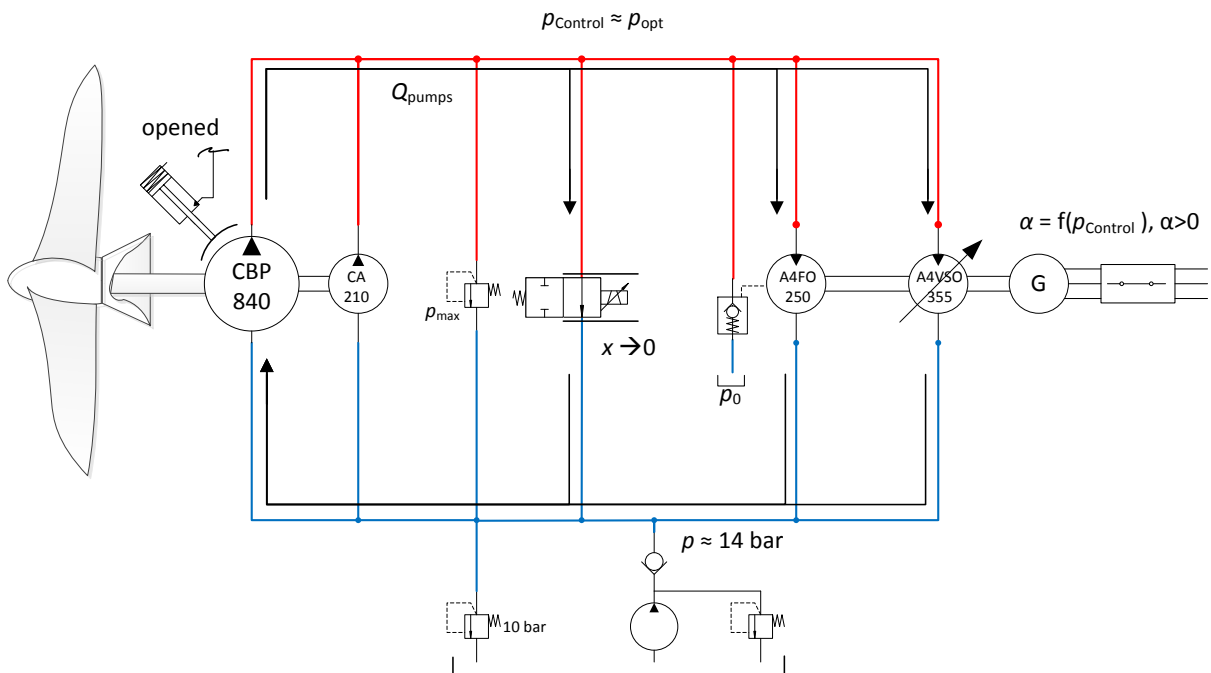


Figure 3-16: Start up of the turbine using the boost pump – Step five

After the servo valve has closed the drivetrain has reached the normal operating conditions depicted in Figure 3-17.

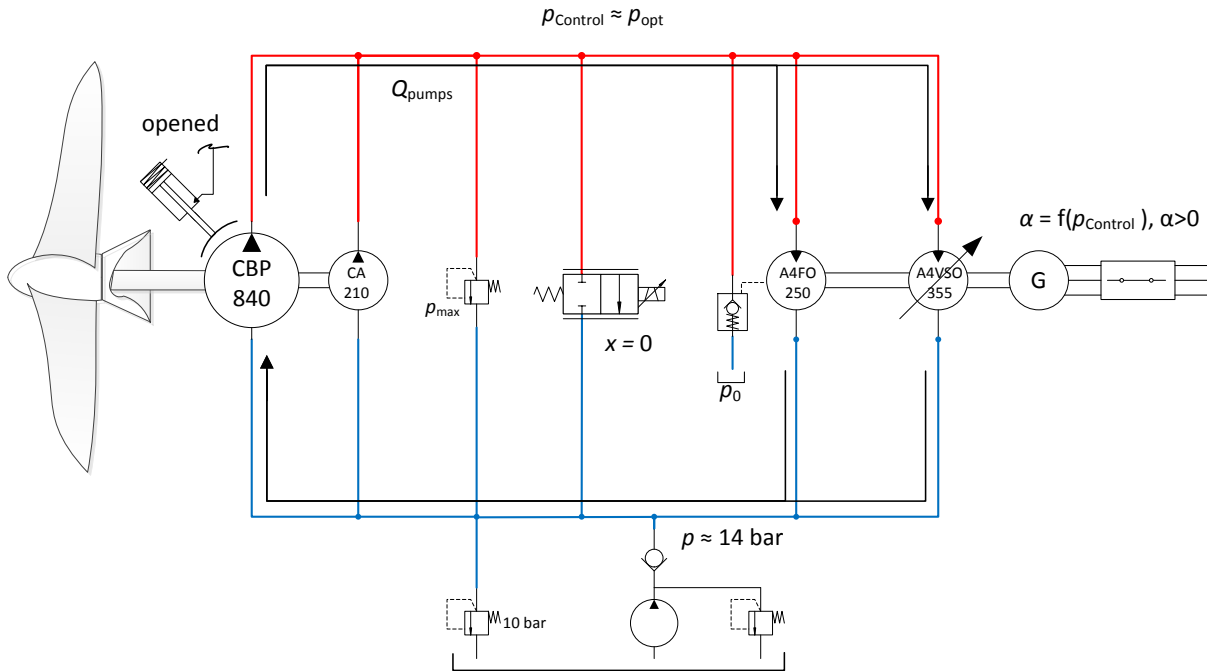


Figure 3-17: Start up of the turbine using the boost pump – Step six

In this strategy the brake torque is generated by the servo valve during start up. During the operation of this valve a large amount of the input power is converted into thermal energy. For this reason the heat build-up of the system should be approximated. The mean system temperature of the system can be calculated by eq. 3-1 [MUR12].

$$P(t)dt = Cd\theta + (\theta - \theta_0)Bdt \quad \text{eq. 3-1}$$

It is assumed that a heat transfer is possible only at the heat exchanger. So the heat transfer at the pumps, motors or the piping is neglected. The constant C is given by the product of the oil density ($\rho_{oil} = 870 \text{ kg/m}^3$), the total oil volume ($V_{oil} = 180 \text{ l}$) and the oil's specific heat capacity ($c_{oil} = 1885 \text{ J/K}$). The outside temperature θ_0 is assumed to be 15°C and a desired system temperature of 50°C . The heat exchanger is approximated to transfer 50 kW at a temperature difference of 35 K and B is approximated to be $50 \text{ kW}/35 \text{ K}$.

Results of the conducted simulations can be found in section 5.1.2.

3.5 Stop procedures for the turbine

For the stop procedure of the turbine two strategies are proposed, that use the hydrostatic drivetrain to slow down the turbine and finally a mechanical brake to lock the rotor. The first strategy uses the pressure controller to generate the hydraulic braking torque whereas the second strategy uses the main pressure relief valve on the high pressure side.

3.5.1 Stop of the turbine using pressure control

The initial conditions of the drivetrain at the beginning of the stop procedure are shown in Figure 3-18. The turbine is operated by the pressure controller along the desired control curve applying the optimal braking torque to the rotor (see 3.2 for the control strategy).

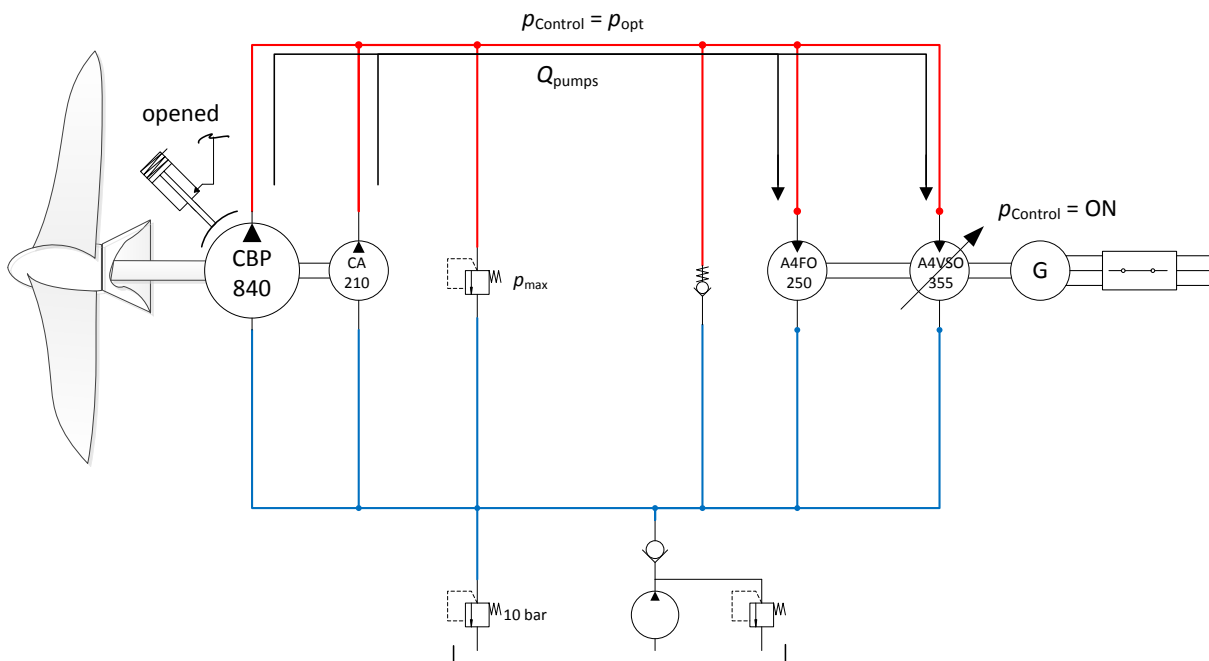


Figure 3-18: Stop procedure using the pressure controller – Step one

If the stop procedure is initiated, the pressure controller keeps the high pressure at a constant level p_{stop} , which is high enough to move the turbine over the torque peak shown in Figure 3.6. At the beginning of the procedure the variable displacement unit on the generator side operates as motor (see Figure 3-19).

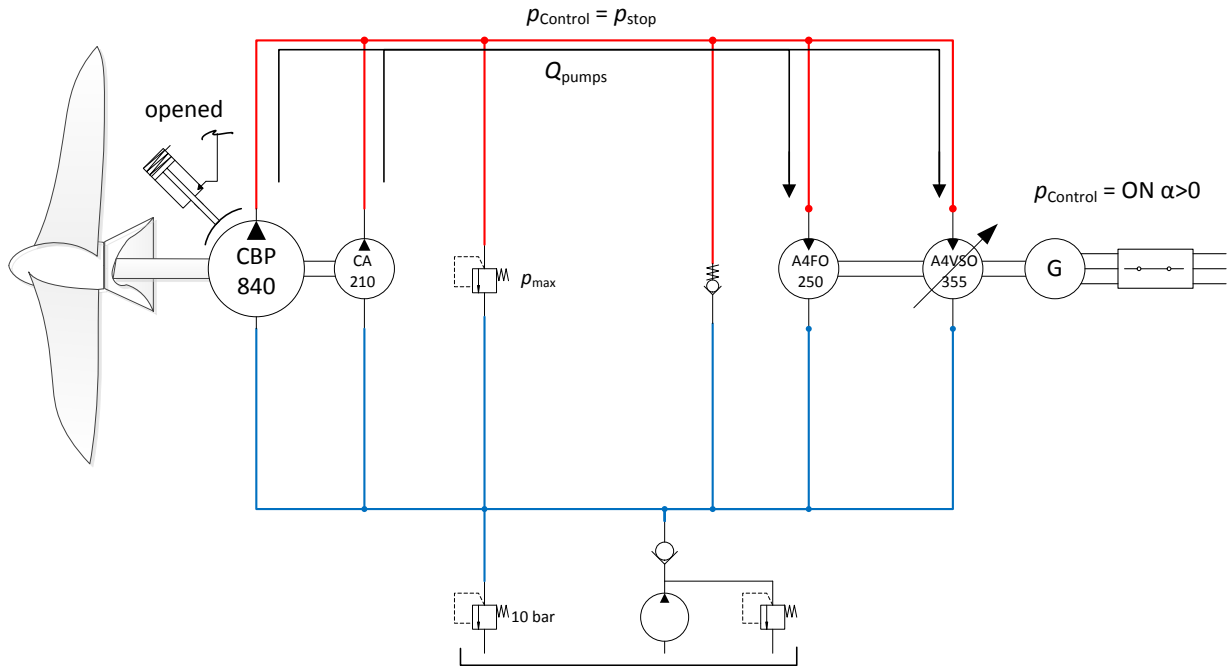


Figure 3-19: Stop procedure using the pressure controller – Step two

The flow generated by the pumps decreases, while the rotor slows down. At a certain rotational speed, the flow of the pumps is smaller than the flow required by the constant displacement unit. At this point the variable displacement unit starts to operate as pump as shown in Figure 3-20. It also transfers oil to the high pressure side to keep the pressure at a constant level.

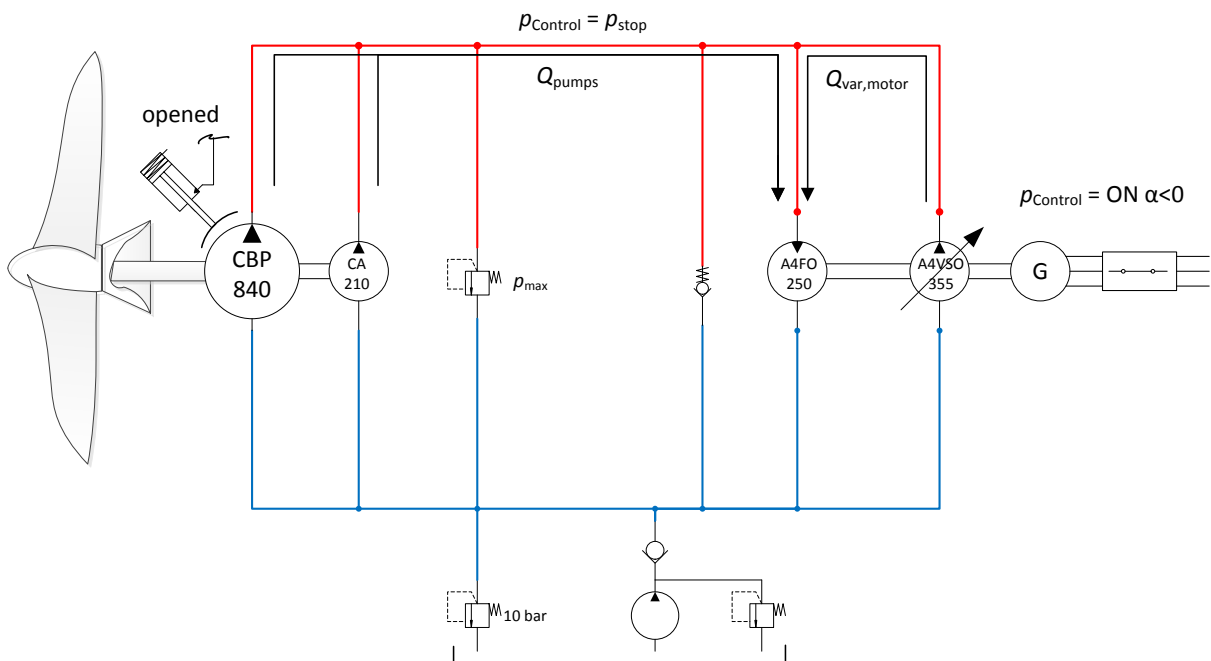


Figure 3-20: Stop procedure using the pressure controller – Step three

For small rotor speeds the rotor torque decreases quadratically (see Figure 3.6 on the left side of the torque peaks) and the initially applied braking torque is considerably higher. To avoid an abrupt stop of the rotor the control strategy is switched to a speed control, which drives the rotor smoothly to a stop. Finally the mechanical brake is locked and the generator gets disconnected from the grid. The generator shaft keeps on turning for a while due to the inertia of the mounted components. Until the shaft has stopped the flow needed for the constant displacement motor is supplied by the variable displacement unit or the check valve.

Simulations results can be found in section 5.4.1.

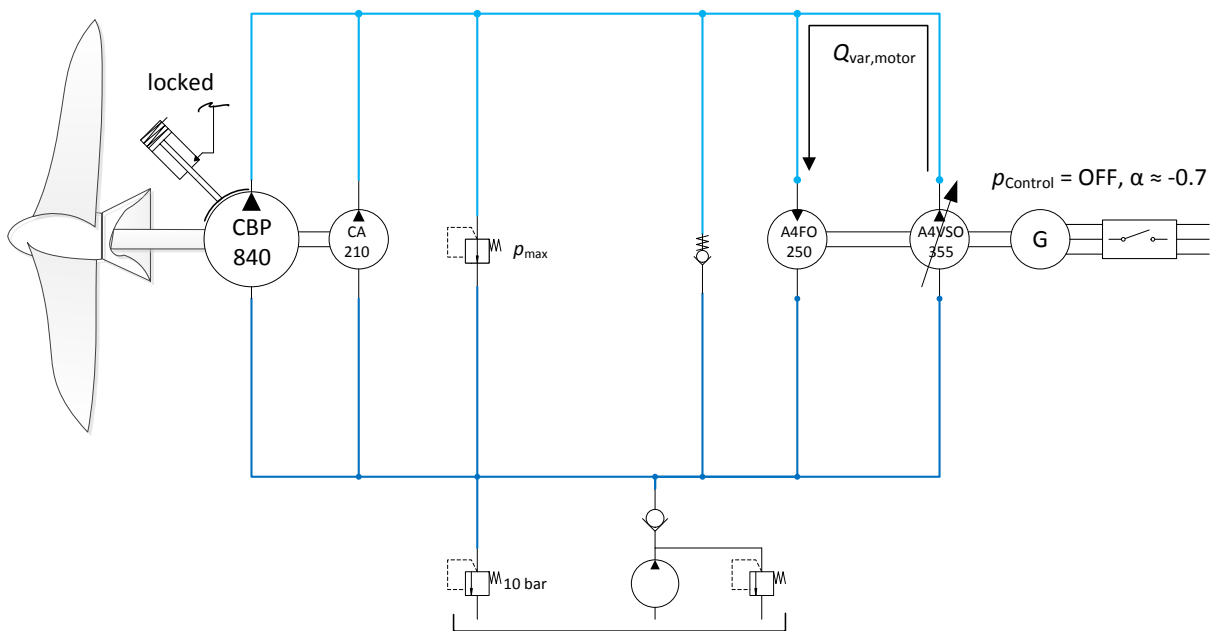


Figure 3-21: Stop procedure using the pressure controller – Step four

3.5.2 Stop of the turbine using the main pressure relief valve (emergency stop)

The first stop procedure uses the pressure controller to stop the turbine. So this strategy is applicable if the control system and the whole drivetrain are able to operate. In an emergency situation this might not be the case. Therefore, a second procedure is presented to stop the turbine without the control system or the generator side using only the pressure relief valve on the high pressure side. The initial conditions before the stop procedure are depicted in Figure 3-22.

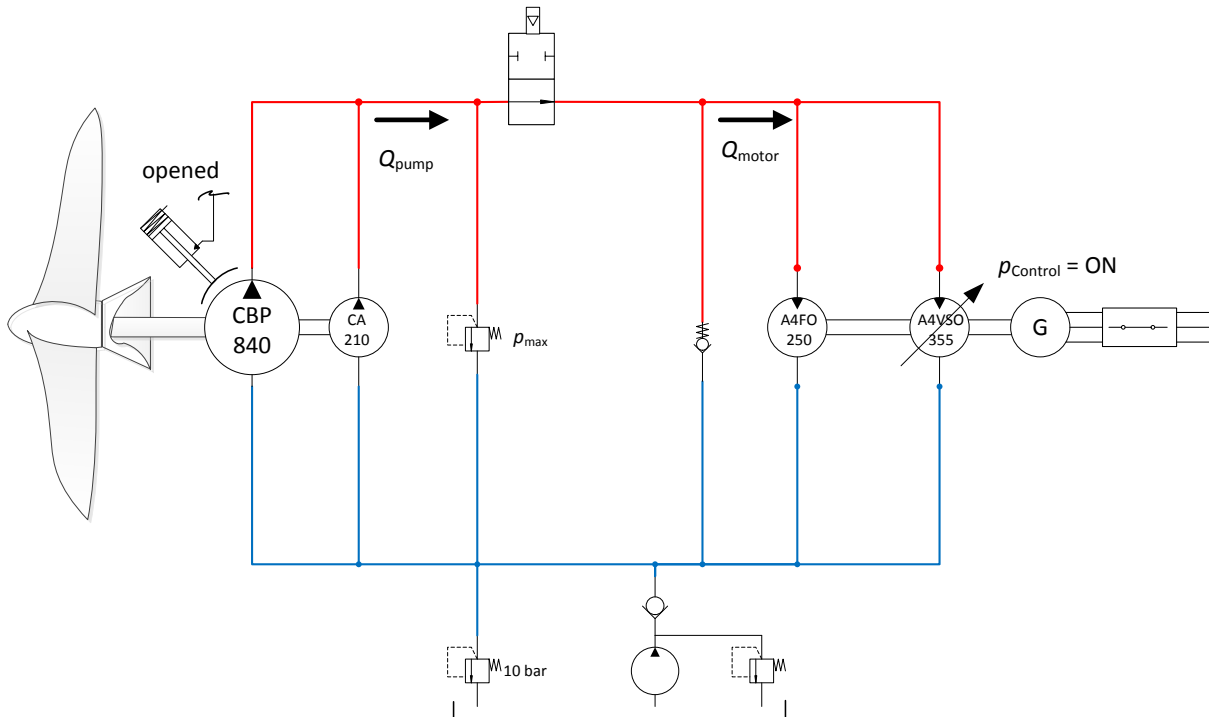


Figure 3-22 :Stop procedure using the PRV – Step one

When the stop procedure is initiated, the valve on the high pressure line is closed decoupling the pump and motor side. As shown in Figure 3-23 the flow of the pumps has to pass the main pressure relief valve setting the pressure to p_{max} , which has to be high enough to move the rotor over the torque peak for any possible current speed. The generator is disconnected from the grid and the displacement of the variable motor is set to zero. On this side of the circuit only the flow of the constant unit needs to be replaced until the generator shaft has stopped. This is done by the check valve, which has been chosen to maintain a pressure difference of at least 5 bar (see 3.4.1). Consequently the pressure on the high pressure side will be at least 5 bar lower compared to the low pressure side resulting in a braking torque loaded onto the generator shaft by the constant displacement motor.

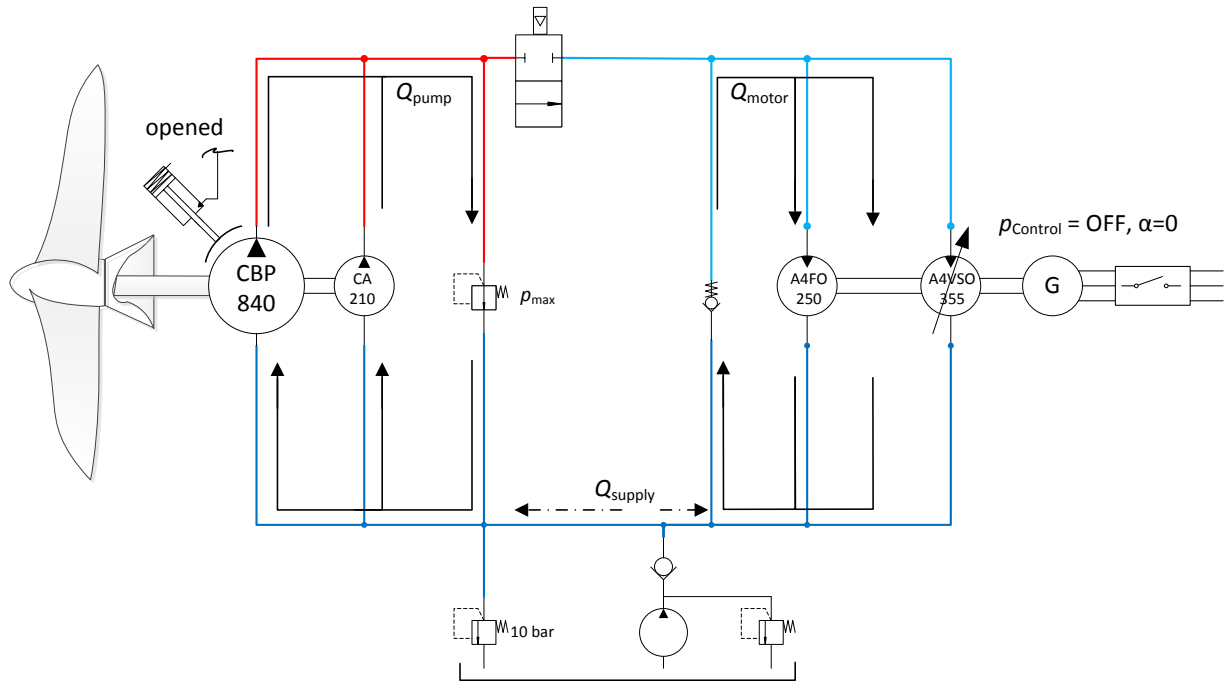


Figure 3-23: Stop procedure using the PRV – Step two

Finally the rotor gets locked by the mechanical brake as depicted in Figure 3-24 and a flow on the generator side keeps on circulating until the generator shaft stops. Further simulation results can be found in section 5.4.2.

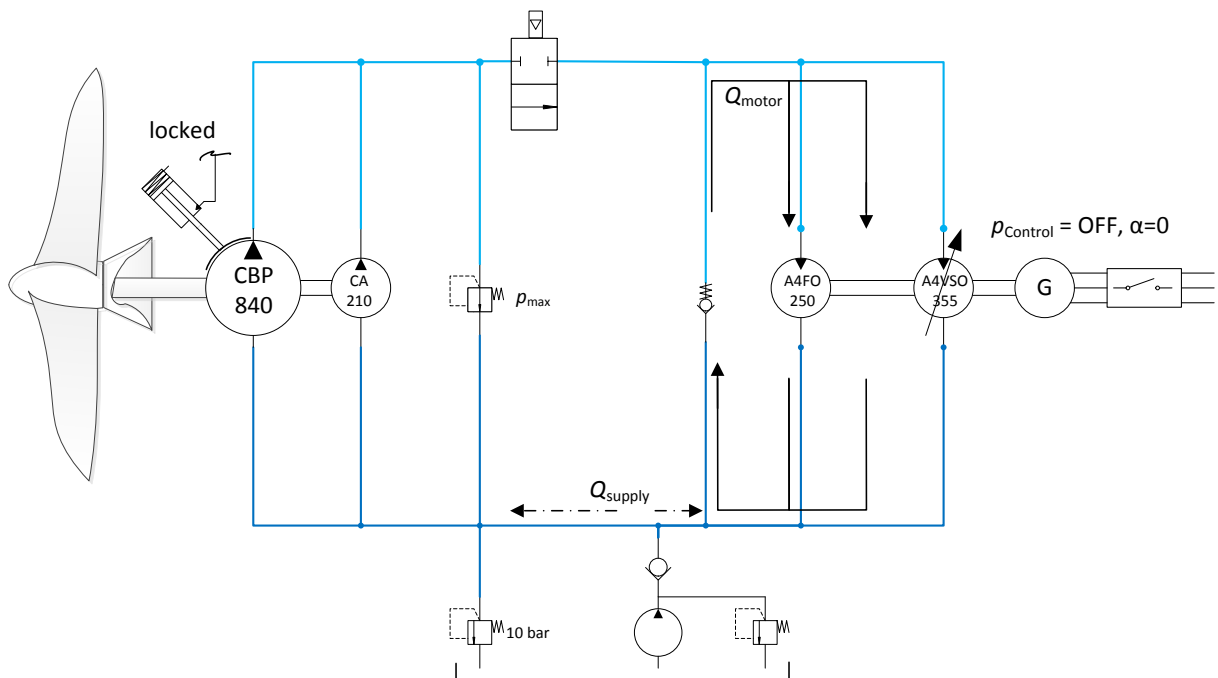


Figure 3-24: Stop procedure using the PRV – Step three

3.5.3 Overview of the different control algorithms

The following section provides an overview of the different control algorithms (Figure 3-25), operation modes and when they are applied during operation. The initial state for the system is called “Standby”. The system is not operating, the mechanical brake is locked and the generator is turned off. When the system’s start-up is initiated (“Start-up” mode), one of the presented start-up strategies (section 3.4.1 and section 3.4.2) is performed. During start-up a control algorithm speeds up the rotor and generator. When the high pressure finally equals the optimal pressure, the control algorithm switches to a “pressure controller” (see section 3.2) and the turbine is operated under normal conditions (“Normal operation”). If the power at the generator shaft rises above 250 kW (regarded as an overload scenario here), the control algorithm switches to a “power controller” (see section 3.3) to limit the input power at the rotor (“Overload Operation” mode). Since the current speed is not measured, it cannot be detected, when the current speed has slowed down and the overload scenario ends. This issue is solved by comparing the pressures which are set by power controller and pressure controller. If the values are the same, the overload situation must have ended and the turbine can be operated under normal conditions again by the pressure controller (“Normal Operation” mode). The stop procedure of the turbine can be initiated regardless of the present operating point. To stop the turbine two procedures have been presented (see 3.5.1 and 3.5.2), which slow down the rotor and disconnect the generator from the grid. When the rotor speed is close to zero rpm the mechanical brake is locked and the system returns to the “Standby-mode”.

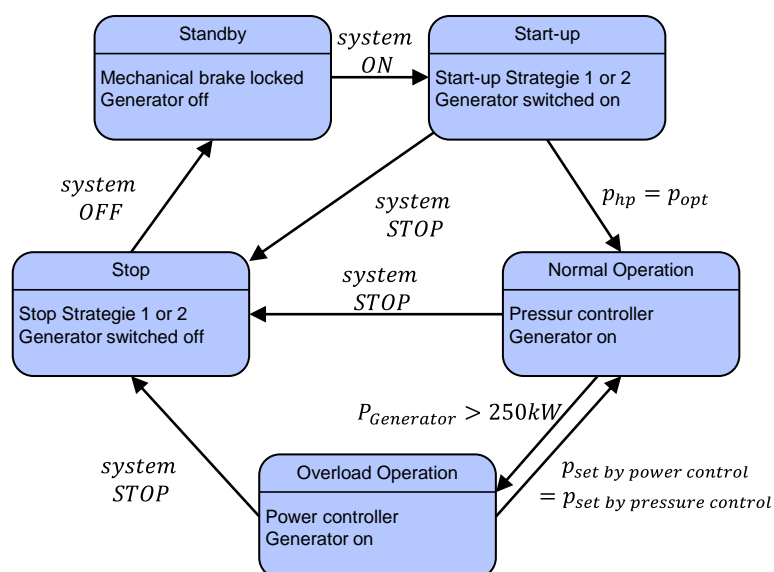


Figure 3-25: Different controllers applied during system operation

3.5.4 Overview of further required components for a hydrostatic drivetrain

In the previous sections different strategies for system start-up, stop or overload situations were presented. For reasons of clarity only components specific for the certain strategies were considered and mentioned. To operate such a system independently in the ocean for a long time additional components are required for different reasons. These are further safety installations (e.g. PRVs or check valves), manifolds to collect or separate the oil flows, accumulators, additional (safety) valves, heat exchangers, boost pumps and oil filters.

At IFAS a “hydraulic transformer” has been designed (Figure 3-26), that integrates most of the peripheral functions. Furthermore this hydraulic transformer is capable of supplying the system with necessary flow rates in an emergency case such as the breakdown of the control system or if some piping or hoses fail. The hydraulic transformer is not discussed in detail here. The final component tree depends on the realised start up and stop strategies as well as the implemented safety functions.

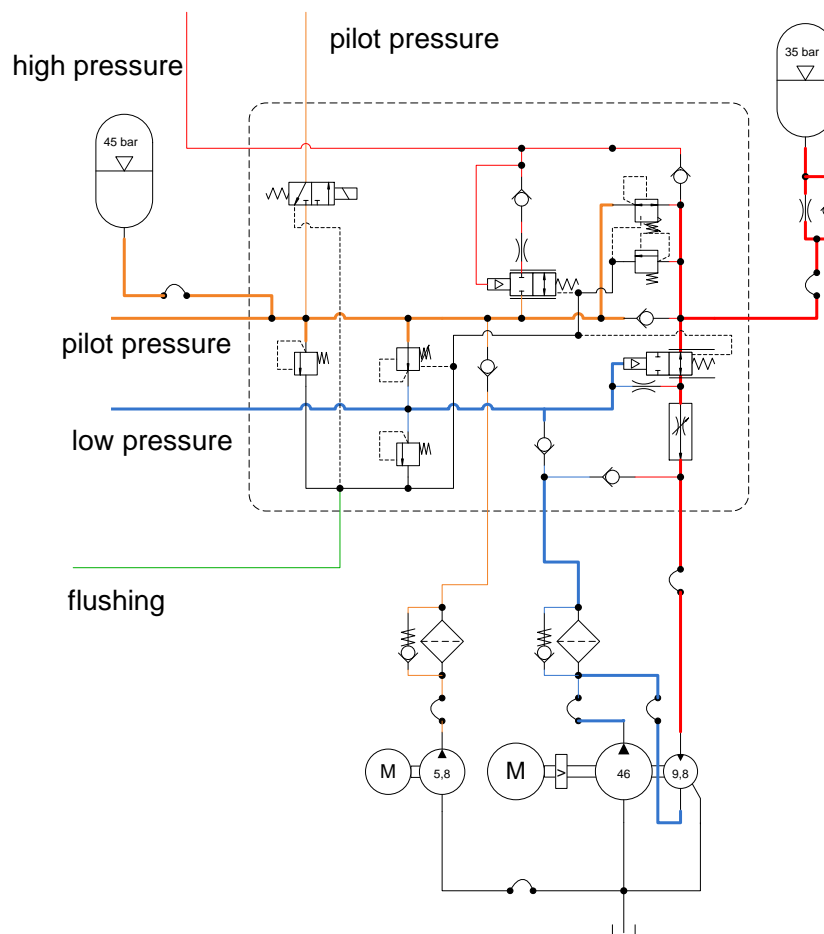


Figure 3-26: Hydraulic transformer

4 Build-up of the Simulation Model

The following section describes the modelling of the basic components of a HDT in the simulation software MatLab/Simulink/Stateflow. A one dimensional simulation considering the volumetric instead of the mass flow is carried out, a simplification often used in simulation of hydrostatic drivetrains. Finally a model of the whole drivetrain is set up including a dynamic model of the turbine, the hydrostatic drivetrain and a simple model of the generator. A control system for operation during the start up phase, standard operation, overload conditions and shut down is set up as well.

To set up the models the well-known equations for the components described in [Mur12] and measurement data of the losses in the pumps and motors are used. The data has been measured using the hydrostatic test bench at IFAS. As the components used within this project are the same as the pumps and motors installed on the test bench, the data is applicable here. In case the displacement of a needed component differs to that component used for measurement, the loss data is linearly scaled up or down using the displacement as a scaling factor.

The simulation of the pump is based on conservation of torque (eq. 4-1) and flow rate balance (eq. 4-2) [MUR12].

$$J_p \cdot 2\pi\dot{n}_{\text{Rotor}} = M_{\text{Rotor}} - \frac{V_p \cdot \Delta p}{2\pi} - M_{L,p}(\Delta p, n_{\text{Rotor}}) \quad \text{eq. 4-1}$$

$$Q_{p,\text{eff}} + Q_{L,p}(\Delta p, n_{\text{Rotor}}) = V_p \cdot n_{\text{Rotor}} \quad \text{eq. 4-2}$$

The modelling of the motor is similar to the pump. The conservation of torque (eq. 4-3) and flow rate (eq. 4-4) are used again.

$$J_m \cdot 2\pi\dot{n}_m = \frac{V_m \cdot \Delta p}{2\pi} - M_{L,m}(\Delta p, n_m, \alpha) \quad \text{eq. 4-3}$$

$$Q_{m,\text{eff}} - Q_{L,m}(\Delta p, n_m, \alpha) = V_m \cdot n_m \quad \text{eq. 4-4}$$

For modelling the underwater turbine the necessary parameters and equations are provided by AQUANTIS and implemented into Matlab/Simulink by IFAS. In addition to the calculation of the nominal torque (eq. 2-5), turbulence, wake and shear effects are incorporated. For the modelling of the generator the load torque curve depicted in Figure 4-1 is provided

by AQUANTIS. The graph shows how the generator torque varies with rotation speed as a percentage of the rated torque (which is 1632 Nm).

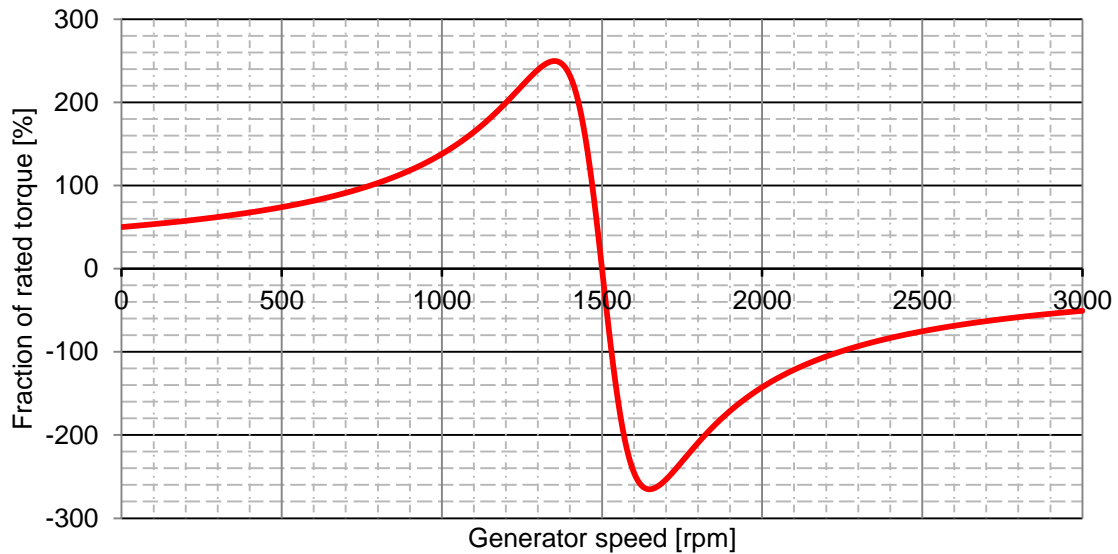


Figure 4-1: Generator torque curve

An accurate profile of the seal friction on the rotor is not provided by AQUANTIS, so only an estimation of the peak value ($\approx 1.4 \text{ kNm}$) for small rotor speeds is used. In line with the Stribeck Curve a decline of the seal friction for higher rotor speeds is assumed. For low rotor speeds the rotor torque becomes comparatively small and the influence of the seal friction is more important, especially during start up. For higher rotor speed the seal friction is much smaller compared to the rotor torque and the influence is negligible. Therefore a constant seal friction value is assumed for higher rotor speeds (200 Nm). The curve used in the simulations is shown in Figure 4-2.

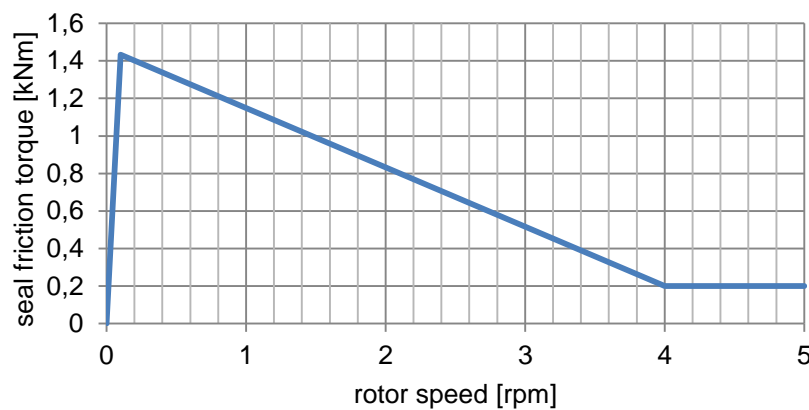


Figure 4-2: Seal friction curve

For the simulation of the drivetrain a simplified model is used and only necessary components for the start up, stop and normal operation phase are considered. A sketch of the system and the components considered is depicted in Figure 4-3 and the basic model used within the simulations is shown in Figure 4-4. For reasons of clarity and length of this report not all models or submodels are presented here in detail.

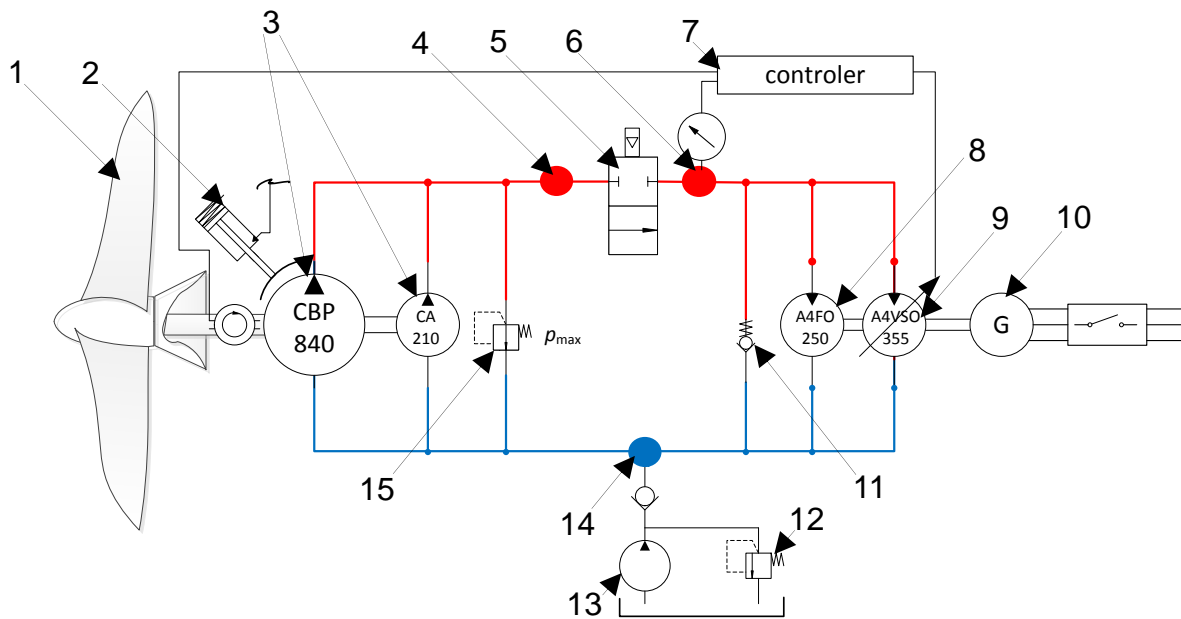


Figure 4-3: Sketch of the simulation model

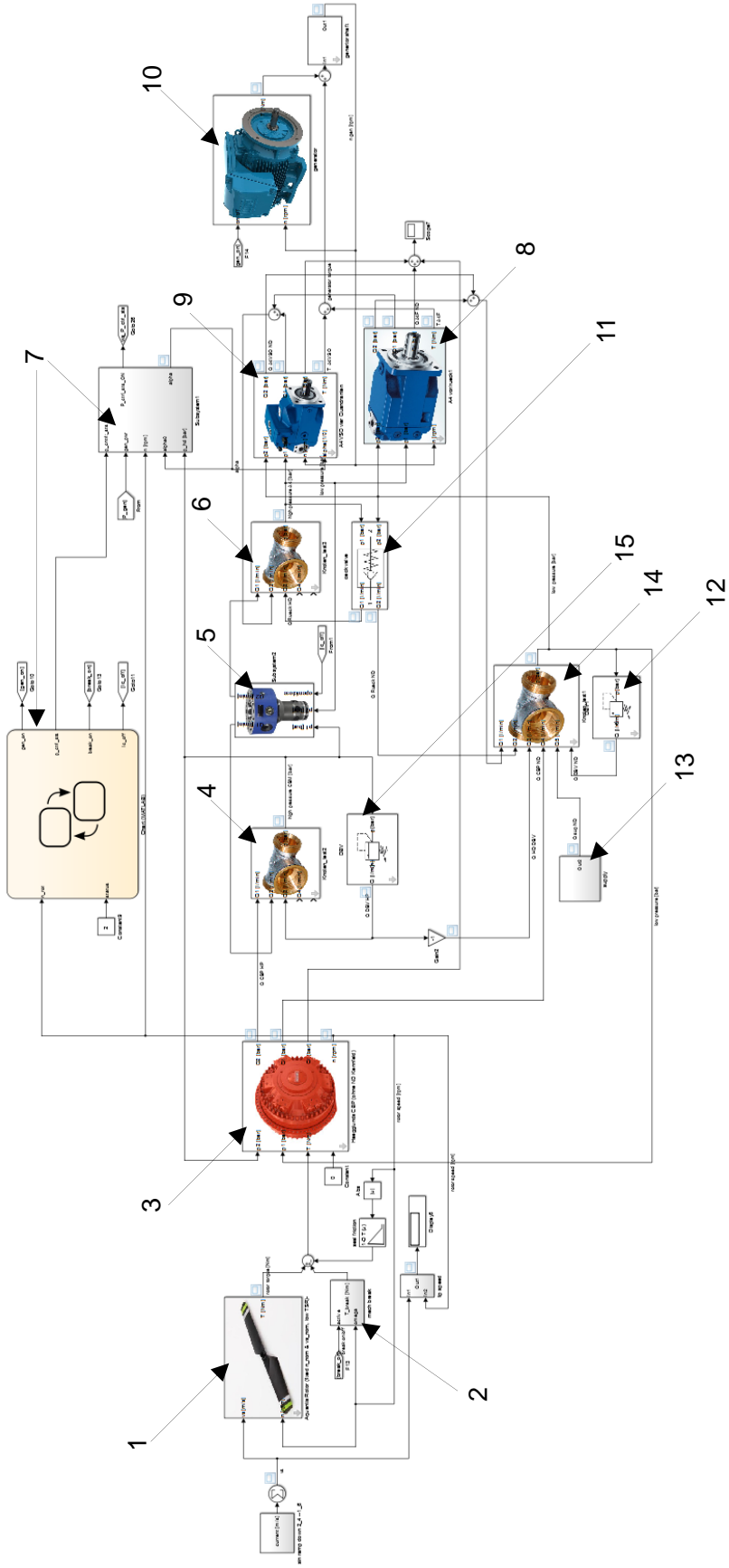


Figure 4-4: Simulink model of the drivetrain in Matlab/Simulink

5 Simulation of the HDT

In the following section the results of the simulations are discussed. An efficiency map of the drivetrain is shown in Figure 5-1 considering all hydraulic components. The efficiency is calculated by dividing the output power at the generator shaft by the input power acting on the rotor shaft. The efficiencies of the rotor and the generator are excluded. At high current speeds the PRV of the high pressure side opens and a certain amount of energy is lost resulting in a low efficiency (see blue marked area in Figure 5-1). For the rated operating point $n_{rotor} = 12 \text{ rpm}$ and $v_s = 1.6 \text{ m/s}$ a maximum efficiency of 0.87 is reached. The power needed to operate all components of the periphery e.g. boost pumps is not considered. So the overall efficiency of a real drivetrain will be lower (approximately 2 %).

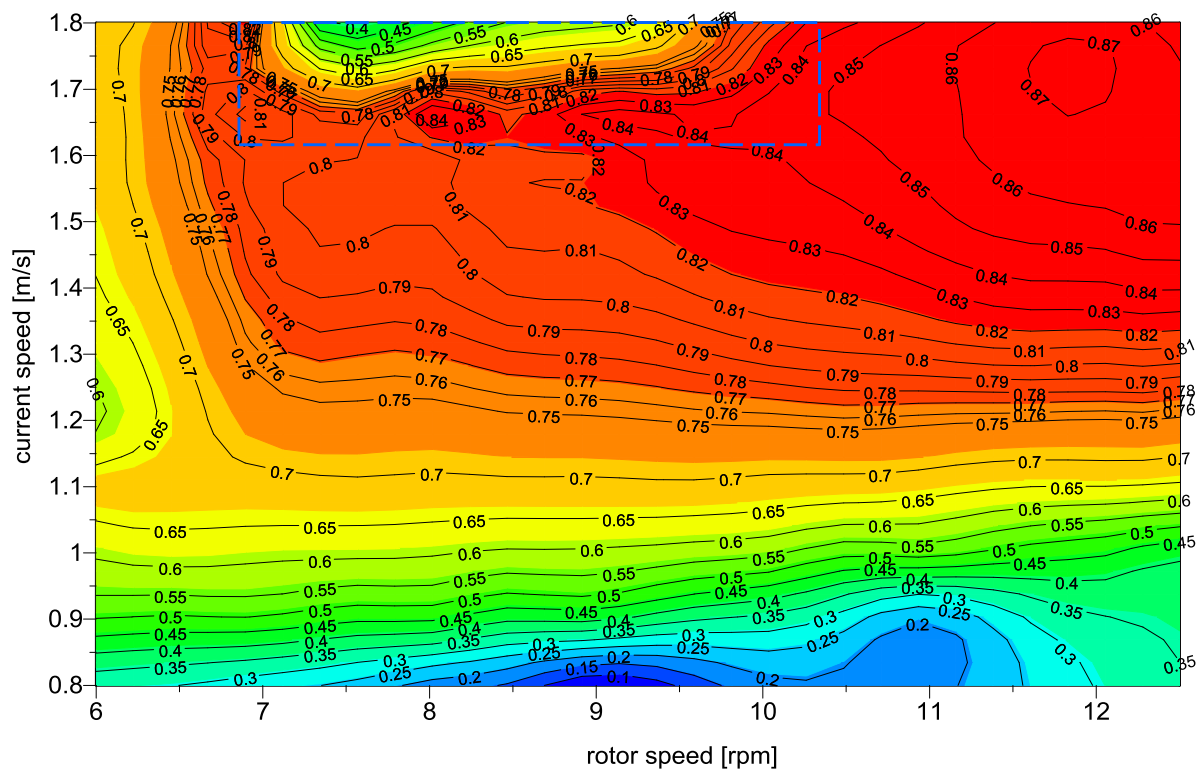


Figure 5-1: Efficiency map of drivetrain

5.1 Start up of the rotor

5.1.1 Start up with the grid

The simulation results for the start up strategy presented in 3.4.1 are depicted in Figure 5-2 and Figure 5-3 for a current speed of 0.8 m/s and an initial rotor speed of 3 rpm and in Figure 5-4 and Figure 5-5 for a current speed of 1.6 m/s and an initial rotor speed of 2.5 rpm. At a rotor speed of 5.7 rpm the flow rate generated by the pumps is large enough to supply the constant displacement motor. The check valve closes (see Figure 5-3 for flow rates) and the pressure controller is activated (see Figure 5-2 at second one). The high pressure is set by changing the displacement of the variable displacement motor and the rotor is sped up until the equilibrium state between rotor and brake torque for the present current speed (here 0.8 m/s) is reached.

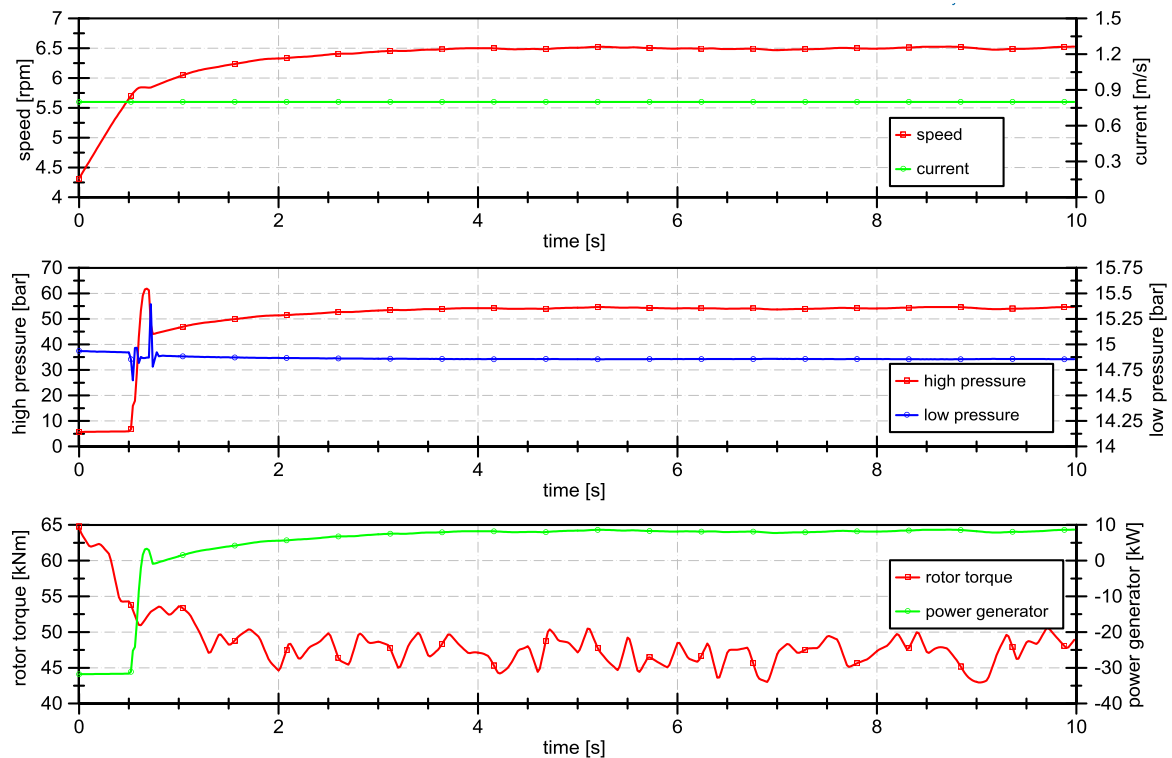


Figure 5-2: Start up at 0.8 m/s using pressure control $\alpha = f(p_{opt})$

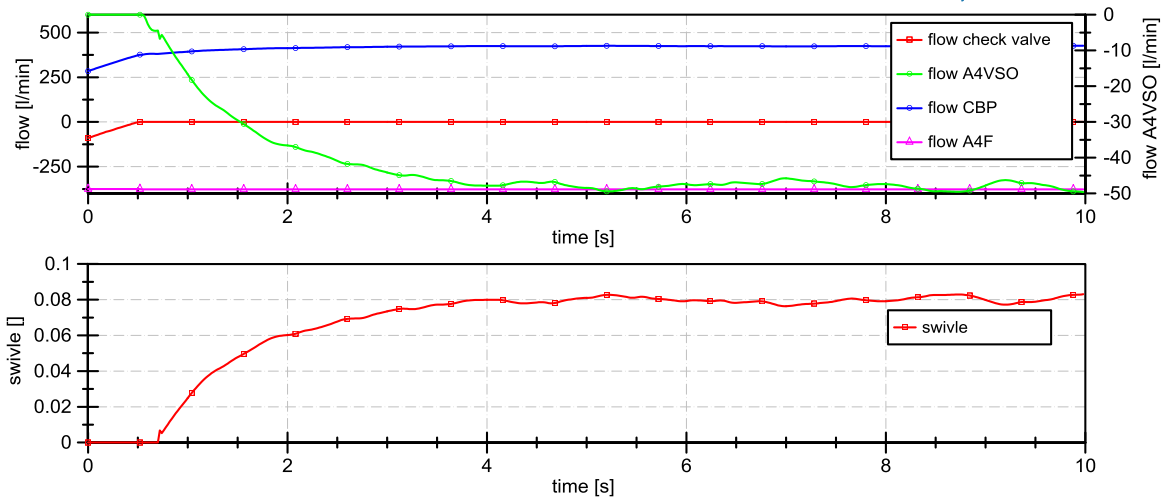


Figure 5-3: Start up at 0.8 m/s using pressure control $\alpha = f(p_{opt})$

For a current speed of 1.6 m/s the results are quite similar (see Figure 5-4 and Figure 5-5). Accordingly, the start up strategy presented in 5.1.1 is feasible for current speeds of 0.8 m/s to 1.6 m/s.

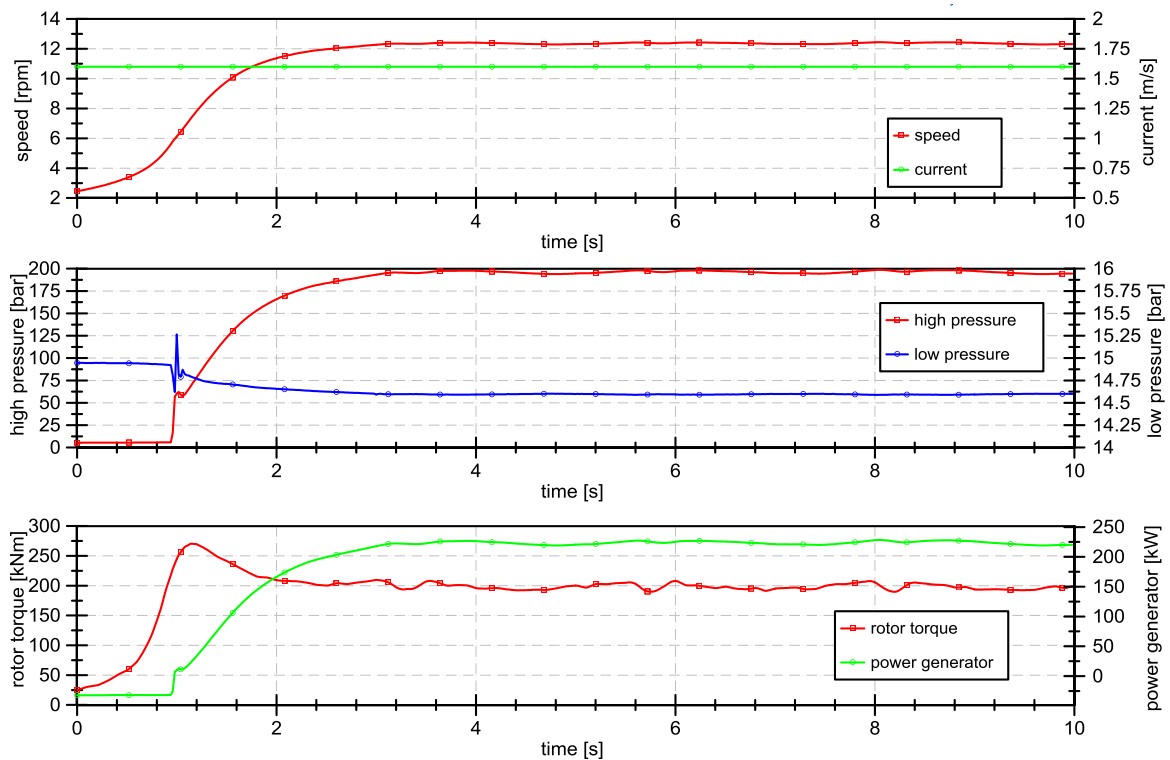


Figure 5-4: Start up at 1.6 m/s using pressure control $\alpha = f(p_{opt})$

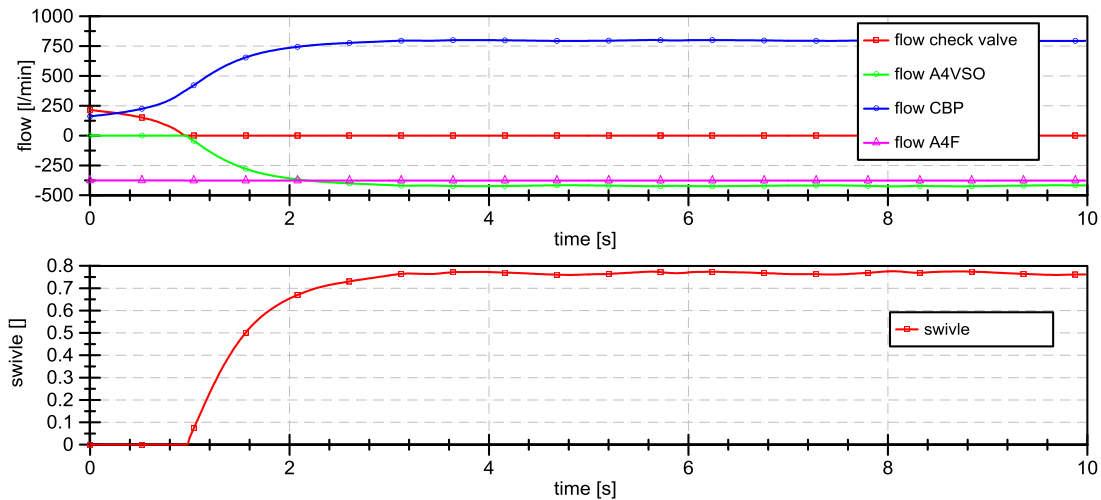


Figure 5-5: Start up at 1.6 m/s using pressure control $\alpha = f(p_{opt})$

The previously shown procedure activates the pressure controller when the rotor reaches a rotational speed of 5.7 rpm and applies a brake torque derived from the optimal control curve. Herby the rotor is stabilized at the optimal operating point for each current speed. Another option for the start up procedure is to use the full displacement of both motors from the beginning. In doing so the pressure controller is not used during the start up (the swivel angle is set to one) and the rotor speeds up until equilibrium state is reached. That state is defined by the flow balance and consequently the rotor speed is given by the flow transferred to the generator side. Without applying a brake torque it is guaranteed that the rotor passes the torque peak and reaches an operating point at the stable side of the characteristic torque curve. Since both motors are used at full displacement the flow passing the check valve during start up increases. Therefore the operation curve of the check valve is modified to generate the same pressure difference at a higher flow rate as in the previous procedure.

For a current speed of 0.8 m/s the results are shown in Figure 5-6 and Figure 5-7. For a current speed of 1.6 m/s the results are depicted in Figure 5-8 and Figure 5-9. For both current speeds it can be seen that the rotor passes the torque peak. For a current speed of 0.8 m/s the rotor approaches the maximum rotational speed with declining acceleration due to the low input torque at higher speeds. For 1.6 m/s the input torque is higher leading to faster speed-up. Here the input torque at the equilibrium state is much higher compared to the state for a current speed of 0.8 m/s, because higher current speeds lead to a higher input torque. The high pressure increases proportionally to the input torque. As the leakage of the components increases with pressure as well as the generator speed with higher load

torques the maximum rotor speed increases for higher current speeds due to the higher flow rate in the system.

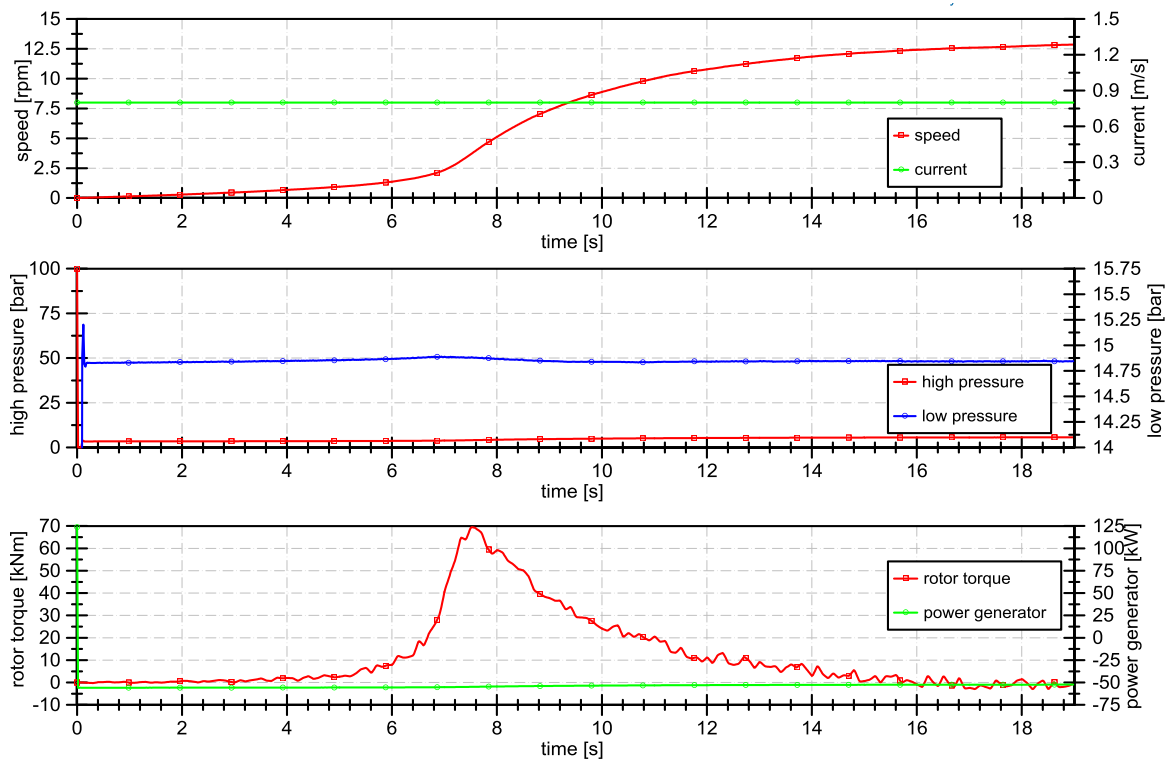


Figure 5-6: Start up at 0.8 m/s using full displacement of variable motor ($\alpha = 1$)

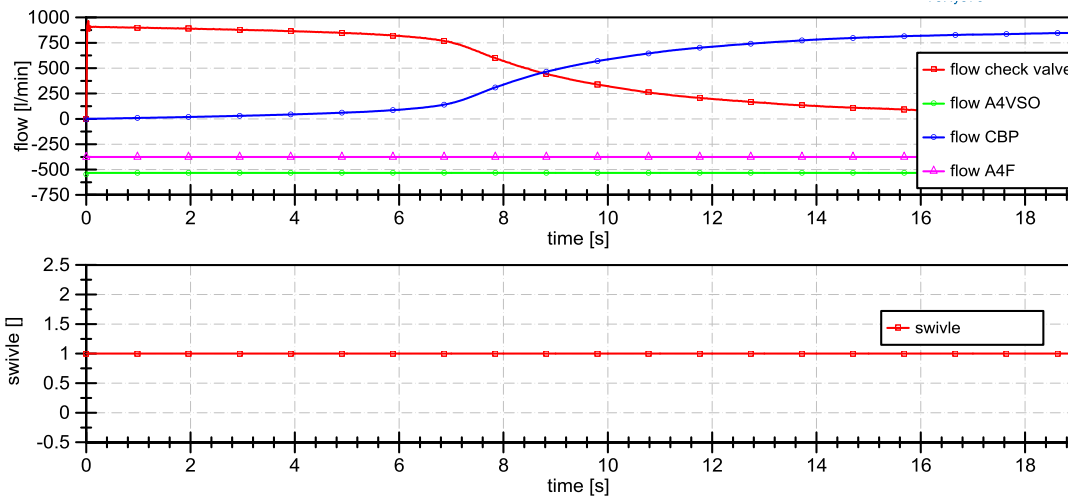


Figure 5-7: Start up at 0.8 m/s using full displacement of variable motor ($\alpha = 1$)

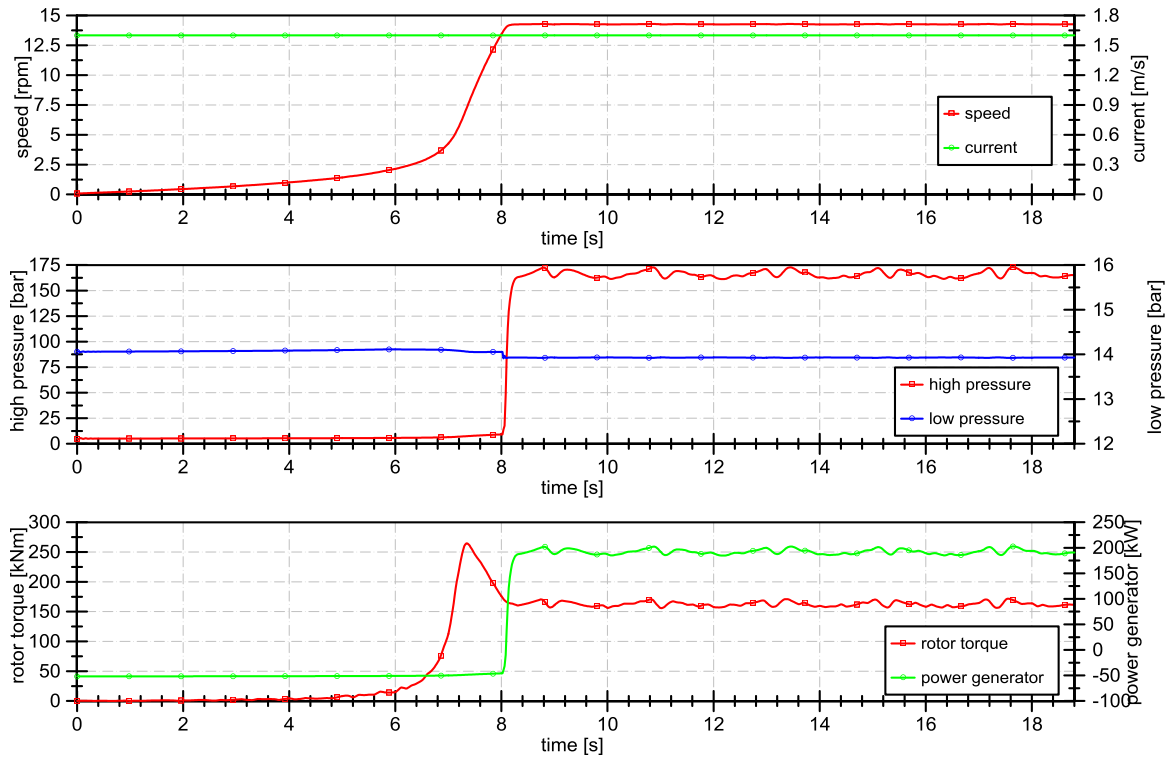


Figure 5-8: Start up at 0.8 m/s using full displacement of variable motor ($\alpha = 1$)

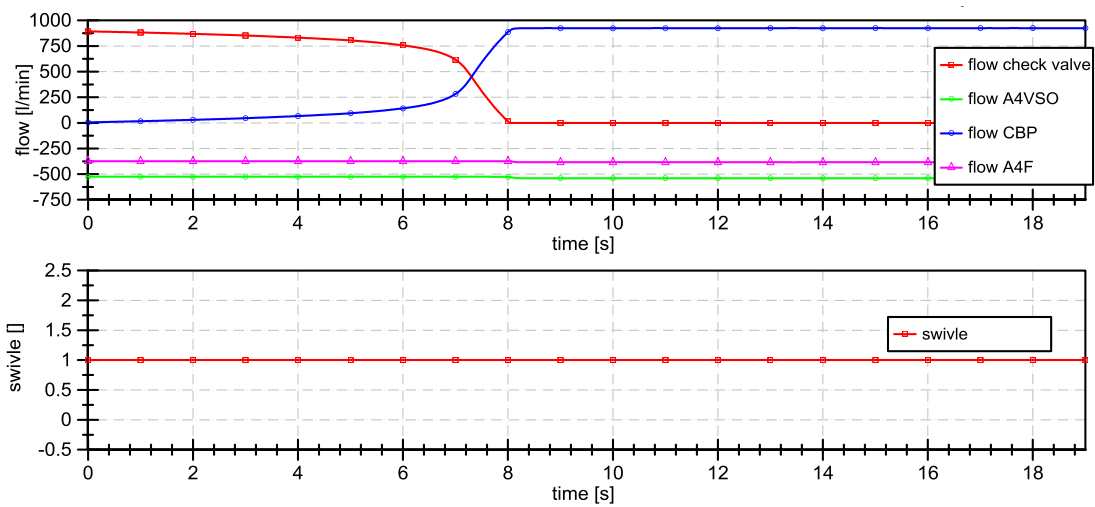


Figure 5-9: Start up at 0.8 m/s using full displacement of variable motor ($\alpha = 1$)

Start up with the grid in an overload scenario

The turbine layout proposed by AQUANTIS uses a passive depth control to reduce the input power level. If an increasing current speed causes the input power to rise above the rated input power the turbine starts to dive deeper into the sea due to the forces acting onto the structure. The structure stops diving at a sea depth where the current speed equals the rated current speed and a new equilibrium state is reached. If the rotor is inactive no thrust is generated and the passive depth control is unable to operate. As a consequence the turbine might be started at a sea depth where the current speed exceeds the rated current speed and the input torque exceeds the rated operating point as well until the passive depth control has moved the turbine deeper into the sea. This scenario is simulated, whereas the change of the current speed caused by the passive depth control is assumed to have a quarter sinusoidal form. After the mechanical brake of the rotor has been unlocked the current speed decreases from 2.4 m/s to 1.6 m/s. For a current speed of 2.4 m/s the input torque is much larger compared to the rated torque. So only half of the torque is applied to the rotor shaft in this simulation. The results are shown in Figure 5-10. Further investigations of the scenario are not conducted.

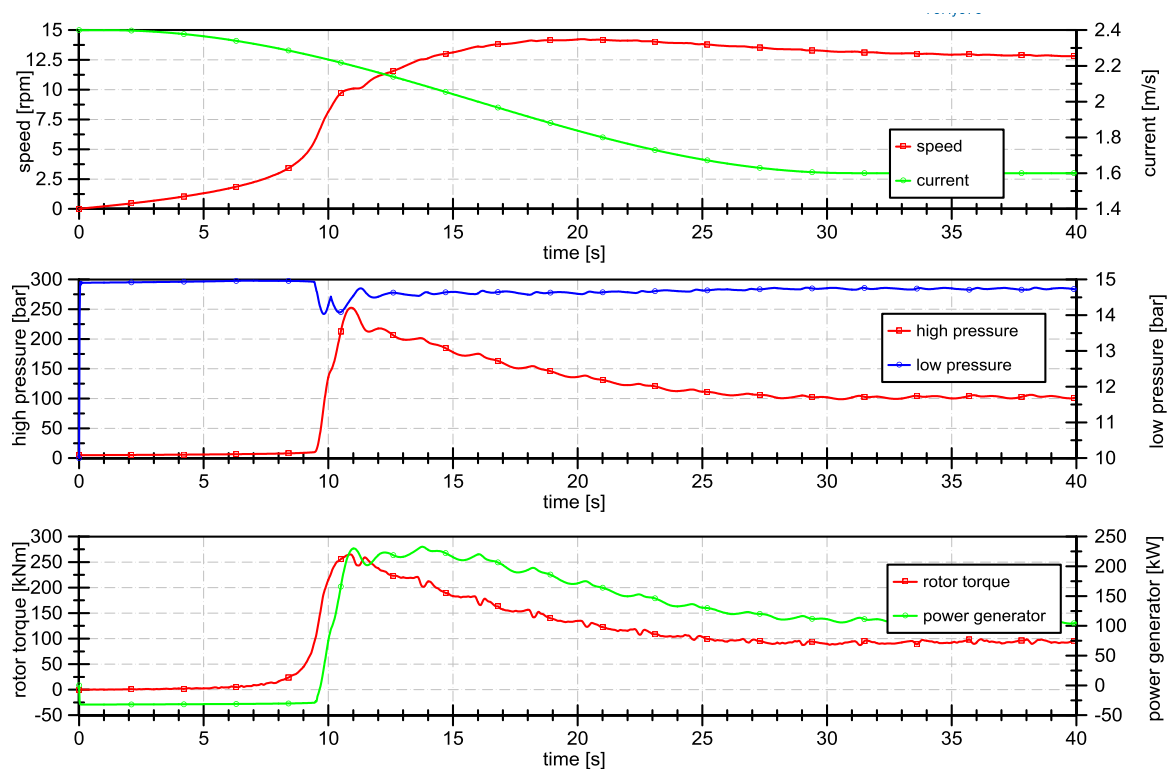


Figure 5-10: Start up at current $v_s = 2.4 \text{ m/s} \rightarrow v_s = 1.6 \text{ m/s}$ using half rotor torque

5.1.2 Start up without the grid

The simulation results for the start up strategy presented in 3.4.2 are depicted in Figure 5-11 and Figure 5-12 for a current speed of 1.6 m/s. At the beginning the rotor is sped up by the flow of the boost pump. The generator is not connected to the grid and no brake torque applied to the generator shaft. To prevent the generator shaft from turning a controller keeps the generator shaft's rotation speed at zero by setting the swivel angle of the variable displacement motor to a negative value. After 12 seconds the pressure controller is activated and operates the servo valve. At the same time the check valve closes. After 20 seconds the optimal rotor operating point for a current speed of 1.6 m/s is reached and the generator is speed up slowly. When the generator has reached the rated speed of 1500 rpm (at second 36) the generator is connected to the grid. The servo valve starts to close slowly and pressure controller starts to operate the variable displacement motor instead. The servo valve is closed by setting a constant speed and without applying any controller.

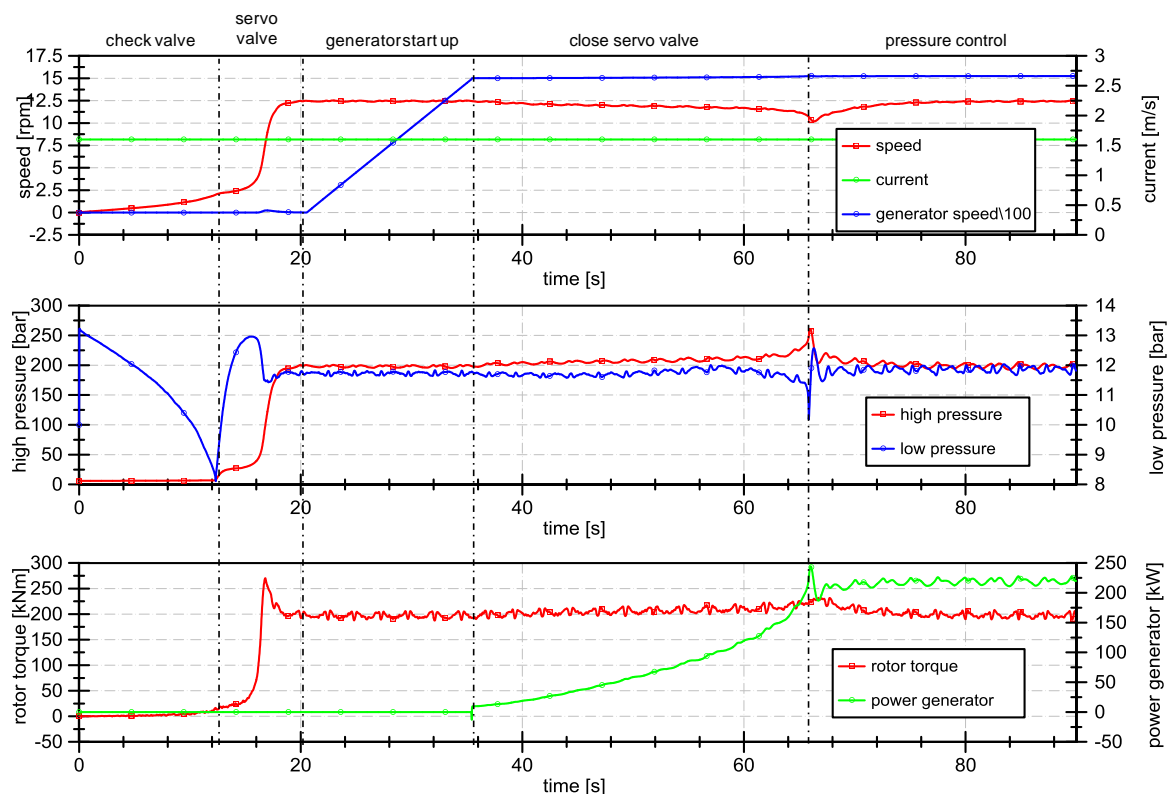


Figure 5-11: Start up at 1.6 m/s with electrical driven boost pump

So the feedback to the pressure controller by the changing flow rate is not compensated by the control algorithm here, which can be seen by the decrease of the rotor speed in Fig-

ure 5-11 from second 36 to 66. To avoid a large reduction of the rotor speed the valve is closed slowly. By applying a more advanced control algorithm the closing of the valve might be performed within a few seconds without affecting the rotor speed much. While the servo valve is active a high amount of the input power is converted into thermal energy. Therefore an approximation of the mean system temperature is depicted in Figure 5-12. The presented start up procedure heats up the system about 28 K. The optimal temperature of the system during operation will be around 40-50 °C and is reached more quickly by this start up procedure compared to the others.

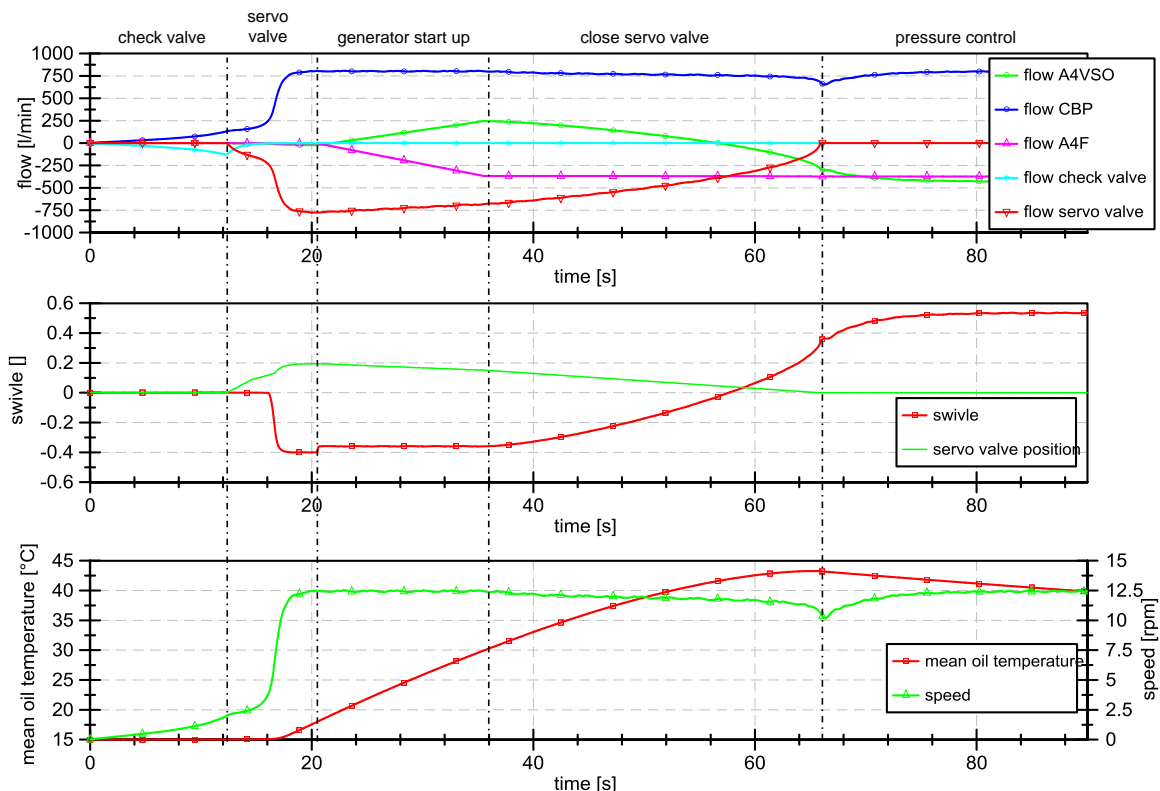


Figure 5-12: Start up at 1.6 m/s with electrical driven boost pump

5.2 Simulation of an overload scenario

The simulation results of the control strategy for overload scenarios presented in 3.3 are shown in Figure 5-13. When the current speed rises above the rated current speed, it will be reduced by the operation of the passive depth control. The impact of the passive depth control on the current speed is not known and the current speed is varied as shown. The acceleration of the current in reality might be much slower. Hence, the simulated scenario is a more conservative approach. When the generator torque exceeds 250 kW the control algorithm changes and instead of using a pressure controller to regulate the high pressure

the generator power is controlled (at second four). The power controller slows down the turbine to reduce the input power. But as the rotor speed decreases the rotor is moved towards the torque peak leading to a higher rotor torque and consequently to a higher system pressure. At the eleventh second a decrease of the current speed due to the control action of the passive depth control is assumed. When the power controller attempts to set the same pressure as the pressure controller, the control algorithm switches back to the pressure controller, which happens around second fourteen. Around the fourteenth second the operating point is close to the point at which the pressure controller is set. At this time the control algorithm switches back to the pressure controller.

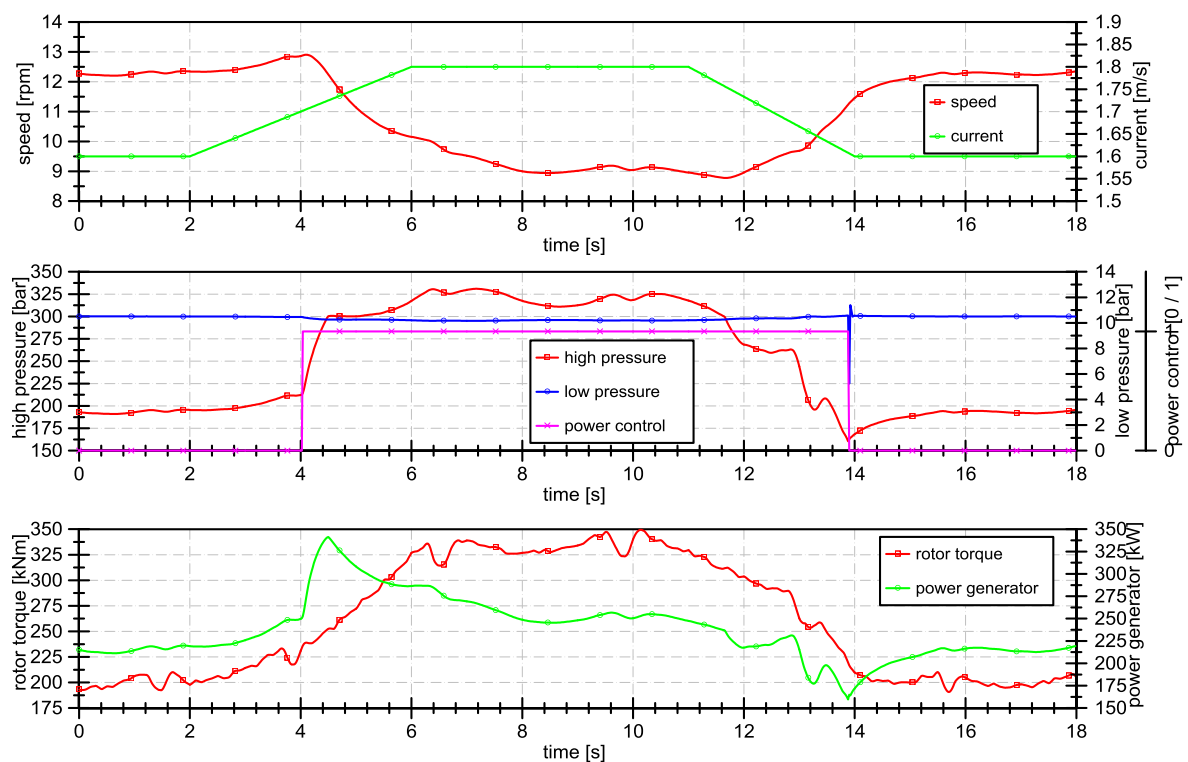


Figure 5-13: Overload scenario ($current\ v_s = 1.6 \frac{m}{s} \rightarrow 1.8 \frac{m}{s} \rightarrow 1.6 \frac{m}{s}$)

5.3 Simulation of an “over speed configuration”

In the previous section 5.2 the input power was reduced by slowing down the rotor, which in turn leads to a higher input torque and a system pressure in unwanted regions. Another option is to overspeed the rotor. From Figure 2-1 it can be seen, that very high tip-speed ratio results in a low power coefficient and consequently a lower input power. The maximum rotor speed is defined by the installed motor displacement. To operate the rotor at higher speeds the motor displacement must be increased. The minimum rotor speed is giv-

en by the related generator speed and the constant motor's displacement. As this parameter shall remain unchanged only the displacement of the variable motor is increased up to 500 ccm³. This modification also affects the efficiency of the drivetrain and therefore an efficiency map of the modified layout is given in Figure 5-14.

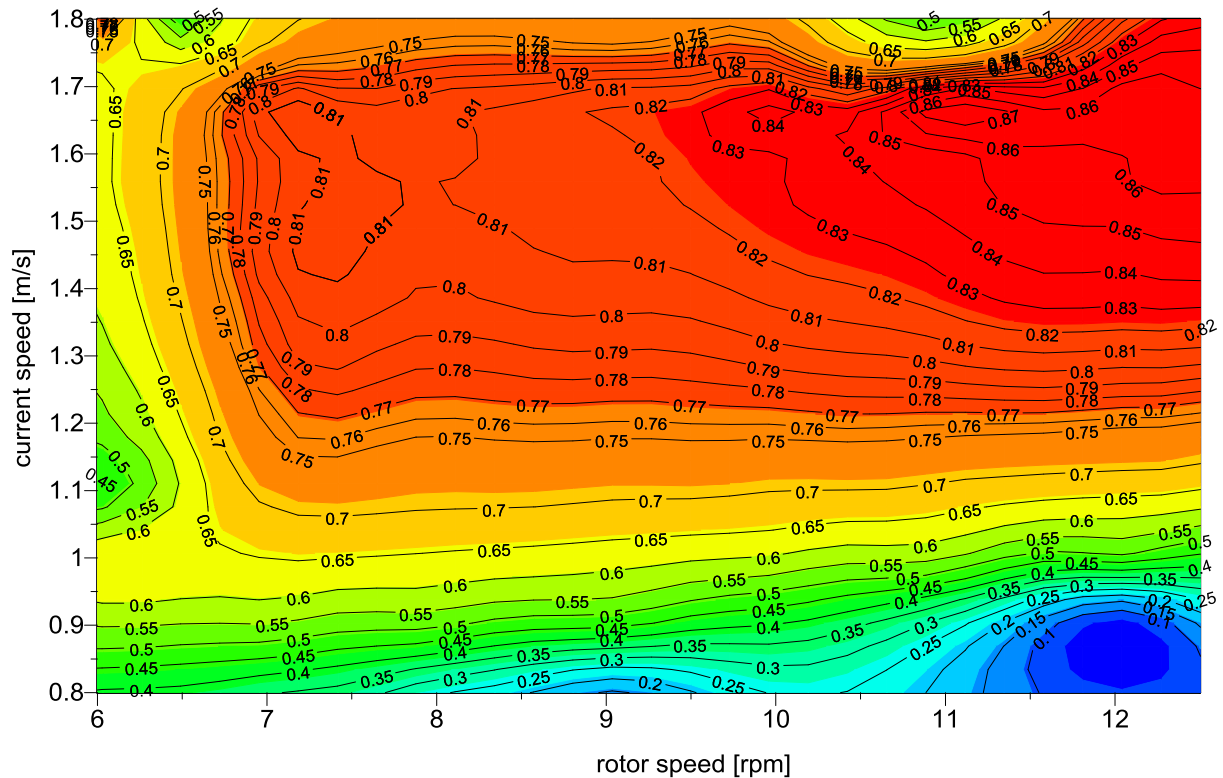


Figure 5-14: Efficiency map of over speed configuration (A4F 250 / A4VSO 500)

The variable displacement motor has a poorer efficiency for low swivel angles. Due to the greater displacement the variable motor is operated at lower swivel angles compared to the standard layout used within this project. This leads to a lower overall efficiency of this modified drivetrain compared to the standard layout and a mean loss in efficiency of about one percent. The results of the simulation are presented in Figure 5-15 and Figure 5-16. The current speed is increased from 1.4 m/s to 1.8 m/s resulting in an overload situation, an input power on the generator shaft greater than 250 kW and a high pressure of 240 bar. After 40 seconds the rotor is sped up leading to a reduction of the input power and the high pressure as well. Compared to the strategy in 5.2 both the generator power and the high pressure are moved into desired areas, which is the main advantage of this strategy. However, the maximum rotor speed is still limited by the total motor displacement and so this strategy remains applicable only up to a certain current speed. Disadvantages are a lower overall efficiency and the costs for a variable motor with larger displacement.

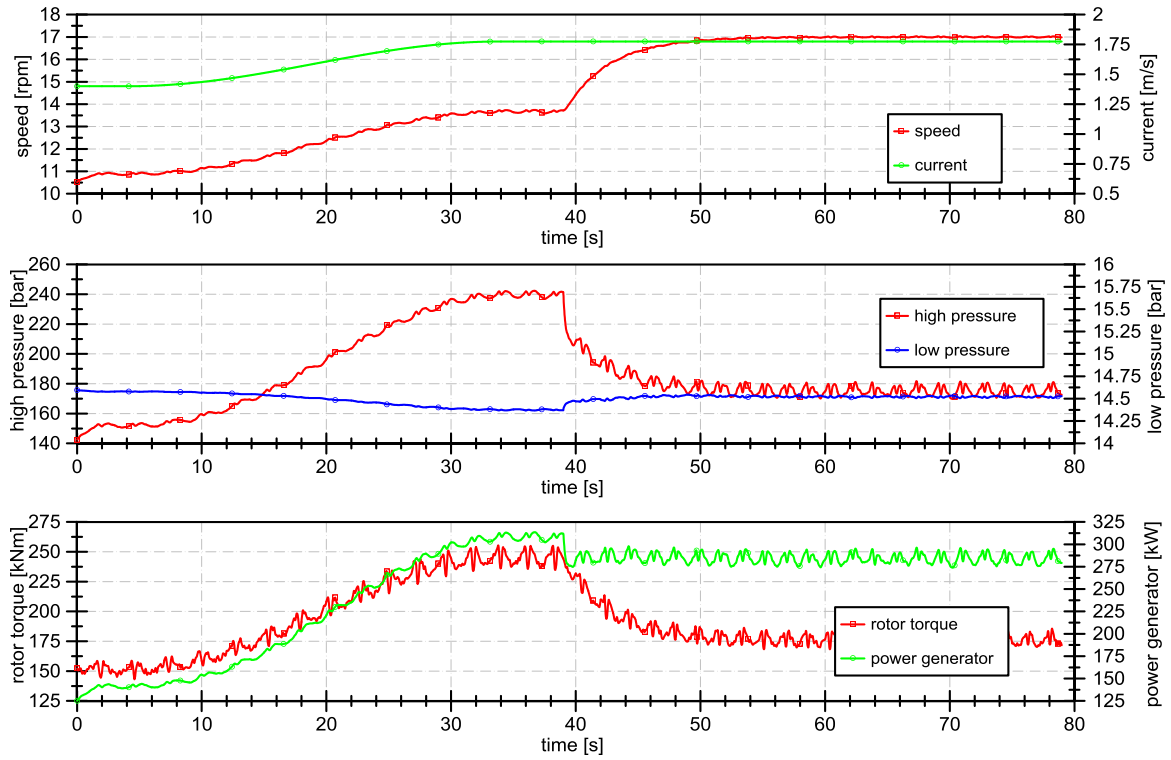


Figure 5-15: Load control using over speed

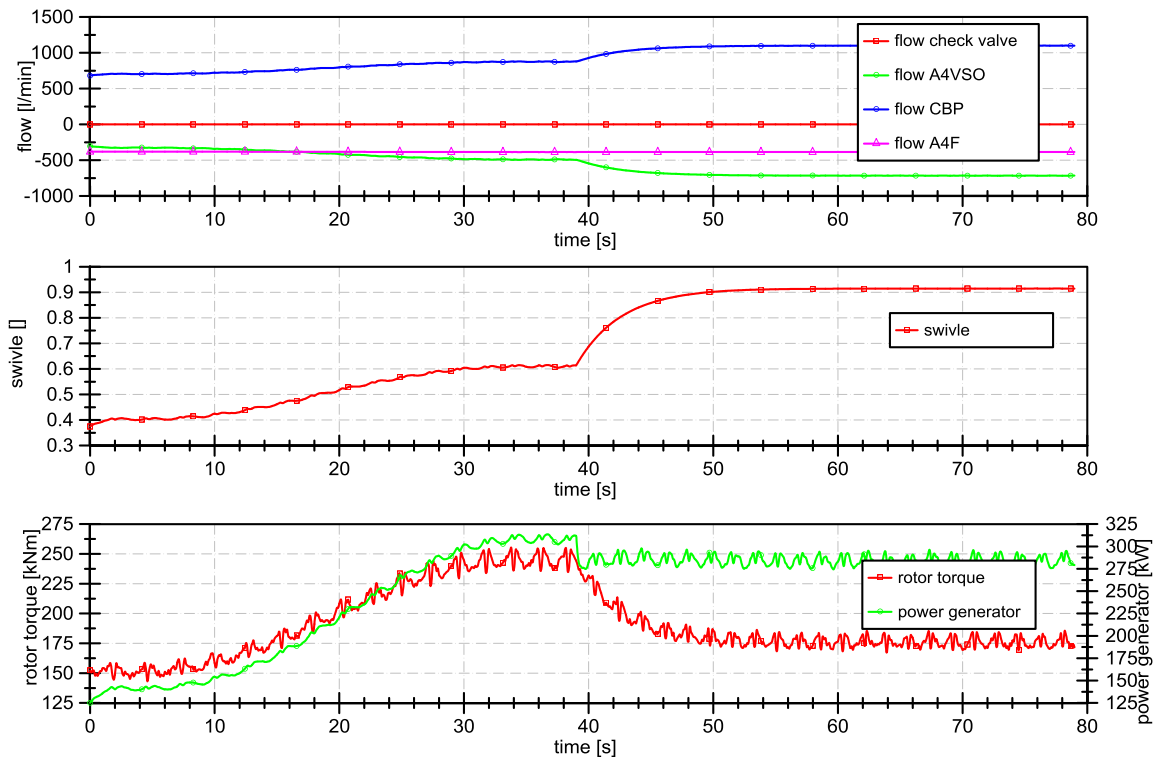


Figure 5-16: Load control using over speed

5.4 Stop procedures for the system

In section 3.5 two stop procedures for the turbine are presented. The simulation results are discussed in the following section.

5.4.1 Stop procedure with braking torque applied by the motors

For a current speed of 1.6 m/s the stop procedure using the motors for the deceleration of the rotor is presented in Figure 5-17. After two seconds the stop procedure is initiated and the pressure controller sets the high pressure to 300 bar to decelerate the rotor. This leads to a generator input power above the rated power at first. When a rotational speed of 6 rpm is reached the control algorithm is changed and the rotor speed is controlled. In doing so the brake torque is lowered for lower rotational speeds and the rotor moves smoothly towards zero rpm. After the rotor has decelerated below one rpm the pressure controller keeps the high pressure at 20 bar. Otherwise the high pressure would decrease proportionally to the rotor speed and the cavitation pressure would be reached. During this phase 20 bar is enough to decelerate the rotor further. As the rotor speed falls below 0.5 rpm the mechanical brake is locked and the rotor is stopped.

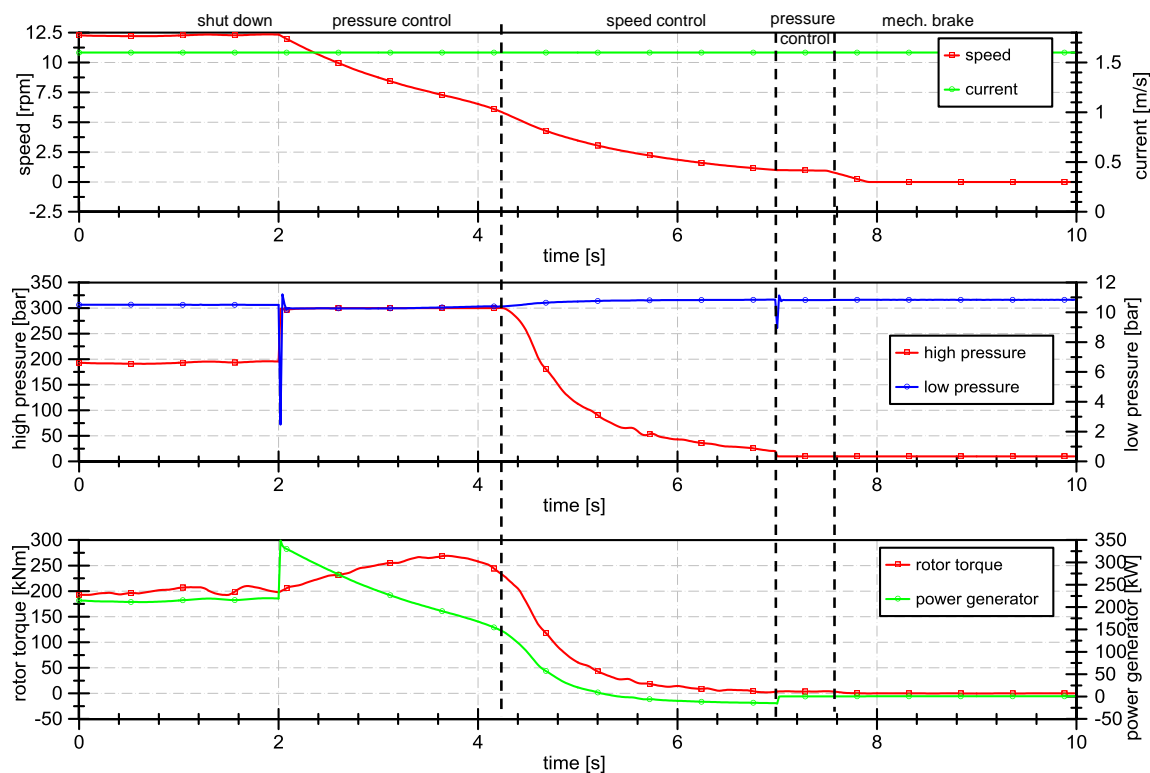


Figure 5-17: Stop at current $v_s = 1.6 \frac{\text{m}}{\text{s}}$, $p_{\text{brake}} = 300 \text{ bar}$

In Figure 5-18 the stop procedure for a current speed of 1.8 m/s is shown. The method remains the same but for such a current speed a system pressure of 300 bar is not enough to move the rotor over the torque peak. Therefore the pressure generating the initial brake torque is increased to 330 bar.

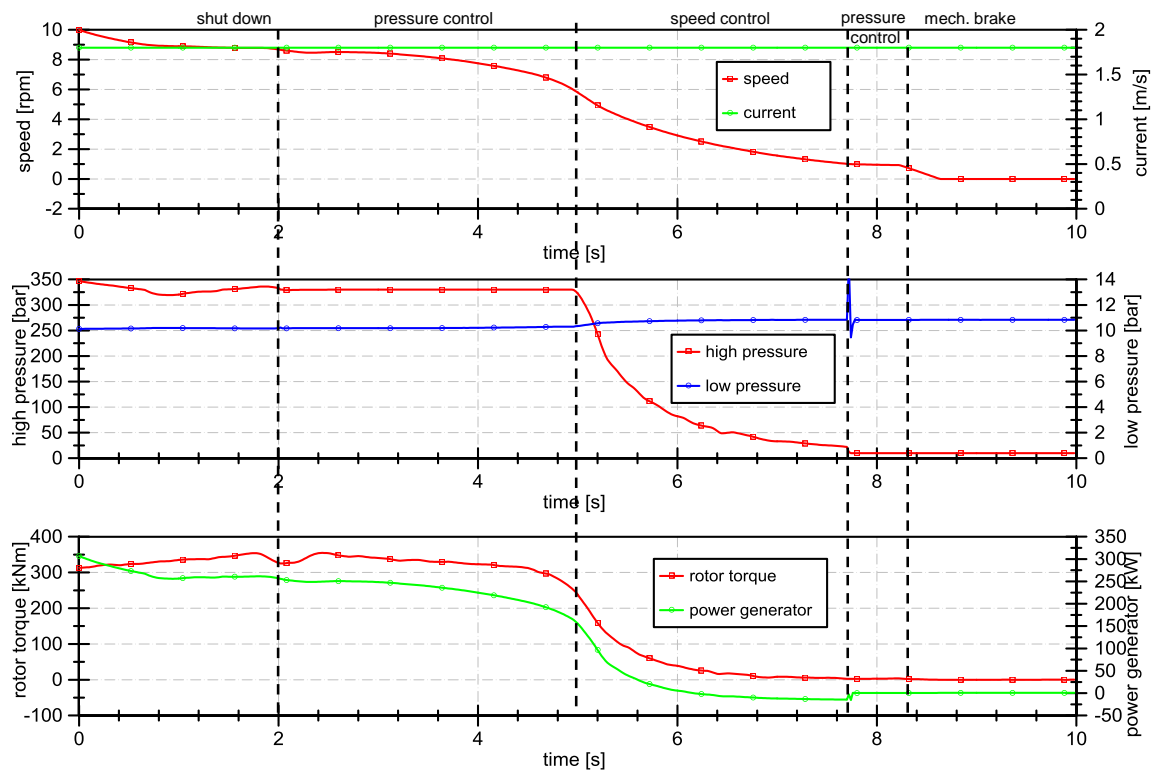


Figure 5-18: Stop at current $v_s = 1.8 \frac{\text{m}}{\text{s}}$ (Overload), $p_{\text{brake}} = 330 \text{ bar}$

However, it is noteworthy that higher current speeds require a higher pressure to generate the initial brake torque for the deceleration of the rotor. As this brake torque is applied to the drivetrain by the generator it must be guaranteed that the generator is able to handle such loads even if it is just for a few seconds. On the other hand for lower current speeds the brake torque can be chosen sufficiently low and unnecessary high pressure loads onto the hydraulic components can be avoided.

5.4.2 Stop procedure with braking torque applied by the PRV

Another opportunity to load a braking torque onto the rotor is to close the main valve in the high pressure circuit. This leads to a pressure build up until the PRV opens. The system pressure and consequently the braking torque during the deceleration are determined by the PRV's operation curve. The simulation results for a current speed of 1.8 m/s are depicted in Figure 5-19. After one second the stop procedure is initialised and the high pressure is

330 bar. The main valve is closed and the generator is disconnected from the grid. If the rotational speed of the rotor is below one rpm the mechanical brake is locked and the rotor stops. The duration of the deceleration is determined by the operation curve of the PRV and the high pressure resulting from it. For a current speed of 1.8 m/s a pressure of 330 bar is sufficient to push the rotor over the torque peak, but for higher current speeds a higher pressure must be applied. So the chosen maximum pressure should be chosen high enough to stop the rotor for all current speeds, which might occur during operation.

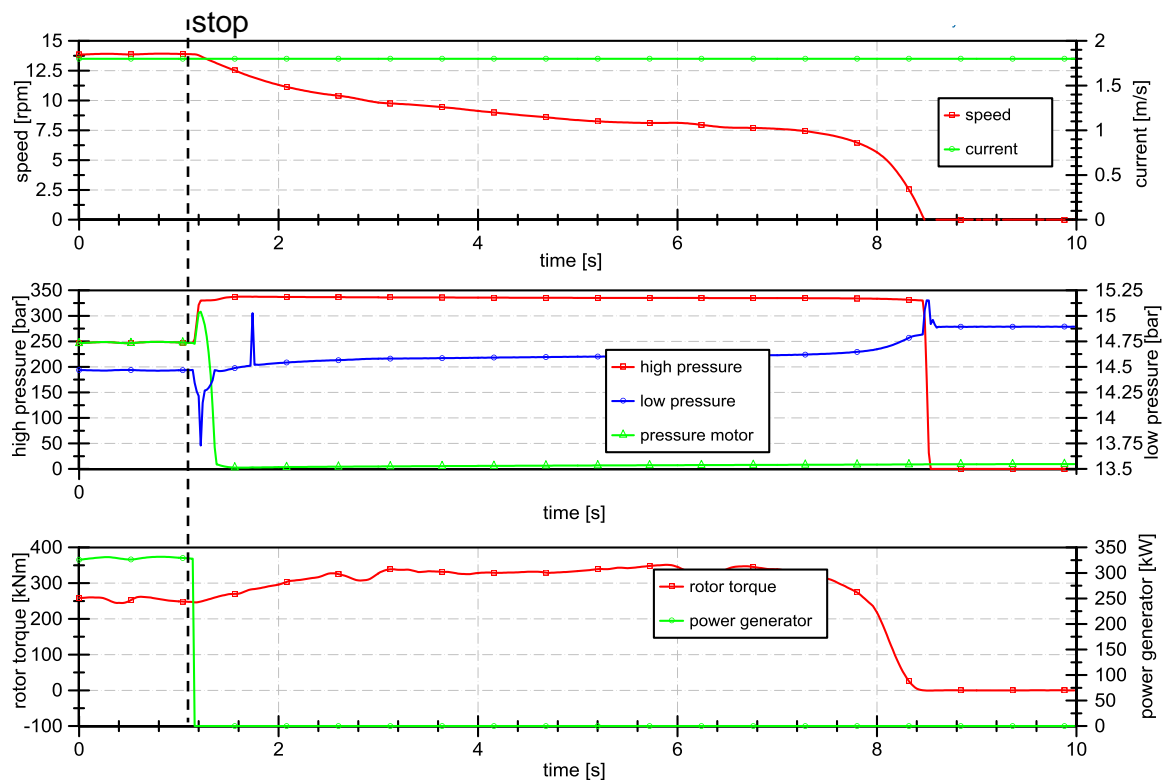


Figure 5-19: Stop procedure at 1.8 m/s using the PRV

In summary, both stop procedures can be applied to the drivetrain in different situations. Strategy one can change the system pressure dynamically and maintain a pressure that is sufficient for the present current speed leading to a smoother and less stressful deceleration process. However, in strategy two to stop the drivetrain only the main valve needs to be closed and the generator is disconnected from the grid. This strategy can be applied in emergency situations as well. If the valve is kept opened by the control system and closes otherwise, this stop procedure is the default state and is initialized either by the control system itself or when the control system breaks down. So depending on the circumstances one of the presented strategies should be applied, especially because the drivetrain layout

does not have to be changed to run one of the two strategies and the needed hydraulic components are the same. Both strategies only differ in the control effort.

5.5 Load-cycle: Start – Overload – Stop

In Figure 5-20 the simulation of a load cycle is shown. At first the turbine is sped up at a current speed of 0.8 m/s (see 3.4.1 for the single procedure). The rotor and the current accelerate and the control system operates the turbine along the proposed optimal control curve (see 3.4.1). After 55 seconds the current speed increases further resulting in an overload situation. The control system reacts by controlling input power of the rotor (see 3.3) and decelerates the turbine. Then the current speed decreases again and the overload scenario ends. The control system switches back to the pressure controller (around second 95) and operates the turbine the optimal TSR again. Finally a stop procedure (see 3.5.1) is initialised.

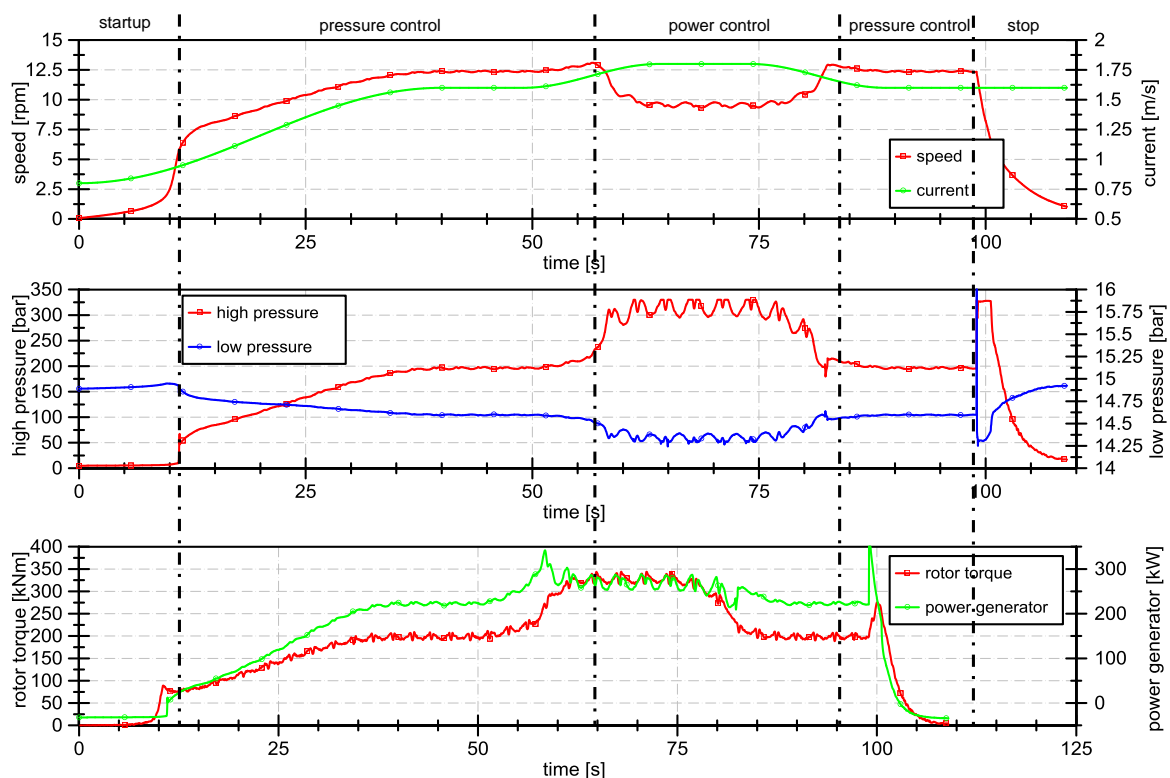


Figure 5-20: Load-cycle - start up, overload, stop

6 Proposed layout for a test bench

The analysis of the proposed drivetrain has so far been conducted using only simulations. To undertake further steps or design a prototype the simulations need to be validated on a test bench. At IFAS a test bench for a 1 MW drivetrain has been developed and proven successfully. This test bench can be used for the necessary validations. Because the test bench has been designed for higher input power the generator side needs to be modified to meet the requirements of this project e.g. the proposed motors, generator and the total output power. In Figure 6-1 such a redesign of the test bench is shown. This figure shows only the hydrostatic drivetrain. The powertrain used to drive it is not shown. The modified part of the drivetrain is marked by the blue area. At the IFAS lab there is no space available to install the new power take off unit (PTO) close to the test bench. So there will be an additional piping (see [2.] in Figure 6-1) for both the low and the high pressure line connecting the PTO to the current test bench. Consequently, on both sides of the piping a manifold is necessary. The test bench pumps use four ports at the low and high pressure side and a manifold [1.] is installed close to them to collect the separate flows. The main valve and the main PRV are mounted there too. On the generator side a second manifold [3.] is installed to connect the motors' hoses to the piping, as well as the check valve for the start up strategy 1 and a PRV protecting the low pressure line. The motors are directly mounted onto the generator shaft [4.]. To the right of the figure all the necessary periphery to operate the drivetrain independently in the field is shown, but not explained in detail here.

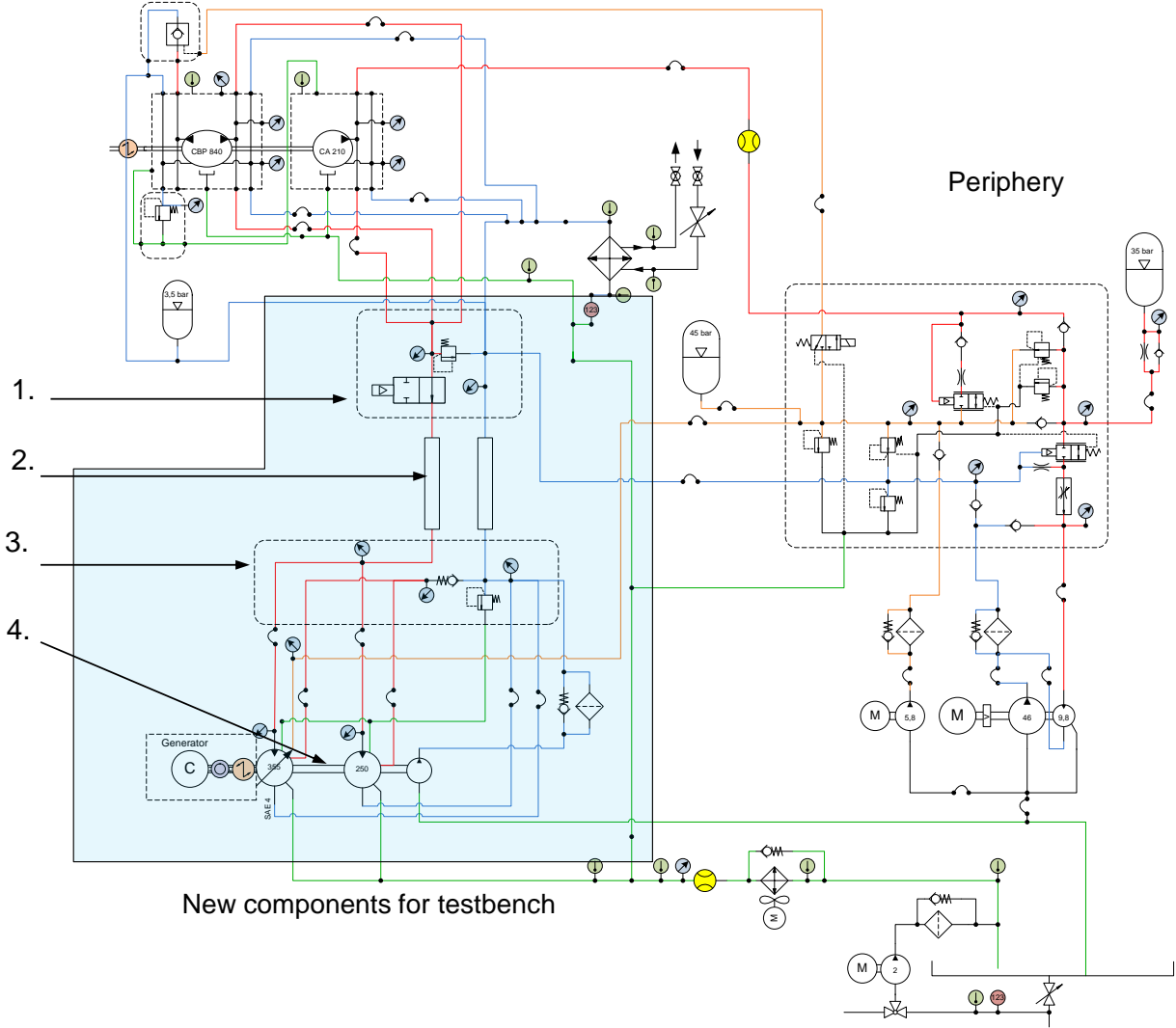


Figure 6-1: Proposed layout of the test bench

7 Summary and Outlook

The design of a HDT for a marine current power system with an electric output power of 250 kW was done for a specific location. Three different configurations of hydraulic pumps and motors were generated. After a first evaluation only one layout was chosen for further investigation.

An analysis of the selected configuration of the HDT was done by setting up a model of the system in Matlab/Simulink. The required data concerning the turbine and the generator was provided by AQUANTIS. Data about the hydraulic components was supplied by IFAS.

Different strategies for the start up, the stop and to react to overloads were developed and simulated. It was shown that the HDT is able to run well over its whole operating area and thus meets all requirements

In a next step the development of a test bench is proposed to validate the simulations. Therefore a modification of the current hydrostatic drivetrain test bench at IFAS has been presented.

Aachen, September 2014



Prof. Dr.-Ing. H. Murrenhoff

- Head of Department -



G. Matthiesen, M.Sc, M.Sc.

- Official in Charge -

III Bibliography

- [HAU08] Hau, E. “Windkraftanlagen”, 4. Edition, Springer-Verlag Berlin Heidelberg, 2008
- [Mur12] Murrenhoff, H. “Grundlagen der Fluidtechnik Teil1 – Hydraulik”, 7. Edition, Shaker, Aachen, 2012
- [Sch12] Schmitz, J., Vatheuer, N., Murrenhoff, H. “Dynamic Analysis and Measurement of a Hydrostatic Transmission for Wind Turbines”, 8th International Fluid Power Conference, Dresden, 2012
- [WAT09] Watton, J. “Fundamentals of Fluid Power Control”, 1. Edition, Cambridge University Press, USA, 2009

IV Table of figures

Figure 1-1:	Concept of a marine current turbine	5
Figure 2-1:	Power-coefficient c_p curves versus tip speed ratio	8
Figure 2-2:	Torque-coefficient c_m curves versus tip speed ratio	9
Figure 2-3:	Optimal power curve of the rotor	10
Figure 2-4:	Sketch of the drivetrain under development	10
Figure 2-5:	Main configurations of the HDT	12
Figure 2-6:	Efficiency curves of the drivetrains at optimal points of operation	13
Figure 2-7:	Pressure curves of the drivetrains at optimal points of operation	14
Figure 2-8:	Points of operation for three configurations	14
Figure 2-9:	Power curves of the drivetrains at optimal points of operation	15
Figure 2-10:	Relative frequency of current velocity provided by AQUANTIS	15
Figure 2-11:	Comparison of weighted power for three drivetrain layouts	16
Figure 2-12:	Comparison of estimated power for three drivetrain layouts	16
Figure 3-1:	Speed Controller	18
Figure 3-2:	Torque Controller	18
Figure 3-3:	Forces acting on rotor shaft	19
Figure 3-4:	Torque control strategy	20
Figure 3-5:	New equilibrium point with change in current speed	20
Figure 3-6:	Limiting the input power by shifting operating points	22
Figure 3-7:	Start up of the turbine using the grid – Step one	23
Figure 3-8:	Start up of the turbine using the grid – Step two	24
Figure 3-9:	Flow rates during start up by strategy one	25
Figure 3-10:	Start up of the turbine using the grid – Step three	25
Figure 3-11:	Start up of the turbine using the boost pump – Step one	26
Figure 3-12:	Start up of the turbine using the boost pump – Step two	27
Figure 3-13:	Start up of the turbine using the boost pump – Step three	28
Figure 3-14:	Torques and flow rates during start up strategy two	29
Figure 3-15:	Start up of the turbine using the boost pump – Step four	30
Figure 3-16:	Start up of the turbine using the boost pump – Step five	30
Figure 3-17:	Start up of the turbine using the boost pump – Step six	31
Figure 3-18:	Stop procedure using the pressure controller – Step one	32
Figure 3-19:	Stop procedure using the pressure controller – Step two	33
Figure 3-20:	Stop procedure using the pressure controller – Step three	33

Figure 3-21: Stop procedure using the pressure controller – Step four.....	34
Figure 3-22 :Stop procedure using the PRV – Step one.....	35
Figure 3-23: Stop procedure using the PRV – Step two	36
Figure 3-24: Stop procedure using the PRV – Step three	36
Figure 3-25: Different controllers applied during system operation	37
Figure 3-26: Hydraulic transformer.....	38
Figure 4-1: Generator torque curve	40
Figure 4-2: Seal friction curve.....	40
Figure 4-3: Sketch of the simulation model	41
Figure 4-4: Simulink model of the drivetrain in Matlab/Simulink.....	42
Figure 5-1: Efficiency map of drivetrain.....	43
Figure 5-2: Start up at 0.8 m/s using pressure control $\alpha = f(popt)$	44
Figure 5-3: Start up at 0.8 m/s using pressure control $\alpha = f(popt)$	45
Figure 5-4: Start up at 1.6 m/s using pressure control $\alpha = f(popt)$	45
Figure 5-5: Start up at 1.6 m/s using pressure control $\alpha = fpopt$	46
Figure 5-6: Start up at 0.8 m/s using full displacement of variable motor ($\alpha = 1$)	47
Figure 5-7: Start up at 0.8 m/s using full displacement of variable motor ($\alpha = 1$)	47
Figure 5-8: Start up at 0.8 m/s using full displacement of variable motor ($\alpha = 1$)	48
Figure 5-9: Start up at 0.8 m/s using full displacement of variable motor ($\alpha = 1$)	48
Figure 5-10: Start up at current $vs = 2.4 \text{ m/s} \rightarrow vs = 1.6 \text{ m/s}$ using half rotor torque.....	49
Figure 5-11: Start up at 1.6 m/s with electrical driven boost pump	50
Figure 5-12: Start up at 1.6 m/s with electrical driven boost pump	51
Figure 5-13: Overload scenario ($current \text{ vs} = 1.6ms \rightarrow 1.8ms \rightarrow 1.6ms$)	52
Figure 5-14: Efficiency map of over speed configuration (A4F 250 / A4VSO 500).....	53
Figure 5-15: Load control using over speed.....	54
Figure 5-16: Load control using over speed.....	54
Figure 5-17: Stop at current $vs = 1.6ms$, $p_{brake} = 300 \text{ bar}$	55
Figure 5-18: Stop at current $vs = 1.8ms$ (Overload), $p_{brake} = 330 \text{ bar}$	56
Figure 5-19: Stop procedure at 1.8 m/s using the PRV	57
Figure 5-20: Load-cycle - start up, overload, stop	58
Figure 6-1: Proposed layout of the test bench	60
Figure 7-1: Failure Mode - Pipe/Hose High pressure Failure	67
Figure 7-2: Failure Mode - Motor Control Broken	68
Figure 7-3: Failure Mode - Motor Control Broken	69

Figure 7-4:	Failure Mode – No Electricity	69
Figure 7-5:	Failure Mode – Broken PRV, check valve	70
Figure 7-6:	Failure Mode – Loss of Controller	70

V List of tables

Table 2-1: Parameters of the turbine model7

VI Appendix

Failure modes and counteractions:

Pipe/Hose High pressure Failure:

Valves will be mounted close to hose. In doing so a broken pipe/hose can be closed by the valve.

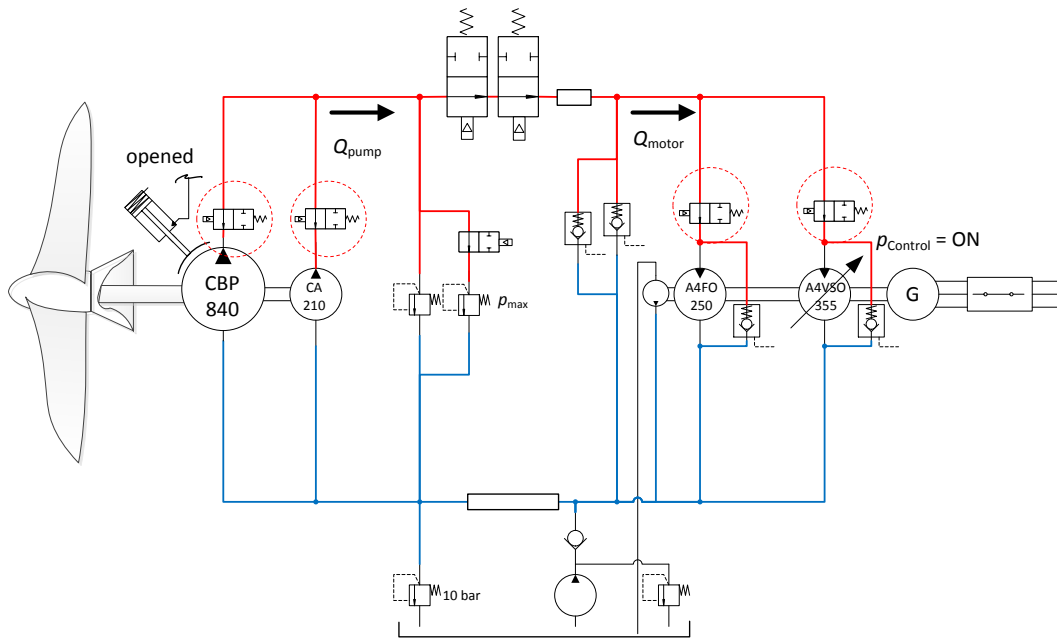


Figure 7-1: Failure Mode - Pipe/Hose High pressure Failure

Motor Control Broken:

Close the main valve and initiate the emergency stop procedure. Flows will be supplied by the hydraulic transformer.

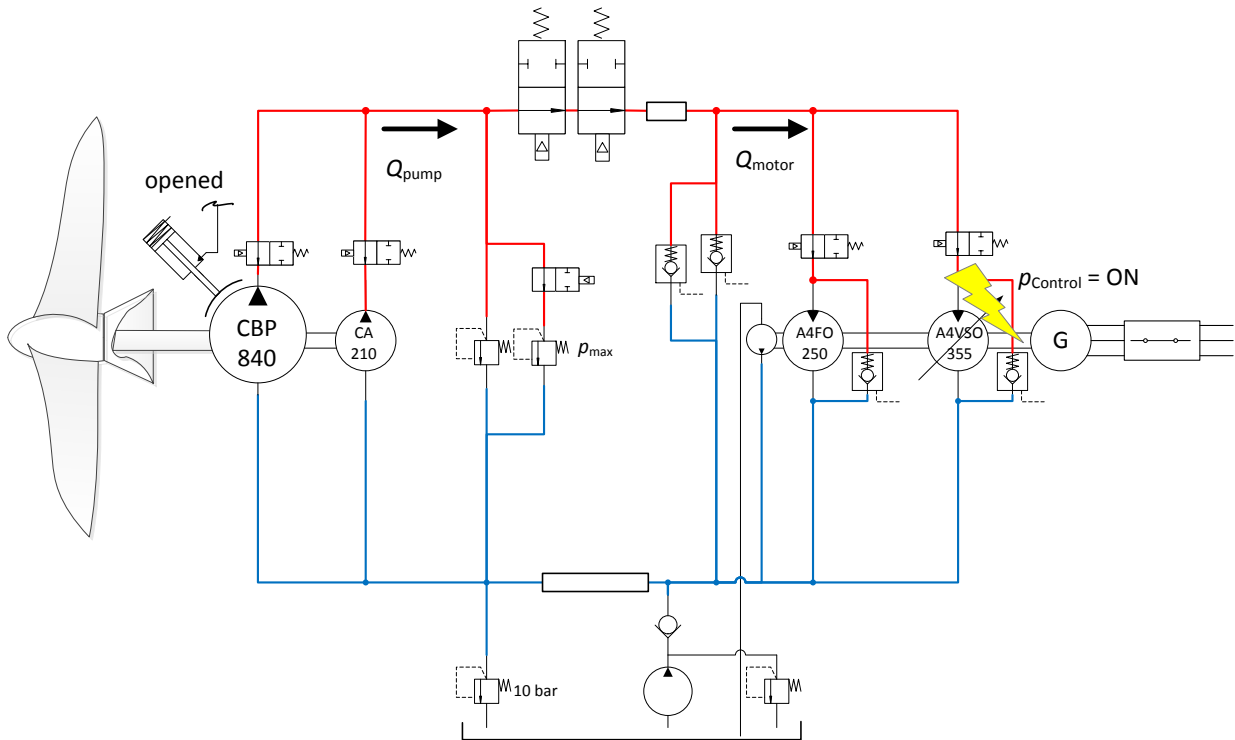


Figure 7-2: Failure Mode - Motor control broken

Boost pump broken:

Use the hydraulic transformer to supply the low pressure and perform an emergency stop.

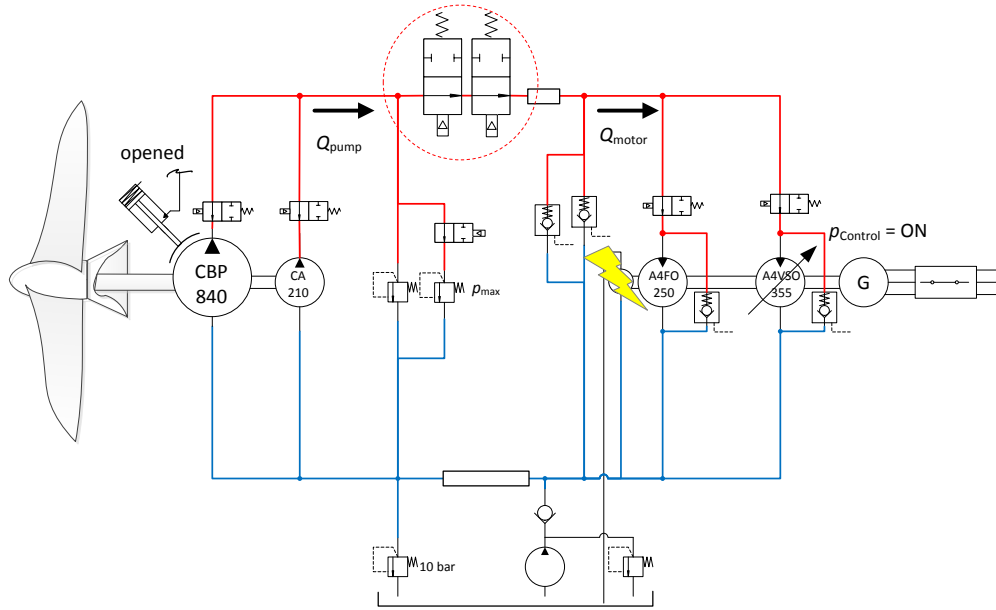


Figure 7-3: Failure Mode - Motor Control Broken

No electricity:

Use the hydraulic transformer to supply the low pressure and perform an emergency stop.

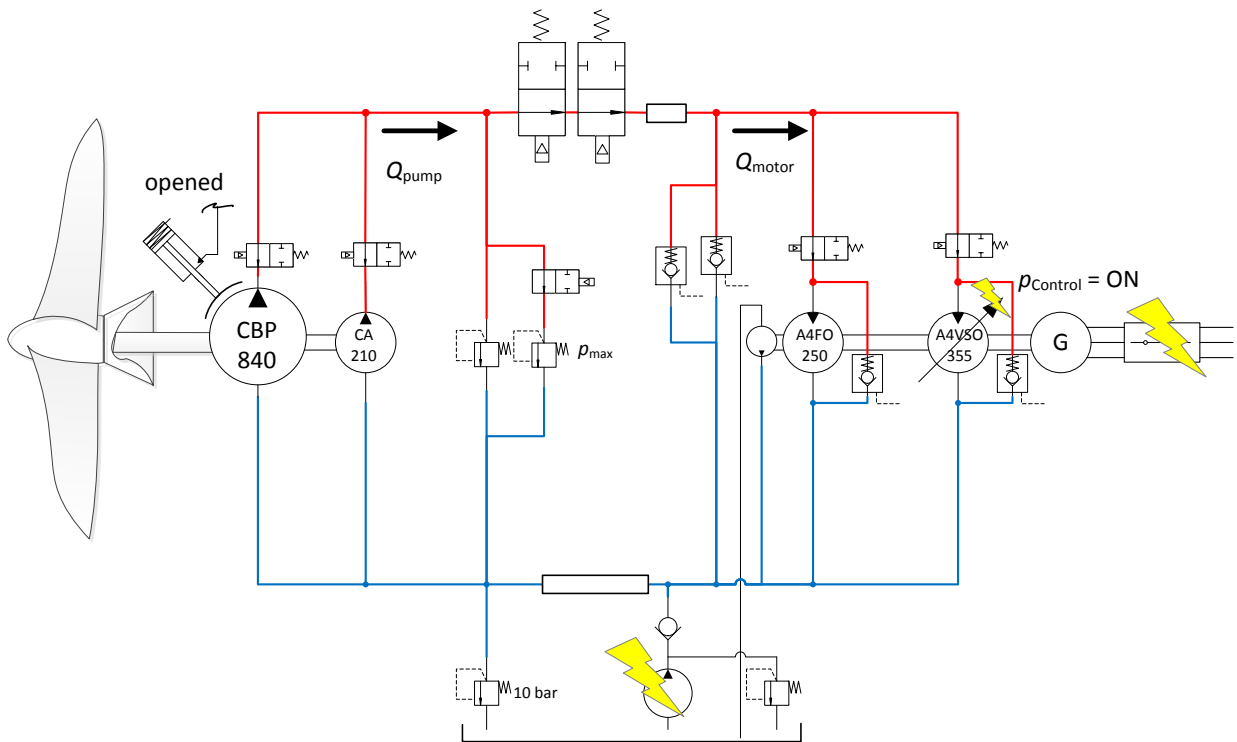


Figure 7-4: Failure Mode – No Electricity

Broken PRV, check valve:

Redundant components

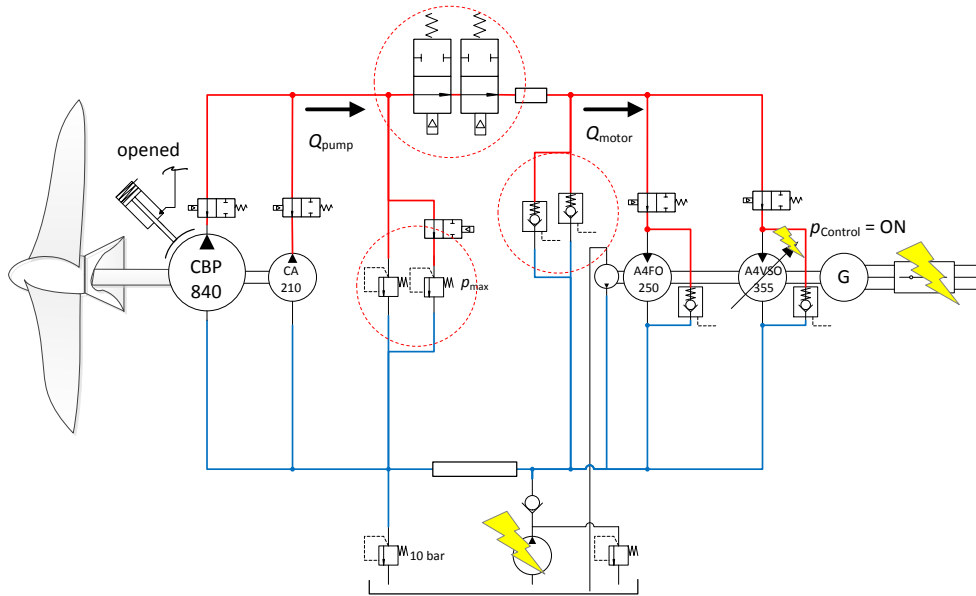


Figure 7-5: Failure Mode – Broken PRV, check valve

Loss of Controller:

Perform emergency stop procedure

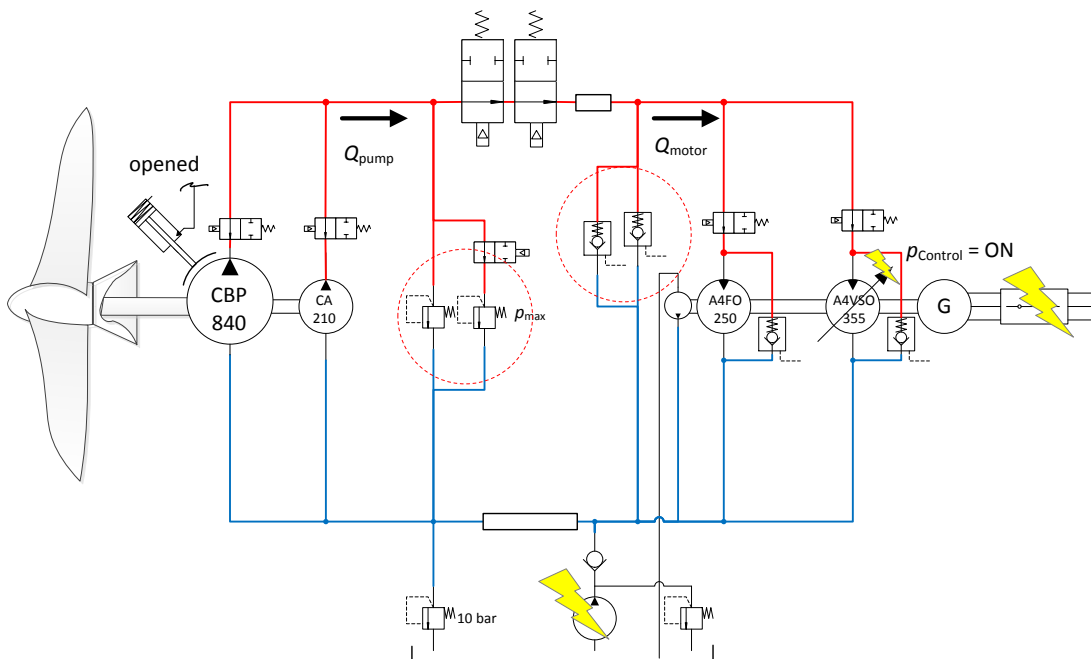


Figure 7-6: Failure Mode – Loss of Controller